Multimodal Transport Networks*

Simon Fuchs — Atlanta Fed

Woan Foong Wong — University of Oregon & CEPR

March 2024

Abstract

Movement of goods utilizes multiple transportation modes, and transport network changes can have large spillovers. This paper studies the economic and environmental effects of improvements and disruptions within the multimodal transport network. We develop a quantitative spatial equilibrium model incorporating multimodal routing and congestion at intermodal terminals, where mode-switching takes place. We estimate intermodal port congestion by investigating ship dwell times and their responsiveness to port traffic using vessel-positioning data. We estimate elasticity of modal substitution in response to infrastructure improvements using highway and rail data. Calibrating the model to US multimodal freight transport for road, rail, waterways, and intermodal terminals, we quantify the gains from improving intermodal terminals. We identify important bottlenecks in central US—switching cost reductions in most beneficial terminals generate welfare gains equivalent to 300-700 million USD of additional GDP (in 2012 USD), alongside environmental gains from modal substitution towards greener rail traffic. Congestion effects compound the impacts of Panama Canal disruption and rail strike scenarios.

JEL Code: F11, R12, R42

Keywords: Multimodal transport, Transport network, Spatial equilibrium, Infrastructure investments

*Contact: simon.fuchs@atl.frb.org and wfwong@uoregon.edu. We are grateful to the NBER, DOT, and NSF for project support under the "Economics of Transportation in the 21st Century" Initiative. We thank Adina Ardelean, Mark Colas, Nelson Lind, Yuhei Miyauchi, Andrii Parkhomenko, as well as seminar and workshop participants at Berkeley Haas, Emory, Minneapolis Fed, Purdue, UCLA, Rochester, CRED Workshop on Urban and Regional Economics 2024, and other conferences for helpful comments. Benjamin Delgado and Philip Economides provided excellent research assistance. The views in this paper are solely the responsibility of the authors and should not necessarily be interpreted as reflecting the views of the Board of Governors of the Federal Reserve System or of any other person associated with the Federal Reserve System. All errors are our own.

1 Introduction

Firms, workers, and locations are intrinsically linked via transport, trade, and production networks. Improvements or disruptions within these networks can have large impacts on economic activity and welfare. Much of the focus on transport networks has been on one mode, like roads or ocean shipping. However, transportation takes place multimodally, driven by geography and containerization, with intermodal terminals—which allow for the switching between modes—playing an important role in integrating the entire network. On top of this, congestion effects at intermodal terminals, like ports, can exacerbate the disruption effects on the entire multimodal transport network or mitigate the positive returns from improvements. These welfare impacts can further generate vastly different environmental consequences: transport modes emit differing levels of emissions (trucks emit 8 times more CO_2 per ton-mile than rail, CBO (2022)).

We study multimodal transport networks and their impact on the economic and environmental returns to infrastructure investments and disruptions. In particular, we focus on how these outcomes will depend on the geography of the multimodal transportation network, the location and congestion levels of intermodal terminals that allow for switches between modes of transportation, as well as the relative cost of transportation across modes. By incorporating these features we provide a framework that allows us to realistically evaluate disruptions and infrastructure policies taking the complete domestic transportation network into account. We highlight that changes within the multimodal transport network can generate direct and indirect effects across modes. Improving the highway network, for example, will directly decrease truck transport costs. Indirectly, there can be two additional effects. First, better road access will improve the general market access of locations via a decrease in overall transport costs, increasing their overall demand for transportation across all modes—a *modal complementarity* effect. At the same time, this improvement increases the relative costs of other transport modes, and the transport use for other modes will decline relative to road—a *modal diversion* effect. This also allows us, for the first time, to evaluate the environmental impact of infrastructure investments that stems from modal complementarity and diversion.

We first develop a quantitative spatial equilibrium model that incorporates transportation across multiple transport modes. Drawing on recent innovations in transportation modeling we characterize the optimal route and sourcing choice of an agent making nested choices along the network in a recursive manner. This modeling choice has two distinct advantages: First, by relying on a recursive characterization we can characterize the optimal routing problem and

the associated (ad valorem) transportation cost without explicitly enumerating all multi-modal paths. Second, the model allows for a flexible nesting structure that can be embedded into the spatial equilibrium equation to express the equilibrium outcomes in terms of edge-level outcomes only. This formulation makes it possible to embed a nested modal choice directly into the equilibrium equations, allowing both a flexible mode choice as well as rich congestion patterns on any mode-specific network. Finally, we derive the counterfactual equilibrium. The counterfactual equilibrium can be easily calibrated using data on observed modal traffic and the spatial distribution of income and labor densities only. Furthermore, it allows for a convenient computational separation of the mode-specific transportation equilibrium at the edge level, which balances mode choice and endogenous congestion and determines the (endogenous) aggregate transport cost, and the aggregate determination of the (counterfactual) spatial equilibrium. This framework allows for a wide variety of counterfactuals that can evaluate mode-specific dis-aggregate investments or disruptions.

In order to calibrate our model, we estimate two central parameters. First, we examine the impact of congestion at intermodal terminals. Using vessel positioning data down to the minute interval, we investigate the time ships take to load and unload at ports which are important intermodal terminals. We then estimate an elasticity of port congestion by investigating how responsive the ship's dwell times are to overall port traffic at the time of the ship's arrival. Since ship dwell times can be endogenous to conditions at port, we develop a shift-share instrument in order to identify the impact of overall port traffic on ship dwell times. We find that a 1 percent increase in port traffic increases ship dwell times by 0.2-0.3 percent.

Second, we estimate an elasticity of modal substitution with respect to infrastructure improvements by building on the seminal work by Duranton and Turner (2011) which finds that a 1 percent increase in interstate highways lead to more truck traffic use in cities by about 1.7-2.1 percent. Matching confidential waybill rail data to cities, we show that this improvement in road access has a positive but imprecise impact on rail traffic use, due to opposing forces from modal complementarity and substitution, that is 4-7 times smaller in magnitude (0.3-0.4). Taking the ratio of rail to truck traffic use, we estimate an elasticity of modal substitution: a 1 percent increase in interstate highways result in a decrease in rail to truck traffic use by 0.9-1.2 percent.

Next, we calibrate the model to fit and reproduce salient features of the US domestic transportation network. We first build a graph representation of the US multimodal transportation system drawing on high-resolution GIS data on road, rail and maritime linkages, as well as the location of intermodal switching facilities. In combination with detailed road traffic and railroad

data the model can then be applied to evaluate infrastructure investments, taking the multimodal nature of the US domestic transport system into account. We employ the model to evaluate a number of counterfactuals.

Our main application compares the welfare impact of investing in different terminals across the country, thus improving the intermodal integration of the multimodal transport network. The analysis points towards substantial and highly heterogeneous welfare gains across space. We find that terminals that generate the largest gains are in the center of US like Chicago and Dallas, highlighting the role of multimodal network transporting goods from coastal regions to the interior. Investments that would lower transportation costs in the most important nodes by only 1 percent would generate an aggregate welfare gain equivalent to $300-700 million of additional GDP (in 2012 USD). These investments result in modal substitution, shifting traffic use from road to rail. Since trucks generate more greenhouse gases relative to trains, these modal substitution effects have important environmental consequences for infrastructure investment in terminals.

Additionally, we quantify the welfare changes and environmental impacts of three policy-relevant scenarios. For each of these scenarios, we show that congestion—at terminals and for both terminals and roads—has a compounding effect on welfare. We further show that modal substitution in response to each of these scenarios result in additional environmental impacts due to the differing levels of emissions for each transport mode. First, we evaluate the value of the rail network in the United States by exploring the potential rail strike from fall 2022. We find that losing access to the rail transport network is equivalent to decreasing US GDP by about $230 billion (in 2012 USD), about half the value of the US highway system as estimated by Jaworski, Kitchens and Nigai (2023). The modal substitution towards trucks results in an even larger social cost. Next, we consider the consequences of repealing the Jones Act from 1920, an active US trade regulation that restricts all ships transporting goods and passengers between US ports to be majority owned and crewed by US citizens, as well as built locally. By reducing the cost of operating US domestic waterways to foreign-flag vessels which is equivalent to letting foreign ships service these waterways, we show that the welfare gain of repealing the Jones Act is equivalent to increasing US GDP by about $3.2 billion (in 2012 USD). Our finding is towards the lower end of the range estimate by US international Trade Commission (USITC), pointing towards our focus on just the continental United States and also the long-run response of the multimodal network to substitute away from this relatively expensive mode. The modal substitution away from trucks and rail results in an even larger social benefit since waterway

transport is greener. Our third scenario is on the impact of the Panama Canal disruptions due to drought conditions. The welfare cost of decreasing access to the canal, allowing for both modal and route substitution, is equivalent to decreasing US GDP by about $2.7 billion (in 2012 USD). Here the environmental consequences are more negative due to the substitution towards both trucks and rail.

Our paper is related to a number of different strands of research. First, this paper contributes to a rapidly expanding literature incorporating realistic transportation network into quantitative spatial equilibrium models (see Redding (2020) for a recent survey). Within that literature, there have been multiple efforts to merge the dis-aggregated network structure of transportation infrastructure with a general equilibrium economic geography model. (Fajgelbaum and Schaal, 2017; Allen and Arkolakis, 2022; Fajgelbaum et al., 2023). In particular, Allen and Arkolakis (2022) proposed a tractable way of incorporating the optimal routing choice into an spatial equilibrium model, allowing the authors to examine the general equilibrium implications of transportation improvements. While much theoretical progress has been made, the literature has often focused on one mode of transportation, approximating transport costs with either road, maritime, or rail transportation costs (Coşar and Demir, 2018; Brancaccio, Kalouptsidi and Papageorgiou, 2020; Heiland et al., 2019; Ganapati, Wong and Ziv, 2021; Wong, 2022; Degiovanni and Yang, 2023). A more recent literature has focused on the contributions of highways and domestic roads to transport costs and port access (Fan, Lu and Luo, 2019; Fan and Luo, 2020; Bonadio, 2021; Jaworski, Kitchens and Nigai, 2023).[1] Our project adds to this literature by studying the general equilibrium analysis of the US multi-modal transportation system—highways, rail, and barges—as well as intermodal switching terminals which allow for transshipments.

Second, our paper is related to a long-standing literature in transportation studies that examines route and mode choice both empirically and theoretically (McFadden, Winston and Boersch-Supan, 1986; Rich, Kveiborg and Hansen, 2011; Beuthe, Jourquin and Urbain, 2014; Winston, 1981). The state-of-the-art in transportation studies solves high-dimensional traffic assignment problems algorithmically accounting for both dis-aggregated heterogeneity in modal and route choice.[2] We employ similar tools to those recently developed in transportation studies. Specif-

[1] Fan, Lu and Luo (2019) and Jaworski, Kitchens and Nigai (2023) focus on domestic road and highways while Bonadio (2021) focuses on roads and road access to ports. Fan and Luo (2020) is a note which characterizes bilateral transport costs and their elasticities with respect to transshipment costs.

[2] For a recent theoretical contribution compare Kitthamkesorn, Chen and Xu (2015) which solves for the traffic assignment problem allowing for both endogenous route and mode choice. A recent applied quantitative contribution in this literature (Li, Xie and Bao, 2022) models the multimodal linkages between the US and China with endogenous route choice and congestion at port locations.

ically, we employ what the transportation literature calls a *stochastic user equilibrium* where routes and modes are chosen subject to a stochastic perception error. However, we go beyond the transportation literature, by fully embedding the stochastic user equilibrium into a spatial general equilibrium framework, where input and output markets across space clear and factor and output prices are endogenously determined.

Third, our paper is related to the recent literature on the environmental impacts of transportation. Most of this literature focuses on the link between international trade and greenhouse gas emissions via transportation, and changes to this relationship in response to environmental regulations (Shapiro, 2016; Mundaca, Strand and Young, 2021; Lugovskyy, Skiba and Terner, 2022) or trade policies (Cristea et al., 2013). We instead highlight how infrastructure investments can have environmental consequences via the multimodal transportation network. While some of these papers have found compositional shifts in transport mode use due to regulation and trade policy changes,[3] our quantitative general equilibrium framework allows us to distinguish between the two modal complementarity and diversion effects. Additionally, our empirical framework allows us to investigate the strength of both of these effects for infrastructure improvements.

The remainder of the draft is structured as follows. Section 2 describes the US multimodal transport network and our data. We then detail the multimodal routing model in Section 3 and describe how we estimate our congestion and modal substitution elasticities in Section 4. We incorporate our elasticities and apply our model to evaluate the welfare impact of terminal investments in Section 5 and conclude in Section 6.

2 Data: US Domestic Freight Transportation

In this section, we introduce our data sources and provide an overview of the US domestic transportation system. As mentioned above, the movement of goods from origin to destination takes place over multiple modes of transportation. Figure 1 plots the value share of freight moved by different modes across various distances within the United States. Trucks are mostly used to move US freight over shorter distances below 100 miles, accounting for 90 percent of value (Figure 1), which is indicative of the denser road network playing an important role in facilitating transportation at the start and end of the movement of goods. This is commonly known as the

[3] Cristea et al. (2013) finds that trade liberalization between countries will increase trade from more distant partner countries, resulting in a proportional increase in air transport use and greenhouse gas emission. Lugovskyy, Skiba and Terner (2022) finds that environmental regulations capping CO_2 emissions from maritime shipping will substitute demand towards air transport, increasing total transport-related CO_2 emissions.

first and last mile in freight transportation (Rodrigue, 2020; Ranieri et al., 2018). Over longer distances, however, freight is increasingly transported using multiple modes. For freight moved over longer distances of 1000 miles or more, multimodal transport accounts for a third of the total value (Figure 1) and almost 50% by weight (Figure A.1). For freight transported over 1,500 miles, multimodal transport accounts for more than half by value and more than two-thirds by weight. For context, the road distance between Los Angeles and Chicago is about 1700 miles. The proportion of freight transported over multiple modes is also increasing over time: intermodal container rail traffic is the fastest growing rail traffic segment, having grown by more than 5 times since 1984 (Surface Transportation Board).

2.1 Rail, Road, Waterways, Ports, and Intermodal Terminals

Rail Geography Network and Traffic We use detailed geo-spatial information from the U.S. Census Bureau's Topologically Integrated Geographic Encoding and Referencing (TIGER) Database to construct a graph representation of the US intermodal rail network. To do so, we subset the original network to those segments that are owned by Class I carriers and are compatible with multimodal transportation.[4]

For rail traffic data, we have obtained access to confidential data from the Surface Transportation Board. This is a stratified sample of carload waybills for all U.S. rail traffic submitted by those rail carriers terminating 4,500 or more revenue carloads annually, covering 48 states (except Alaska and Hawaii). The carload waybills report the origin rail station, destination rail station, and the interchange stations in between that these freight cargo are transported through. The rich geographical information in this confidential data set allows us to study the routing of these commodities through the railroad network. Additionally, this data set also contains commodity-specific information including number of car loads, weight, whether it is a domestic or international shipment, and its inter-modality—primarily indicating if the freight movement involved other transport modes, which is almost entirely containers. Since we are focused on multimodal freight movement, we restrict our sample to intermodal freight transported by Class I carriers, the largest carriers.

Figure 2a shows the rail intermodal traffic flows for the United States. Thicker lines, indicating higher traffic flows, link the US West and East coastal regions to interior locations like Chicago,

[4]Class I railroads are the largest carriers operating on the US railroad system. They were originally in 1992 defined to be those carriers above $ 250m dollars of revenue, a cutoff that has been adjusted for inflation since. In 2021 the threshold stands at approximately $943m. There are currently seven class I carriers and they make up the large majority of the domestic rail freight market.

Figure 1. US Transport Mode Value Shares by Distance

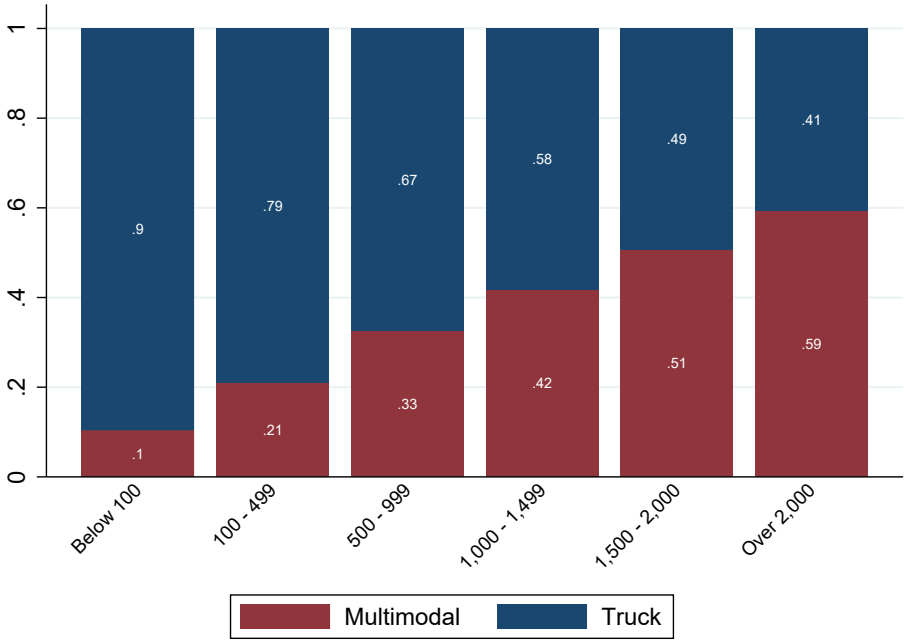

Notes: This figure plots the observed value share of cargo transported by different modes across various distances in 2018. Multimodal indicates cargo movement that involves more than one mode. Source: Freight Analysis Framework, US Department of Transportation, and authors' calculations.

Dallas, and Atlanta. Examples of such routes include Los Angeles and Chicago, New York City and Chicago, as well as Los Angeles and Dallas. Echoing Figure 1, the rail network serves to transport freight over long distances.

Road Geography Network and Traffic We follow Allen and Arkolakis (2022) for the construction of road traffic flows data. We summarize their procedure in three steps: First, they create a sparse graph representation of the underlying road network by collapsing the high-dimensional geo-spatial information contained in the original shapefiles and only preserving nodes that are either endpoints or intersections. Furthermore, core-based statistical areas (CBSAs) are represented by a singular node along the network. Their resulting graph consists of 228 nodes and and 704 edges. Second, they construct a weighted graph by including traffic data. To do so they obtain the average annual daily traffic from the the 2012 Highway Performance Monitoring System (HPMS) dataset by the Federal Highway Administration and allocate it to individual links by constructing a length-weighted average of the annual daily traffic.

Figure 2b shows a graph representation of the interstate highway system with thicker lines indicating higher road traffic flows. The highway flow patterns are quite different from rail traffic flows (Figure 2a). Here, heavier highway traffic connects large cities that are densely

Figure 2. Traffic along the US Domestic Freight Transport System

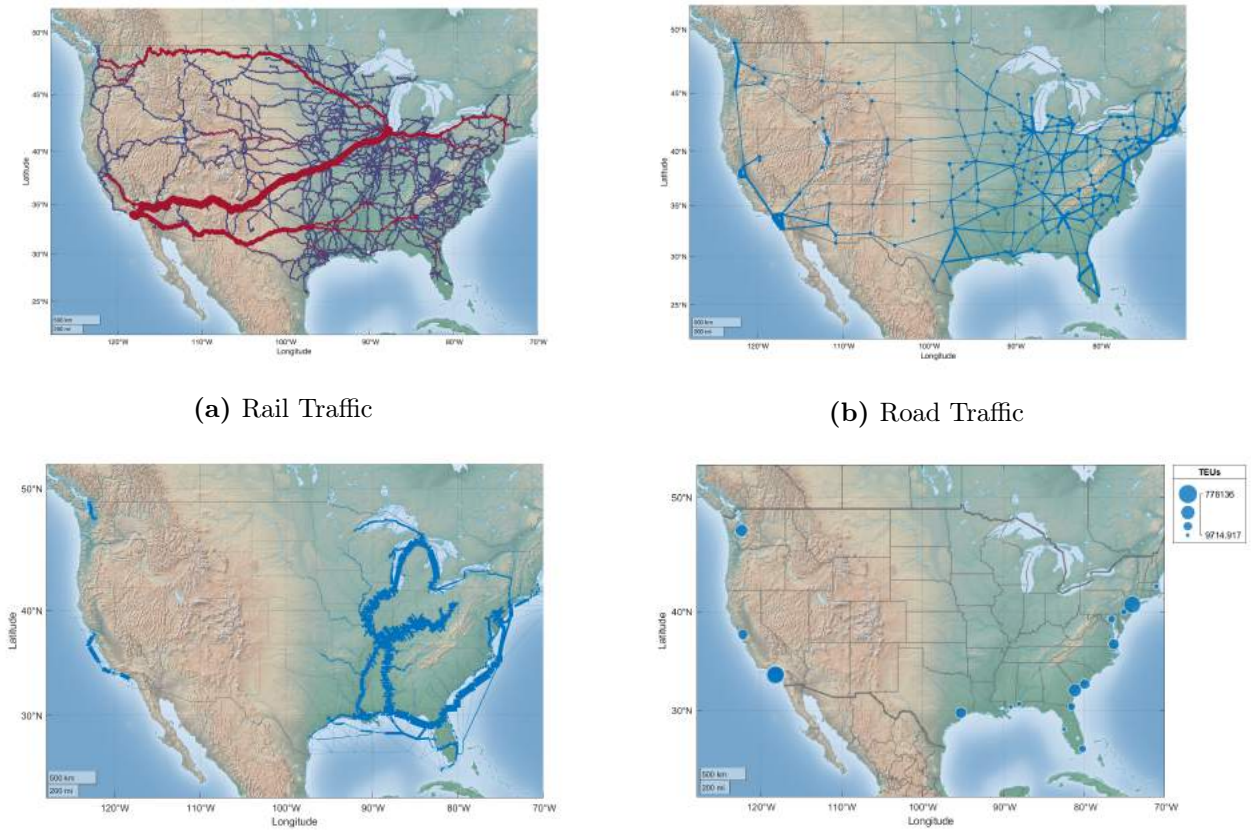

(a) Rail Traffic

(b) Road Traffic

(c) Waterway Traffic

(d) Port Traffic

Notes: Panel (a) presents the US domestic rail traffic data for Class I carriers (the largest rail carriers) conditional on intermodal capability. Shortest routes are imputed between origin, interchange stations, and destination to assign total tonnage to individual rail segments along network. Thicker lines indicate higher traffic flows. Panel (b) presents the traffic along the graph representation of the interstate highway system. Thicker lines indicate higher traffic flows. Panel (c) presents the domestic waterborne traffic data for manufactured goods, where the shortest routes are imputed between origin and destination to assign total tonnage to individual segments of the domestic water network. Thicker lines indicate higher traffic flows. Panel (d) presents the container traffic volume at international ports. Larger circles indicate higher container volumes. Sources: Authors calculations, Confidential Carload Waybill, Surface Transportation Board; Highway Performance Monitoring System, the Federal Highway Administration; Waterborne Commerce statistics, US Army Corps of Engineers (USACE); and Port Performance Freight Statistics Program, Department of Transportation (DOT).

populated either on the coast or in the interior regions, like Los Angeles and San Diego, Boston to Philadelphia, and the surrounding areas around Chicago.

Waterway Traffic We next capture goods that are transported via US waterways by bringing in waterborne traffic data from the US Army Corps of Engineers (USACE). Focusing on manufactured goods, we primarily capture freight transported by barges. Figure 2c visualizes this data.

Port Location and Traffic The geospatial data on port location is obtained from the US Army Corps of Engineers. The container volumes at these ports have been collected from the Port Performance Freight Statistics Program maintained by the Department of Transportation (DOT). Both these data are visualized in a geographic bubble map in Figure 2d.

Intermodal Terminals Some of the intersections between the road and rail network also represent terminal stations where a transfer from rail-to-road or road-to-rail is possible. In order to isolate these intermodal terminals, we include information from the National Transportation Atlas Database (NTAD) maintained by the Department of Transportation (DOT) on the location of intermodal freight facilities.

US Multimodal Transport Network To construct the US multimodal transport network, we start by combining all the geo-spatial information on each of the rail, road, and waterway networks. On top of that, we add the locations of ports and intermodal terminals, resulting in the graph representation of the US multimodal transport network in Figure 3.

2.2 AIS Vessel Traffic Data

We utilize automatic identification system (AIS) vessel traffic data from Marine Cadastre, a joint initiative between the Bureau of Ocean Energy Management and the National Oceanic and Atmospheric Administration. This data captures vessel location in US waters at 1-minute intervals using 200 land-based receiving stations. We observe the vessel's identifying information, its longitude and latitude location down to the minute, speed, and navigation status. The vessel's identifying information includes its International Maritime Organization Vessel number (IMO). The vessel's navigation status captures whether the vessel is being propelled (under way using engine), or moored—held in position at a pier.[5] Using information on the ship's speed and navigation status, we define a ship's dwell time to be the time it spends being moored at a pier and has zero speed. This is a conservative measure of ship dwell time at ports because (1) a ship will spend time navigating within the port area as it prepares to moor at a pier and (2) a ship can also end up waiting outside of the port area at anchor before navigating to the port (New York Times, 2021). In future work, we plan on investigating additional measures of dwell times,

[5]There are additional AIS navigational statuses than the ones described here, for example being propelled via sail (underway sailing) or at anchor (held in position by an anchor but not at a dock). Future work will consider utilizing additional statuses.

Figure 3. US Multimodal Transportation Network

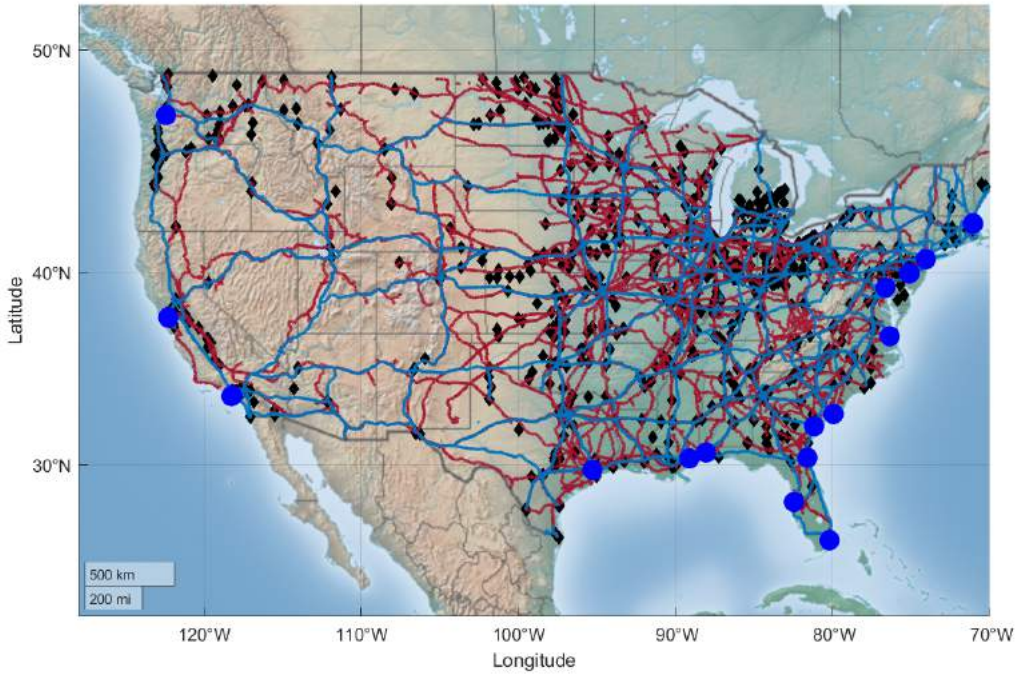

Notes: This figure shows the combined US multimodal freight network. The original GIS information is obtained from the U.S. Census Bureau's Topologically Integrated Geographic Encoding and Referencing (TIGER) Database. The red lines indicate the Class I multimodal railroad network. The blue lines indicate the interstate highway system (IHS). Black diamonds indicate freight terminals that are owned by Class I operators allow for road-to-rail or rail-to-road intermodal movements. The blue circles indicate the top 18 ports.

including the entire time a ship spends within the port areas (not just when they are moored), as well as the time a ship spends at anchor within or just outside of port areas.

In order to match these ships to the ports they are located at, we next require geographical information of the ports. We use the Port Statistical Area shapefiles from the US Army Corps of Engineers and match these ships to the top 30 container ports in the US. These port polygon areas also allow us to calculate the total amount of time a ship spends within the port region on top of the time it spends moored at a dock. Additionally, in order to identify the cargo capacity of these ships and their containership status, we match these ships to the Port Entrance and Clearance dataset from the US Army Corps of Engineers using their identifying information and when they are at these ports. The ship cargo capacity measures the volume of the ship that can be used for loading cargo (also known as net tonnage of a ship). This cargo capacity measure for each ship will contribute to our port traffic measure at each port every day.

Port Traffic Our measure of port traffic is defined as the sum of the net tonnage of each ship moored at the port each day, multiplied by the percent of the day they spend at the port—

crucially including ships that arrived prior to that day but still remained moored at port. To be more specific, if a ship remained moored at port all the way without exiting, its contribution to port traffic would be 100% of their net tonnage (100% of the time it spent at the port). If a ship left at any point during that day, its net tonnage contribution would be less than 100% and instead determined by the amount of time it spent moored at port that day.

With this daily port traffic measure, we calculate moving averages of the port-level traffic for varying amounts of time. We have done this for 3, 7, 14, 21, and 28 days. We present the 28-day moving average results and have included the rest in the appendix.[6]

Summary Statistics Our matched dataset from 2015 to 2021 has 3,755 unique vessels with 1,444 containerships. The top 30 ports in our dataset account for around 95% of all US container trade annually. Figure 4 plots the average of containership dwell times at the top 30 US ports from June 2015 to December 2021. The average dwell time over this period is around 33.3 hours per ship with a standard deviation of 5 hours. However, as seen in Figure 4, there is a significant increase in the ship dwell times post 2021. The average ship dwell time after 2021 is 42.8 hours.

3 Economic Geography Model with Multimodal Routing

In this section, we embed a recursive formulation of the multimodal routing problem into an otherwise standard economic geography model with domestic trade between a discrete number of locations and freely mobile labor reallocation across locations as in Allen and Arkolakis (2014), Redding (2016). We follow recent contributions in the spatial equilibrium literature and embed an optimal route choice along a graph representation of the underlying infrastructure network into the spatial equilibrium model as in Fajgelbaum and Schaal (2017) and Allen and Arkolakis (2022).[7] The technical challenge is that the number of feasible routes for even low-dimensional graphs can be too large to characterize explicitly - a curse of dimensionality that affects path enumeration and makes brute force solutions infeasible. In contrast to previous contributions, we rely on a recursive formulation of the routing problem that implicitly tackles the path enumera-

[6] It is acknowledged here that this measure could be interpreted as an upper bound measure of the amount of traffic at each port since using the net tonnage measure of a ship assumes that it is filled to capacity. Future work will incorporate the draft information we observe for these ships which will allow us to infer net capacity change. Additionally, an alternative lower bound measure of port traffic is a count of ships currently at the port (since smaller ships would have equal weight as large ships).

[7] The latter approach is intimately related to the previous canonical contribution by Akamatsu (1997) who showed that a class of logit traffic assignment models can be restated as an optimization problem with only link-level variables.

Figure 4. Containership Dwell Times at Port

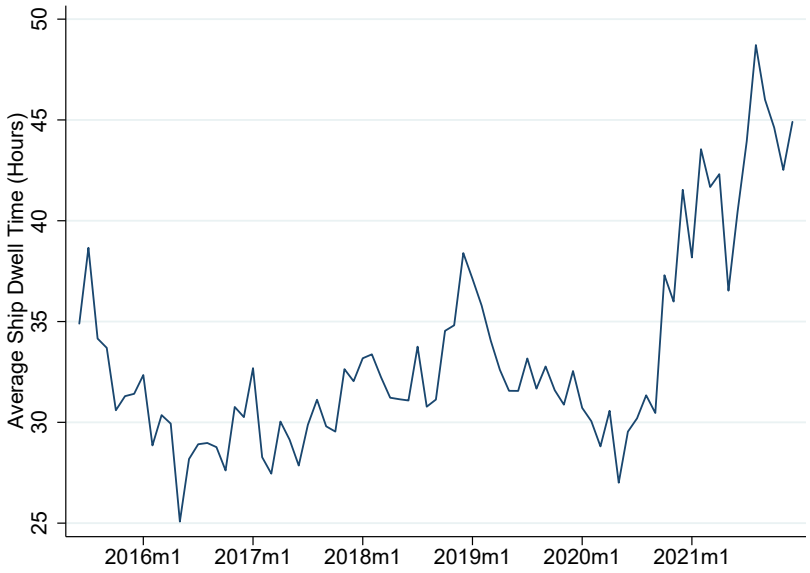

Notes: This figure plots the average of containership dwell times at the top 30 US ports from June 2015 to December 2021. Weighted by ship net tonnage.

tion problem. Specifically, rather than explicitly solving the problem, we can obtain a closed-form expression that is recursive in neighboring transportation cost and can be directly embedded into the equilibrium equations, thus allowing us to restate the spatial equilibrium in terms of choices and flows between neighboring nodes along the topology of the transportation network.

In what follows, we assume perfect competition in our freight transport companies. While this is a simplifying assumption since the focus of this paper is on the multimodal network transport structure, the transportation literature has also established that multimodal container transport is generally more competitive relative to unimodal transport (Zgonc, Tekavčič and Jakšič, 2019), and within rail transport relative to non-containerized shipments (Surface Transportation Board, 2009).[8]

3.1 Geography and Transportation

Let $\mathcal{G} \equiv (\mathcal{N}, \mathcal{L})$ be a multigraph representing a (multi-)modal transportation network where $\mathcal{N}$ and $\mathcal{L}$ are the set of nodes and links respectively. We define the set of successor nodes $\mathcal{F}(i)$ and

[8] Zgonc, Tekavčič and Jakšič (2019) studies the impact of distance on multimodal road-rail transport compared to unimodal road transport and finds that multimodal transport can be competitive relative to unimodal transport even over relatively short distances. In a study on the US freight rail industry, (Surface Transportation Board, 2009) reports that multimodal rail shipments have lower markups than other shipments, and that rail rates are lower for locations that are closer to alternative transport modes. With data on door-to-door container shipments, one would be able to study the issue of market power in container freight transport in more detail. However, to the best of our knowledge, this data is not available in a comprehensive manner.

the set of predecessor nodes $\mathcal{B}(i)$ for each node $i \in \mathcal{N}$. Furthermore, let $\mathcal{G}_m \equiv (\mathcal{N}_m, \mathcal{L}_m)$ be the subgraph representing the transportation network for mode m, where $\mathcal{N}_m \subseteq \mathcal{N}$ and $\mathcal{L}_m \subseteq \mathcal{L}$ are the mode-specific nodes and links respectively. We also define the mode-specific successor and predecessor nodes $\mathcal{F}_m(i)$ and $\mathcal{B}_m(i)$. Each link $ij \in \mathcal{L}_m$ is associated with a generalized link travel cost $t_{ij,m}$ which can be flow dependent. The set of OD pairs is defined as $\mathcal{W}$.

Moving goods from origin i to destination j along route r, which involves a series of links index from 0 to K, is indicated by vector $r \equiv \{i = r_0, r_1, \ldots, r_K = j\}$. We define a primary modal network, $m = 0$, that represents the dense road network on which all cities and road intersections are located. All other modes ($m \neq 1$) are secondary transport networks (i.e. rail, barges etc.). A subset of nodes on the primary and non-primary networks are intermodal terminals which allow for switches between modal networks.

3.2 Consumption and Production

A representative agent lives in location j, supplies her unit endowment of labor inelastically, earns a wage rate w_j, and purchases quantities of a continuum of consumption goods, $\nu \in [0, 1]$. She is endowed with constant elasticity of substitution (CES) preferences where the elasticity of substitution is given by $\sigma \geq 0$. Her preferences are given by,

$$U_j = \left(\sum_{\nu} q_{ij}^{\frac{\sigma-1}{\sigma}}(\nu) \right)^{\frac{\sigma}{\sigma-1}}$$

where U_j aggregates the quantities produced from all other locations i. Furthermore, we define aggregate income as Y^W, the total labor endowment as $\bar{L}$, and average per capita income as the numeraire, i.e. $Y^W/\bar{L} = 1$.

Each location i produces each good $\nu \in [0, 1]$ subject to a constant returns to scale technology and transports it to each destination j along each feasible route. We assume perfect competition which implies that the price of good ν in destination j from origin i along route r is given by

$$p_{ij,r} = \frac{w_i}{A_i} \left(\prod_{k=1}^{K} t_{r_{k-1},r_k} \right) = \frac{w_i}{A_j} \tau_{ij} \tag{1}$$

where the marginal cost of production in i is $\frac{w_i}{A_i}$, local wages are w_i, and each worker can produce A_i units of goods. Trade cost is route-specific and multiplicative over all links along route r. In what follows next, we will introduce a recursive routing and - eventually - sourcing choice.

Figure 5. Recursive Routing on a Directed Graph

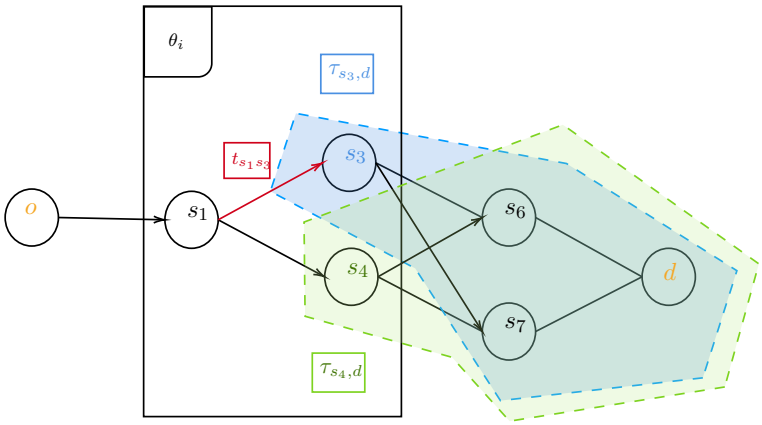

Notes: The figure illustrates a directed transport network from an origin o to a destination d. Nodes are represented as circles and linked via edges. Each link is associated with an (iceberg) transport cost. The figures illustrates the recursive routing choice at node s_1 where an agent chooses between neighboring nodes s_4 and s_3, both of which have a continuation value that captures the cost minimizing transport cost to destination d along the (appropriately colored) subnetwork.

3.3 Recursive Sourcing in Equilibrium

To characterize the optimal combined route and sourcing choice we draw in recent innovations in (discrete) route choice modeling (Oyama, Hara and Akamatsu, 2022; Daly and Bierlaire, 2006). In general, the technical challenge is to overcome the curse of dimensionality associated with constructing the choice set of any agent traveling between any two nodes on a graph - the path enumeration problem. One solution is to implicitly characterize the choice set by recursively solving the routing problem. The most common approach exploits a markovian representation of the routing problem together with the tractability and flexibility of a (nested) extreme value discrete choice framework. We will sequentially introduce this modeling technique, first by introducing the recursive routing choice in this subsection, and then by fully characterizing the route and sourcing choice in the next subsection, before eventually fully embedding it into the market clearing conditions to characterize the spatial equilibrium.

We follow Papola and Marzano (2013) and characterize the individuals' routing and sourcing choice as a joint choice of elemental links of the route in an ordered sequence from the residential location o toward the sourcing destination d. Such a joint choice can be modeled as a recursive choice subject to extreme value preference shocks without discounting. The individual then makes a recursive cost-minimizing routing choice, comparing at each node i, the cost of moving

towards a neighboring node k, i.e. t_{ik}, and continuing onwards from there towards the final destination d facing a continuation value τ_{kd}. That is the agent solves the following problem,

$$\min_{k \in \mathcal{N}(i)} \left\{ \frac{t_{ik}\tau_{kj}}{\varepsilon_{kj}} \right\} \tag{2}$$

where we have assumed that trade cost is route-specific and multiplicative over all links as in (1) where we assume that ε_{kj} is independently identically Frechet distributed across neighboring nodes $k \in \mathcal{N}(i)$ with a - potentially node-specific - dispersion parameter θ_i.[9] We can exploit the properties of the Frechet distribution to derive a closed-form expression for transportation cost that is recursive in iceberg transport cost along the topology of the network, i.e.

$$\tau_{ij} = \mathrm{E}\left[\min_{k \in \mathcal{N}(i)} \left\{ \frac{t_{ik}\tau_{kj}}{\varepsilon_{kj}} \right\} \right] \propto \left(\sum_{k \in \mathcal{N}(i)} \left(t_{ik}\tau_{kj} \right)^{-\theta_j} \right)^{-\frac{1}{\theta_j}} \tag{4}$$

which in closed form relates transportation costs along the network topology to each other. A couple of characteristics should be highlighted. First, the definition of the transportation cost explicitly relies on the topology of the network, as the choice set of the agent at node i explicitly depends on the set neighboring nodes, $N(i)$, and the elemental cost associated with traversing the connecting edges. Second, we will show that in principle this formulation allows for different dispersion elasticities that can vary along the topology of the network, allowing for a more flexible route - and eventually - sourcing characterization than the isoelastic case. Third, it is straightforward to show that for homogenous dispersion elasticities, $\theta_i = \theta$ this characterization

[9] While we present the model in terms of a sequentially drawn Frechet cost shock, it is worth noting that an alternative and isomorphic way of presenting and deriving the model is by describing a GEV type model where the Frechet shocks are recursively related along the network topology. The generalized extreme value (GEV) family of models (McFadden, 1977) allows for the relaxation of independent error draws and more generalized substitution relationships among alternatives. It does so by introducing a correlation function, $G(\cdot)$ where the choice probability of alternative i is given by,

$$P_i = \frac{Y_i G_i}{G} \tag{3}$$

where Y_i is the choice-specific return and G_i the partial derivative of G with regard to i. The isomorphic description of the model presented here is sometimes called a Network-GEV model as introduced in Daly and Bierlaire (2006) and effectively uses the topological structure of the observed network to provide a nesting structure for the choice model. Specifically, the Network-GEV model is defined by a correlation function $G(\cdot)$ that is recursively defined as follows:

$$G_{ij}^{d} = \begin{cases} t_{ij}^{-\theta_i} \sum_{k \in \mathcal{F}(j)} \left(G_{jk}^{d} \right)^{\theta_i/\theta_k} & \text{if } j \neq d, \\ t_{ij}^{-\theta_i} & \text{if } j = d. \end{cases}$$

Furthermore, using results from Lind and Ramondo (2023) this routing choice can be extended to define a sourcing choice where the correlational structure is defined by the observed topology of the (transportation) network.

is isomorphic to the routing characterization in Allen and Arkolakis (2022)[10], but allows for an analytical convenient implicit characterization of the optimal routing choice. This feature that we will utilize when restating the equilibrium equation in terms of edge-level outcomes and that furthermore will allow us to extend the problem to allow for nested mode choice as well as a rich characterization of congestion at the mode level.

3.3.1 Sourcing, Gravity, and Recursive Equilibrium

We proceed by extending the recursive route choice to allow for a combined route-sourcing choice and then embed the closed-form expression route-sourcing shares into the equilibrium conditions, thus deriving a set of equilibrium equations in terms of edge-level outcomes. To do so, we proceed in three steps. In the first step, we combine the recursive routing choice in Equation (4) with the stochastic sourcing choice in Eaton and Kortum (2002) to derive a closed-form characterization for both route and sourcing choice. In a second step, we then proceed to formulate the equilibrium conditions using market access terms. In the final step, we then embed the recursive route and sourcing choice into the equilibrium conditions.

Sourcing and Routing We begin by combining the recursive routing choice from the previous subsection to allow for a combined routing and sourcing choice. We assume that under perfect competition agents (recursively) source their products by choosing the lowest-cost route-source combination, i.e.

$$p_i(\nu) = \min_{(k,j)\in\mathcal{N}(i)\times N} \frac{t_{ik}\tau_{kj}w_j}{\varepsilon_{kj}(\nu)} \tag{5}$$

where, following Eaton and Kortum (2002), we assume that $\varepsilon_{kj}(\nu)$ is iid Fréchet distributed across neighboring nodes $k \in \mathcal{N}(i)$ and sourcing partners j with scale parameter $1/A_i$, where A_i captures origin-specific efficiency (the same A_i as earlier) and shape parameter θ regulates the inverse of shock dispersion.[11] Given the preference shocks, the probability that j purchases a

[10] As shown in Detail in Online Appendix B.4. This isomorphism between one-shot decisions over the universe of paths and sequential decision-making relying on dynamic programming has been previously noted, most notably by Antràs and Gortari (2020) who explore a one-shot sequential sourcing decision in their main text and introduce a dynamic programming formulation in their Appendix A.1.3. In our work we go beyond this formulation in two distinct ways. First, by following the transportation literature and explicitly formulating decision-making on a graph. Second, by embedding the solution into the equilibrium conditions to derive a computationally convenient representation of the spatial equilibrium in terms of outcomes at edges.

[11] Notice that the properties of the Frechet distribution imply that the inclusive value takes on the following

good from i using route r is given by,[12]

$$\begin{aligned}\pi_{ij,k} &= \frac{(w_i/A_i)^{-\theta_j}(t_{jk}\tau_{ki})^{-\theta_j}}{\sum_{i\in\mathcal{N}}(w_i/A_i)^{-\theta_j}\sum_{k'\in\mathcal{F}(i)}(t_{jk}\tau_{k'})^{-\theta_j}} \\ &= \frac{(t_{jk}\tau_{ki})^{-\theta_j}}{\sum_{k'\in\mathcal{F}(i)}(t_{ik'}\tau_{ki})^{-\theta_j}}\frac{\tau_{ij}^{-\theta_j}p_i^{-\theta_j}}{\sum_{i\in\mathcal{N}}\tau_{ij}^{-\theta_j}p_i^{-\theta_j}}\end{aligned} \tag{6}$$

where in the first line, we have the combined probability of sourcing from origin i and using neighboring link k to do so. In the second line, we have decomposed the probability into two terms. The first term represents an implicit route choice probability, characterizing the likelihood of choosing a neighboring node k amongst all neighboring nodes when sourcing from destination j. The second term represents the sourcing probability and is identical to the sourcing probability in Eaton and Kortum (2002).

Market Access, Gravity, and Equilibrium Before defining and deriving the equilibrium conditions, we reformulate the expression for bilateral trade flows (8) using market access terms (Anderson and van Wincoop, 2003; Redding and Venables, 2004). We follow the standard procedure and impose firstly, that good markets clear, i.e. total income in a location, Y_i, is equal to its total sales, and secondly, that trade is balanced, i.e. total expenditure, E_i, is equal to total expenditures in each location:

$$Y_i = \sum_{j=1}^{N} X_{ij}, \qquad E_i = \sum_{j=1}^{N} X_{ji} \tag{7}$$

This allows us to rewrite the gravity equation using market access terms, i.e.

$$X_{ij} = \tau_{ij}^{-\theta_j} \times \frac{\gamma_i}{\Pi_i^{-\theta_j}} \times \frac{\delta_j}{P_j^{-\theta_j}} \tag{8}$$

where we have used the expression for route-sourcing shares in equation (6) in combina-

form, i.e.

$$p_i = \mathbb{E}\left[\min_{(k,j)\in\mathcal{N}(i)\times N}\frac{t_{ik}\tau_{kj}w_j}{\varepsilon_{kj}(\nu)}\right] = \left(\sum_{(k,j)\in\mathcal{N}(j)\times N}(t_{ik}\tau_{kj}w_j)^{-\theta_i}\right)^{-\frac{1}{\theta_i}} = \left(\sum_{k\in\mathcal{N}(j)}t_{ik}^{-\theta_i}\sum_{j\in N}(\tau_{kj}w_j)^{-\theta_i}\right)^{-\frac{1}{\theta_i}}$$

where in the last line we have re-arranged the sums to highlight that under homogenous dispersion parameter ($\theta_i = \theta$) the formula takes on a recursive form ($p_i^{-\theta} = \sum_{k\in\mathcal{N}(j)} t_{ik}^{-\theta} p_k^{-\theta}$ since $p_k^{-\theta} = \sum_{j\in N}(\tau_{kj}w_j)^{-\theta}$) and relates expected sourcing prices along the network topology.

[12] See detailed derivations in Appendix B.1.

tion with the market clearing conditions to derive a gravity equation with varying substitution parameters.[13] Furthermore, the producer and consumer price index are given respectively by,

$$\Pi_i \equiv \left(\sum_{j=1}^{N} \tau_{ij}^{-\theta_i} E_j P_j^{\theta_i} \right)^{-\frac{1}{\theta_i}} = A_i L_i Y_i^{-\frac{\theta_i+1}{\theta_i}}, \qquad P_j = \left(\sum_{i=1}^{N} \tau_{ij}^{-\theta_j} Y_i \Pi_i^{\theta_j} \right)^{-\frac{1}{\theta_j}} \tag{9}$$

As in Allen and Arkolakis (2014), we impose welfare equalization, i.e. $W_j = \frac{w_j}{P_j} u_j$ (Allen and Arkolakis, 2014) and assume localized productivity (A_i) and amenity spillovers (u_i) that depend on the density of workers in a locality, i.e.

$$A_i = \bar{A}_i L_i^{\alpha}, \qquad u_i = \bar{u}_i L_i^{\beta} \tag{10}$$

where $\bar{A}_i$ is exogenous component of productivity at location i and α determines the extent to which productivity is affected by the local population L_i (productivity spillovers), $\bar{u}_i$ is the exogenous utility derived from living in location i and β governs the extent to which amenities are affected by the location population (amenity spillovers). To obtain the equilibrium conditions we impose balanced trade, the market clearing conditions (7), and our expression for trade flows (8), together with our recursive sourcing-route probability (6). We obtain the following equilibrium condition:[14]

$$\Pi_i^{-\theta_i} = t_{ii}^{-\theta_i} \frac{\delta_i}{P_i^{-\theta}} + \sum_{k \in \mathcal{N}(i)} t_{ik}^{-\theta_i} \Pi_k^{-\theta_i} \tag{11}$$

$$P_i^{-\theta_i} = t_{ii}^{-\theta} \frac{\gamma_i}{\Pi_i^{-\theta_i}} + \sum_{k \in \mathcal{N}(i)} t_{ki}^{-\theta_i} P_k^{-\theta_i} \tag{12}$$

where the equilibrium conditions solve for the endogenous market access terms, $\{\Pi_i, P_i\}$. Assuming welfare equalization, i.e. $W_j = \frac{w_j}{P_j} u_j$ and combining the parameterization of spillovers, (10), with the definition of price indices (9), we can relate equilibrium price indices to the spatial distribution of income and labor as well as a global scalar that determines aggregate welfare. Specifically, we have,

$$P_i = \frac{1}{\bar{W}} \bar{u}_i L_i^{\beta-1} Y_i \qquad \Pi_i = \bar{A}_i L_i^{1+\alpha} Y_i^{-\frac{\theta_i+1}{\theta_i}} \tag{13}$$

where the price indices jointly determine the spatial allocation of labor, income and the aggregate level of welfare, $\bar{W}$. We can furthermore rewrite the equations in terms of rescaled variables, i.e. $\{y_i, l_i\}$, where we define shares of world income in location i, $y_i \equiv \frac{Y_i}{Y^W}$, and

[13] Detailed derivations in Online Appendix B.2.

[14] See Online Appendix D.1 for detailed derivations.

shares of total labor in location i, $l_i \equiv \frac{L_i}{L^W}$. The equilibrium system is similar to the one in Allen and Arkolakis (2022), but explicitly embeds the network structure of the economy. Specifically, given the fundamentals $\left\{\bar{A}_i, \bar{u}_i, \tau_{ij}\right\}$, the system of $2N$ equations can be solved for the $2N$ endogenous equilibrium values. The equilibrium system determines the endogenous variables via the interaction of price indices along the network topology. Transportation cost is endogenous and is implicitly being solved as part of the equilibrium system. The result recasts the equilibrium problem in terms of edge-level outcomes. This allows us to incorporate richer edge-level decision making and substitution margins, which we will do in the following subsection by incorporating a nested modal choice into the framework and into the equilibrium conditions. In principle, the fact that the equilibrium system allows for arbitrary substitution elasticities along the topology of the network (θ_i) is highly desirable and could allow for a more flexible framework with a particular focus on bottleneck analysis. We leave those investigations for future work and instead focus on the modal choice in what follows and assume a homogeneous route choice elasticity ($\theta_i = \theta$) below. Finally, in contrast to Allen and Arkolakis (2022) no matrix inversion is necessary to obtain this equilibrium system.

3.4 Multimodal Routing and Aggregate Transport Cost

In a final step, we introduce multimodal routing into our framework. As presented in the previous section, we consider a consumer that resides in location j and makes a route-sourcing choice by choosing sequentially edges along the graph. To furthermore accommodate multimodal routing choices, we incorporate a nested modal choice. In that setting, conditional on the neighboring node chosen, the consumer makes a modal choice by choosing the cost minimizing mode out of all modes along the edge, i. to traverse the edge (subject to an extreme value distributed cost shock). To fix ideas, consider a consumer in location j having chosen to route towards the neighboring node k. The consumer then compares all the different modes that are available along this edge, i.e. $m \in \mathcal{M}_{jk}$, where $\mathcal{M}_{jk}$ is the set of modes available between nodes j and k, and where the edge mode specific transport costs given by,

$$t_{jk,m} = \begin{cases} \tilde{t}_{jk,1} & \text{if} \quad m = 1 \\ s_{jj,m}\tau_{jk,m}s_{kk,m} & \text{if} \quad m \neq 1 \end{cases} \tag{14}$$

where for the primary mode no switching cost is required, but for any non-primary mode ($m \neq 1$) a switching cost is imposed, while $\tau_{jk,m}$ refers to the iceberg transport cost of traversing

Figure 6. Multimodal routing a multi-layered graph

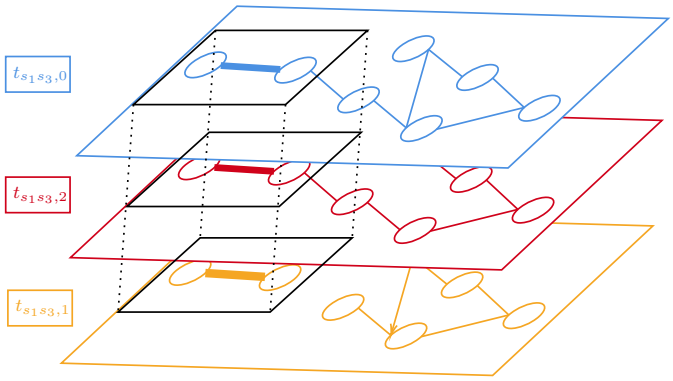

Notes: The figure illustrates the multimodal routing problem that is associated with the directed graph in Figure 5. Nodes are represented as circles and linked via edges. Each link is associated with an (iceberg) transport cost. Three distinct mode-specific graphs are visible. The overall figure represents the multi-layered graph that corresponds to the aggregate (collapsed) representation in Figure 5.

the edge between node j and k along mode m. Notice that this specification is general and allows for geographies where non-primary modes might connect an entirely different set of nodes than primary nodes. The consumer then faces a cost minimizing choice subject to an extreme-value distributed cost shock with a dispersion parameter η, i.e.

$$t_{ik} = \mathbb{E}\left[\min_{m \in \mathcal{M}(i,k)} \left\{ \frac{t_{ik,m}}{\varepsilon_{ik,m}} \right\}\right] = \left(\sum_{m \in \mathcal{M}(i,k)} t_{ik,m}^{-\eta} \right)^{-\frac{1}{\eta}} \tag{15}$$

where we can write the expected aggregate transport cost as a sum of the endogenous mode-specific transport cost, $t_{ik,m}$, that are available between neighboring nodes i and k, i.e. $\mathcal{M}(i,k)$. Notice that the set of endogenous nodes is not always complete and depends on the existing infrastructure. This is akin to making a modal choice on a multi-layered graph, where the individual layers represent the mode-specific transportation network and the agent chooses on for each edge on which layer of the graph to route as illustrated in Figure 6.

This setup then extends the model in Allen and Arkolakis (2022) to allow for a tractable description of mode choice. Mode choice in our setting arises as a routing choice along a multi-layered graph, where the agent makes a cost-minimizing modal choice at the link-level giving rise to an endogenous characterization of the aggregate transport cost, which the agent then in turn takes into account to make a cost-minimizing route choice.[15]

[15] An alternative method to introduce mode choice is to simply allow for mode-specific subnetworks. This

While the introduction of multimodal transportation on a segmented transportation system introduced added conceptual complexity to the problem, the equilibrium system remains *as tractable* as the system presented in Allen and Arkolakis (2022). The only added complexity is that in order to solve for the equilibrium, the traffic equilibrium at the modal level needs to be solved. Below we will discuss how this can be achieved for the system of equations that determines the counterfactual equilibrium.

3.5 Traffic flows and congestion

We proceed by deriving the implied traffic flows. We will proceed in three steps. In a first step we will derive the traffic flows on the aggregate network. In a second step, we will then derive the traffic on the modal networks before then proceeding towards characterizing traffic at terminals. The purpose of deriving these objects is to introduce traffic and congestion in the equilibrium conditions (11) and (12). Specifically, we will be interested in introducing switching costs that depend on the throughput at any given terminal, thus creating bottlenecks in the multimodal transportation system.

Traffic on the Aggregate Network. We begin by characterizing the traffic on the aggregate network across any more.[16] We utilize our recursive framework to characterize the number of times a link (k,l) is used in trade between (i,j), π_{ij}^{kl}, which - analogously to AA2022 - we refer to as link intensity. To obtain the link intensity we construct the probability that a route i to j is used and the likelihood that a particular link (k,l) is chosen, i.e.

$$\pi_{ij}^{kl} = \left(\frac{\tau_{ij}}{\tau_{ik} t_{kl} \tau_{ij}}\right)^{\theta} \tag{16}$$

In the appendix we show how the formula follows directly from our recursive routing choice. We can then use these derivations to characterize traffic on the primary network,

$$\Xi_{kl} = \sum_{i \in \mathcal{N}} \sum_{j \in \mathcal{N}} \pi_{ij,kl} E_j = \sum_{i \in \mathcal{N}} \sum_{j \in \mathcal{N}} \pi_{ij}^{kl} X_{ij} \tag{17}$$

naturally gives rise to a setting where mode choice is then *implied* by route choice. A previous version of this paper presents such a model. The drawback of such a modeling strategy is that tractability requires that the modal substitution elasticity needs to be identical to the route choice elasticity. As we will argue below, this is contradicted by our estimates.

[16] Detailed derivations for traffic on the primary and non-primary network as well as traffic at terminal stations is given in Appendix B.5.

Combining the market access and the link intensity expression (16) allows us to derive the expression for equilibrium traffic,

$$\Xi_{kl} = t_{kl}^{-\theta} \times P_k^{-\theta} \times \Pi_l^{-\theta} \tag{18}$$

Equation (18) is a gravity equation for traffic on the primary network. The expression connects traffic flows to inward, $P_k^{-\theta}$ and outward market access measures, $\Pi_l^{-\theta}$. Both market access measures depend on the transportation cost across the multimodal transport network.

Traffic on the Modal Networks. In the next step, we now turn towards characterizing the probability of sourcing from location j to location i choosing neighboring node k as the cost-minimizing routing choice and opting for mode m between node i and k. The nested choice implies that this choice probability is given by,

$$\pi_{ijk,m} = \frac{t_{ik,m}^{-\eta}}{t_{ik}^{-\eta}} \frac{\left(t_{ik}\tau_{kj}\right)^{-\theta} p_i^{-\theta}}{\sum_{i\in\mathcal{N}} \tau_{ij}^{-\theta} p_i^{-\theta}}$$

which can be decomposed into the sourcing share, link choice probability conditional on sourcing choice, and the modal share conditional on both sourcing and link choice, i.e.

$$\begin{aligned}\pi_{ij,kl,m} &= \frac{t_{kl,m}^{-\eta}}{t_{kl}^{-\eta}} \frac{\tau_{ik}^{-\theta} t_{kl}^{-\theta} \tau_{lj}^{-\theta}}{\tau_{ij}^{-\theta}} \frac{\tau_{ij}^{-\theta} p_i^{-\theta}}{\sum_{i\in\mathcal{N}} \tau_{ij}^{-\theta} p_i^{-\theta}} \\ &= \pi_{ik}^{m} \times \pi_{ij}^{k} \times \pi_{ij}\end{aligned}$$

Given this choice probability, we can characterize the mode-specific traffic between neighboring nodes k and l, i.e.

$$\begin{aligned}\Xi_{kl,m} &= \sum_{i\in\mathcal{N}} \sum_{j\in\mathcal{N}} \pi_{ijk,m} E_j \iff \\ &= t_{kl,m}^{-\eta} \times t_{kl}^{\eta-\theta} \times P_k^{-\theta} \times \Pi_l^{-\theta}\end{aligned} \tag{19}$$

which gives us an expression for mode-specific traffic in terms of market access measures and the aggregate and mode specific iceberg transport cost along the edge. Note, that the nested formulation implies that mode-specific traffic is the conditional mode specific share of aggregate traffic, i.e. $\Xi_{kl,m} = \pi_{ik}^{m} \times \Xi_{kl}$. Equation (19) is the natural counterpart to equation (18) for the mode-specific traffic. It also reflects a gravity equation and connects traffic flows to market access measures. Crucially, bilateral traffic here depends on the transportation cost of the mode-

specific network and the switching costs incurred when transitioning from the primary to the non-primary network.

Traffic at Terminals. Finally, we turn towards characterizing traffic at terminals where switches between the primary and non-primary modal network occurs. We can derive the traffic in a straightforward manner by summing the modal traffic at any origin terminal k, i.e.

$$\Xi_{kk,m} = \sum_{l \in \mathcal{F}_m(k)} \Xi_{kl,m} = P_k^{-\theta} \times \sum_{l \in \mathcal{F}_m(k)} t_{kl,m}^{-\eta} \times t_{kl}^{\eta-\theta} \times \Pi_l^{-\theta}$$

where $\mathcal{F}_m(k)$ denotes the set of mode-specific successor nodes of k. Combining with the definition of mode-specific transportation cost in Equation (14), we obtain,

$$\Xi_{kk,m} = (s_{kk,m})^{-\theta} \times P_k^{-\theta} \times \sum_{l \in \mathcal{F}_m(k)} \tau_{k'l'}^{-\theta} s_{l'l}^{-\theta} \Pi_l^{-\theta}, \tag{20}$$

Equation (20) differs slightly to the previous traffic equations in that they feature an additional summation term. This summation term is a higher order market access term that reflects the fact that in- and outgoing traffic at a terminal depends on the sum of traffic that is generated by nodes that can be reached via that terminal along the non-primary network. This higher order market access term is also a natural measure of the centrality of the terminals in terms of connecting primary and non-primary network and thus - in a sense - their capacity to become a bottleneck to the overall transportation network.

Taking stock, Equation (18) characterizes aggregate traffic along the multi-layered network, Equation (19) characterizes traffic on the modal networks and Equation (20) characterizes traffic at terminals.

Congestion. In a final step, we incorporate congestion on the primary network and at terminal stations.[17] The motivation and parameterization for congestion on the primary network follows Allen and Arkolakis (2022). We assume that the direct cost of traveling over a particular link on the primary network depends on the amount of traffic that travels through that link. Specifically,

[17] While in principle it is possible to extend the framework to allow for congestion on the non-primary network our choice to introduce congestion at terminals mirrors the observation that except for roads all alternative modes do not experience congestion at the route level, but typically the key bottleneck occurs at the intermodal transfer with a prime example being port congestion. Additionally, incorporating congestion at the route-level would come at the cost of added complexity and decreased traceability.

we assume,

$$t_{kl} = \bar{t}_{kl} \left(\Xi^1_{kl}\right)^{\lambda_1}, \tag{21}$$

where λ_1 determines the strength of congestion on the primary network, and $\overline{\mathbf{T}} \equiv [\bar{t}_{kl}]$ is the infrastructure network for the primary network and Ξ^1_{kl} represents the traffic on the primary network. Intuitively, as long as $\lambda_1 > 0$, this expression increase transport cost as traffic on a link increases. While somewhat different to the more commonly used Bureau of Public Roads (BPR) function (Boyles, Lownes and Unnikrishnan, 2021), it is both analytically convenient and can be micro-founded in a simple model where transportation costs are log-linear in travel time and speed is a log-linear function of traffic congestion as shown in Allen and Arkolakis (2022). This expression allows us to derive equilibrium traffic flows in terms of the fundamental transport cost of each edge. First note, that transport cost is now a function of the market access terms, i.e.

$$t_{kl,1} = \bar{t}_{kl,1}^{\frac{1}{1+\eta\lambda_1}} \times t_{kl}^{\frac{\lambda_1(\eta-\theta)}{1+\eta\lambda_1}} \times P_k^{\frac{-\theta\lambda_1}{1+\eta\lambda_1}} \times \Pi_l^{\frac{-\theta\lambda_1}{1+\eta\lambda_1}}$$

Combining this with the expression for equilibrium traffic flows on the primary network (18), we obtain,

$$\Xi_{kl,0} = \bar{t}_{kl}^{-\frac{\theta}{1+\theta\lambda_1}} \times t_{kl}^{\frac{-\theta\lambda_1(\eta-\theta)}{1+\eta\lambda_1}} \times P_k^{-\frac{\theta}{1+\theta\lambda_1}} \times \Pi_l^{-\frac{\theta}{1+\theta\lambda_1}} \tag{22}$$

where now overall traffic depends on the inward and outward market access terms, the fundamental transport capacity of each link, as well as the strength of the congestion externality, λ_1. Intuitively, as better market access improves traffic flow on each link this also increases congestion. Therefore the impact taking congestion into account is somewhat muted.

Secondly, we introduce congestion at terminals. We assume that the direct cost of transiting through a terminal depends on the overall traffic at the terminal, i.e.

$$s_{kk,m} = \bar{s}_{kk,m} \left[\Xi_{kk,m}\right]^{\lambda_m} \tag{23}$$

where λ_m determines the strength of congestion at terminals, and $\overline{\mathbf{S}} \equiv [\bar{s}_{kk,m}]$ is the switching matrix that connects primary and non-primary modes and $\Xi_{kk,m}$ represents the traffic at the terminal station. Combining with the expression for terminal traffic (20), and expressing the overall transport cost for non-primary modes (14), we obtain,

$$\begin{aligned} \tilde{t}_{kl,m} &= \bar{s}_{kk,m}\tau_{kl,m}\bar{s}_{Ul,m} \left[\Xi_{kk,m}\right]^{\lambda_m} \left[\Xi_{ll,m}\right]^{\lambda_m} \\ &= \bar{s}_{kk,m} \times \tau_{kl,m} \times \bar{s}_{ll,m} \times P_k^{-\theta\lambda_m} \times \Pi_l^{-\theta\lambda_m} \times P_{k,m}^{-\theta\lambda_m} \times \Pi_{l,m}^{-\theta\lambda_m} \end{aligned} \tag{24}$$

where $P_{l,m} \equiv \sum_{k \in \mathcal{B}(l)} t_{kl,m}^{-\eta} \times t_{kl}^{\eta-\theta} \times P_k^{-\theta}$ and $\Pi_{k,m} \equiv \sum_{l \in \mathcal{F}(k)} t_{kl,m}^{-\eta} \times t_{kl}^{\eta-\theta} \times \Pi_l^{-\theta}$ define mode-specific market access measures. Intuitively, as long as $\lambda_m > 0$, this expression increases transportation cost as traffic at the terminal location increases. Combining (24) with our expression for modal traffic (19) we obtain the modal traffic for the non-primary modes taking into account endogenous congestion at terminals, i.e.

$$\Xi_{kl,m} = \bar{s}_{kk,m}^{-\eta} \times \tau_{kl,m}^{-\eta} \times \bar{s}_{ll,m}^{-\eta} \times P_{k,m}^{\eta\theta\lambda_m} \times \Pi_{l,m}^{\eta\theta\lambda_m} \times t_{kl}^{\eta-\theta} \times P_k^{-\theta(1-\eta\lambda_m)} \times \Pi_l^{-\theta(1-\eta\lambda_m)} \tag{25}$$

Taking stock, Equation (22) develops the traffic that arises once congestion on the primary network is taken into account, while Equation (25) characterizes traffic on the non-primary network once congestion costs at terminals are taken into account. Traffic is generally increasing in market access which is properly to be understood as market access across the primary and secondary transportation network. Terminals can become important bottlenecks and congestion at terminals can lower the attractiveness of multimodal paths and thus traffic on the non-primary network, as is apparent by Equation (25).

3.6 Counterfactuals

We now turn towards deriving a system of equations that determines the counterfactual equilibrium for arbitrary dis-aggregated mode-specific infrastructure changes. This allows us to evaluate the welfare impact of infrastructure investments along either the primary, non-primary network or terminal locations in a setting where agents make sophisticated routing and mode choices while also allowing for a rich characterization of congestion across the multimodal transport system. To do so we extend the equilibrium system in Equations (11) and (12) to allow for mode choice as in Section 3.4 and for congestion as in Section 3.5. We then follow Dekle, Eaton and Kortum (2008) and employ 'Hat Algebra' to express the equilibrium in terms of changes of the endogenous variables. In the following we denote with hats changes in variables, $\hat{\gamma}_i \equiv \frac{\gamma_i'}{\gamma_i}$. The structure of the model allows for a convenient separation of the edge-specific transportation equilibrium *given* market access terms, and the determination of the aggregate equilibrium. We will split the presentation of the counterfactual equilibrium into two different parts, first describing the transportation equilibrium and then introducing the aggregate equilibrium.[18] The proposition below formulates the transportation equilibrium.

[18] Detailed derivations for both are provided in Online Appendix E.1

Proposition 1 (Counterfactual Equilibrium (a): Transportation equilibrium) *Consider an economy in equilibrium with a primary transport network,* $\overline{\mathbf{T}} \equiv [\bar{t}_{kl,0}]$*, and a terminal transport network connecting primary and non-primary network,* $\overline{\mathbf{S}} \equiv \left[\bar{S}_{kk'}\right]$*, as well as the non-primary transport network* $\overline{\mathbf{T}} \equiv [\bar{t}_{kl,m}]$*. Consider any change either in the underlying infrastructure network denoted by* $\hat{\bar{t}}_{kl,m}$*, or any change in the intermodal switching cost,* $\hat{\bar{s}}_{kk,m}$*. Furthermore, consider a candidate solution for the aggregate counterfactual equilibrium (to be defined below) given by* $\left\{\hat{P}_i, \hat{\Pi}_i, \hat{\gamma}, \hat{\delta}\right\}$*, then equilibrium change in endogenous transportation costs* $\left(\hat{t}_{ik}^{-\theta}, \hat{t}_{ik,m}^{-\theta}\right)$ *is the solution to the edge-level transportation equilibrium and given by:*

$$\hat{t}_{ik}^{-\theta} = \left(\sum_{m \in \mathcal{M}(i,k)} \frac{\Xi_{ik,m}}{\Xi_{ik}} \hat{t}_{ik,m}^{-\eta} \right)^{\frac{\theta}{\eta}} \tag{26}$$

and changes in the endogenous transport cost on the primary mode are given by,

$$\hat{t}_{kl,0} = \hat{\bar{t}}_{kl,0}^{\frac{1}{1 \cdot \lambda_0}} \times \hat{t}_{kl}^{\frac{\lambda_0 (n - \theta j}{1 \ln \lambda_0}} \times \hat{P}_k^{\frac{-\theta \lambda_0}{1 + \gamma \lambda_0}} \times \hat{\Pi}_l^{\frac{-\theta \lambda_0}{1 \cdot r \lambda_0}} \tag{27}$$

and changes in the endogenous transport cost on any alternative mode are given by,

$$\hat{t}_{kl,m} = \hat{\bar{s}}_{kk,m} \hat{\tau}_{kl,m} \hat{\bar{s}}_{ll,m} \hat{P}_k^{-\theta \lambda_m} \hat{\Pi}_{k,m}^{-\theta \lambda_m} \hat{\Pi}_l^{-\theta \lambda_m} \hat{P}_{l,m}^{-\theta \lambda_m} \tag{28}$$

where the mode specific market access terms are defined as,

$$\hat{P}_{l,m}^{-\theta} \equiv \sum_{k \in B(l)} \frac{\Xi_{kl,m}}{\sum_{k \in \mathcal{B}(l)} \Xi_{kl,m}} \hat{t}_{kl,m}^{-\eta} \times \hat{t}_{kl}^{\eta - \theta} \times \hat{P}_k^{-\theta} \tag{29}$$

$$\hat{\Pi}_{k,m}^{-\theta} \equiv \sum_{l \in \mathcal{F}(k)} \frac{\Xi_{kl,m}}{\sum_{l \in \mathcal{F}(k)} \Xi_{kl,m}} \times \hat{t}_{kl,m}^{-\eta} \times \hat{t}_{kl}^{\eta - \theta} \times \hat{\Pi}_l^{-\theta} \tag{30}$$

Proposition 1 thus allows us to calculate the transportation equilibrium that is consistent with a spatial distribution of price indices. This notion of equilibrium at the edge level therefore serves as a nested subroutine in the determination of the overall aggregate spatial equilibrium. A computational benefit arises because the problem is entirely disentangled from the determination of the aggregate spatial equilibrium. In what follows we show how to construct the aggregate counterfactual spatial equilibrium employing Proposition 1 as a nested subroutine:

Proposition 2 (Counterfactual Equilibrium (b): Aggregate Equilibrium) *Consider an economy in equilibrium with a primary transport network,* $\overline{\mathbf{T}} \equiv [\bar{t}_{kl,0}]$*, and a terminal transport*

network connecting primary and non-primary network, $\overline{\mathbf{S}} \equiv \left[\bar{S}_{kk'}\right]$*, as well as the non-primary transport network* $\overline{\mathbf{T}} \equiv [\bar{t}_{kl,m}]$*. Consider any change either in the underlying infrastructure network denoted by* $\hat{\bar{t}}_{kl}$*, or any change in the switching cost,* $\hat{\bar{s}}_{kk'}$*. Given observed traffic flows* $(\Xi_{ik}, \Xi_{ik,m})$*, economic activity in the geography* (Y_i, E_j)*, and parameters* $\{\alpha, \beta, \{\theta_i\}, \lambda_1, \lambda_2\}$*, the equilibrium change in economic outcomes* $\left(\hat{y}_i, \hat{l}_i, \hat{\chi}\right)$ *is the solution of the following system of equations:*

$$\hat{\Pi}_i^{-\theta} = \left(\frac{\delta_i}{\delta_i + \sum_{k\in\mathcal{F}(i)} \Xi_{ik}}\right) \frac{\hat{\delta}_i}{\hat{P}_i^{-\theta}} + \sum_{k\in\mathcal{F}(i)} \left(\frac{\Xi_{ik}}{\delta_i + \sum_{k\in\mathcal{F}(i)} \Xi_{ik}}\right) \hat{t}_{ik}^{-\theta} \hat{\Pi}_k^{-\theta} \tag{31}$$

$$\hat{P}_i^{-\theta} = \left(\frac{\gamma_i}{\gamma_i + \sum_{k\in\mathcal{F}(i)} \Xi_{ki}}\right) \frac{\hat{\gamma}_i}{\hat{\Pi}_i^{-\theta}} + \sum_{k\in\mathcal{F}(i)} \left(\frac{\Xi_{ki}}{\gamma_i + \sum_{k\in\mathcal{F}(i)} \Xi_{ki}}\right) \hat{t}_{ki}^{-\theta} \hat{P}_k^{-\theta} \tag{32}$$

where $\hat{t}_{ki}^{-\theta} = F\left(\{P_i, \Pi_i\}\right)$ *is the endogenous transportation cost that given a candidate solution for the price indices is solved by the transportation equilibrium in Proposition 1, while changes in the market access terms pin down changes in income and labor densities, i.e.*

$$\begin{aligned} \hat{P}_i &= \hat{y}_i \hat{l}_i^{\beta-1} \hat{W}^{-1} \\ \hat{\Pi}_i &= \hat{l}_i^{\alpha+1} \hat{y}_i^{-\frac{\theta+1}{\theta}} \end{aligned} \tag{33}$$

where we define shares of world income in location i*,* $y_i \equiv \frac{Y_i}{Y^W}$*, and shares of total labor in location* i*,* $l_i \equiv \frac{L_i}{L^W}$

Proposition (2) indicates that given observed traffic flows on the primary network, bilateral flows on the non-primary network[19], $(\Xi_{ik}, \Xi_{ik,m})$ as well as knowledge of the model parameters, $\{\alpha, \beta, \{\theta_i\}, \lambda_1, \lambda_2\}$, we can employ the model to evaluate infrastructure improvements along the primary network or at terminal stations, thus improving the connectedness of the primary and non-primary transport network. The proposition provides a straightforward extension of equation (28) and (29) in AA2022. The only difference is the presence of a nested subroutine, which given a candidate solution for spatial equilibrium, $\{P_i, \Pi_i\}$, solves the transportation equilibrium at the edge-level, i.e. Equations (26), (27) and (28). This implicitly determines the modal choice taking into account endogenous congestion and generates an endogenous aggregate transportation cost. This adjustments adds a novel channel towards evaluation infrastructure improvements. In this

[19]Notice the slight abuse of notation here. While $\Xi_{ij,1}$ refers to the edge-specific traffic along the primary network, $\Xi_{ij,m}$ instead refers to modal flows between i and j along the non-primary networks and is therefore not necessarily edge-specific. However, $\Xi_{ij,m}$ summarizes modal traffic in the sense that it refers to any flows between i and j no matter their origin or destination on the primary network. This is convenient - as we will argue below - since this is the data moment that is directly observed in the rail traffic data.

setting, the impact of improving transportation infrastructure has the same direct and general equilibrium effect as in AA2022 where route choice is impacted, congestion can be alleviated, input and output markets can adjust and where all this adds up to welfare gains. In our setting, additionally, we also feature a direct interplay between the primary and non-primary network. Mode-specific infrastructure investments can lead to modal diversion and thus alleviate congestion on the alternative transport network. The extent to which this might occur depends on the cross-sectional variation in the access to the non-primary transportation system, which is reflected by variations in the weights on the final term across space.

As a corollary we can also characterize the change in the equilibrium traffic flows along the primary and secondary transport system.

Corollary 1 *Given the equilibrium changes in market access terms* $\left(\hat{P}_i, \hat{\Pi}_i, \right)$*, as well as the equilibrium changes of mode and aggregate transport costs,*$\left(\hat{t}_{ik}, \hat{t}_{ik,m}, \right)$*, the resulting change in the traffic flows can be computed using the following formulae:*

$$\hat{\Xi}_{ik} = \hat{t}_{ik}^{-\theta} \times \hat{P}_i^{-\theta} \times \hat{\Pi}_k^{-\theta} \tag{34}$$

$$\hat{\Xi}_{ik,m} = t_{ik,m}^{-\eta} \times \hat{t}_{ik}^{\theta-\eta} \times \hat{P}_i^{-\theta} \times \hat{\Pi}_k^{-\theta} \tag{35}$$

Corollary 1 allows us to account for the changes in the observed traffic flows. This can be a convenient tool to analyse the implied traffic and environmental impact of infrastructure investments.

4 From Theory to Data

In order to quantify our model, we require two key elasticities. As in Proposition 1 and 2, the counterfactual equilibrium crucially depends on the model parameters, in particular the strength of the congestion forces on the primary network and at terminals (λ_1, λ_2).[20] While our calibration broadly follows Allen and Arkolakis (2022) who provide an estimate for the strength of congestion on the primary network, we have introduced a new parameter that pins down congestion at intermodal terminals, λ_2. In this section we present how the relationship between dwell times at intermodal facilities and throughput can be used to estimate the strength of congestion and the magnitude of this parameter. Next, to motivate the key mode choice channels in our model, we

[20] In what follows we assume one common congestion parameter for intermodal terminals to any non-primary mode (λ_2). Below we will estimate the strength of congestion at intermodal terminals at ports, but we will also argue that similar estimates on railroad terminals do not contradict our port estimates.

require an elasticity of substitution between transport modes. In order to estimate this elasticity, we revisit and build upon the seminal work by Duranton and Turner (2011) within the context of multimodal transportation.

4.1 Estimation of Intermodal Terminal Congestion

In this subsection, we measure port congestion by estimating the elasticity of ship dwell time with respect to port traffic. We estimate the following regression (Column (3), Table 1):

$$\ln \text{Ship Dwell Time}_{spdmy} = \beta_1 \ln \text{Port Traffic}_{pdmy} + \delta_{dmy} + \alpha_{spy} + \epsilon_{spdmy} \tag{36}$$

where Ship Dwell Time$_{spdmy}$ is the number of hours ship s spent at port p on day of the week d month m and year y, Port Traffic$_{pdmy}$ is the 28-day moving average amount of port traffic at port p ending on day d month m and year y, δ_{dmy} is day-month-year fixed effects, and α_{spy} is ship-port-year fixed effects. The key parameter of interest, β_1, captures the elasticity of ship dwell times with respect to port traffic. Standard errors are two-way clustered at the ship and port level.

The ship-port-year fixed effects control for fixed and time-varying characteristics at the ship-port level. Fixed ship-port characteristics include time-invariant comparative advantage differences for different ports that result in larger ships being received at these ports which mechanically take longer time to unload, for example ports with deeper natural harbors. It also includes fixed ship characteristics like ship sizes and fixed port characteristics like its geography. Time-varying ship-port characteristics account for potential technology changes over time that ports can undertake that might affect ship dwell times, for example technology upgrades at ports over time to accommodate larger ships. Additionally, the day-month-year fixed effects control for aggregate events that impacts all ships.

We find that a one percent increase in port traffic is correlated with a statistically significant increase in ship dwell times by 0.1 percent (Column (3), Table 1). This elasticity is robust to specifications with ship fixed effects and port-year fixed effects separately (Column (1), Table 1) as well as with ship-port fixed effects and port-year fixed effects separately (Column (2), Table 1).

In order to account for the extraordinary pandemic period, we include an indicator for the pandemic period (post March 2020) in order to estimate separate elasticities for port congestion. We find that our pre-March 2020 estimate is within one standard error of the baseline results

Table. 1. OLS Elasticity of Port Traffic with respect to Ship Dwell Times

	(1)	(2)	(3)	(4)	(5)
Port Traffic	0.0955**	0.100**	0.103**		0.241***
	(0.0374)	(0.0399)	(0.0394)		(0.0534)
Port Traffic × Before Mar 2020				0.0955**	
				(0.0408)	
Port Traffic × After Mar 2020				0.122***	
				(0.0389)	
Day-Month-Year FE	✓	✓	✓	✓	✓
Ship-Port-Year FE			✓	✓	✓
Port-Year FE	✓	✓			
Ship-Port FE		✓			
Ship FE	✓				
West Coast Ports					✓
Observations	86094	86094	86094	86094	21205
R^2	0.70	0.78	0.83	0.83	0.87
F	6.53	6.29	6.85	5.60	20.35

***Notes*:** Robust standard errors in parentheses are clustered by port. All variables are in logs. Port traffic is the 28-day moving average of total daily net tonnage at the port. Weighted by ship net tonnage.

(Column (4), Table 1). As expected, our estimate post-March 2020 is slightly higher in magnitude compared to the pre-period elasticity. Additionally, the West Coast ports have a history of port strikes and slowdowns. They also have naturally deeper harbors which allow for larger ships, and service large volumes of US-Asia trade—LA and Long Beach are the top two US ports. These factors can result in longer dwell times for ships that are servicing these busy ports. We show that the elasticity for West Coast ports is much larger in magnitude by limiting our samples to just West Coast ports (Column (5), Table 1).

The baseline results use a 28-day moving average of total daily net tonnage at the port. Using a shorter period of the moving average calculation, we find that the elasticity of port traffic with respect to ship dwell times decreases in magnitude. With a shorter period of moving average calculation, the ship dwell times respond less to changes to the average tonnage at the port. Column (1) reproduces our baseline results using the 28-day moving average from Table 1, Column (2) presents the 21-day moving average, Column (3) presents the 14-day moving average, and Column (4) presents the 7-day moving average.

In order to establish the causal impact of port traffic on ship dwell times, we require demand shifter for port traffic that is uncorrelated with unobserved ship dwell times determinants ϵ_{spdmy}. Our IV strategy uses aggregate compositional changes for imports at the region- and product-

Table. 2. OLS Elasticity by Time Aggregations

	(1)	(2)	(3)	(4)
Port Traffic	0.103**	0.0848***	0.0527**	0.0266**
	(0.0394)	(0.0297)	(0.0203)	(0.0113)
Day-Month-Year FE	✓	✓	✓	✓
Ship-Port-Year FE	✓	✓	✓	✓
Moving Average (Days)	28	21	14	7
Observations	86094	86094	86092	86058
R^2	0.83	0.83	0.83	0.83
F	6.85	8.17	6.74	5.59

***Notes*:** Robust standard errors in parentheses are clustered by port. All variables are in logs. Column (1) estimates the elasticity using the 28-day moving average of total daily net tonnage at the port and is replicated from the baseline results in Column (3) Table 1. Column (2) presents the 21-day moving average, Column (3) presents the 14-day moving average, and Column (4) presents the 7-day moving average. Weighted by ship net tonnage.

level into the top 30 US ports to predict demand for traffic at each port:

$$\text{Port Trade Exposure }_{pmy} \equiv \sum_{O} \sum_{N} X_{on\backslash p,my} \times \omega_{onp,2003}$$

where the lagged weighted sum of top 30 US ports imports from origin o and product n excluding port p at month m and year y, and the weights are region- and product-level shares are lagged by at least 13 years from the start of the available sample period (2003). The weights sum to 1 across products and origins for each port-year observation. This import trade data is available from the Census Bureau at the monthly level and by both value (dollars) and weight (kg).

For this IV strategy to be valid, the port trade exposure measure has to be generally uncorrelated with unobserved ship dwell times determinants controlling for fixed characteristics at the ship-port level, time varying characteristics at the port-level, and aggregate time-varying events that impact all ships. Following Borusyak, Hull and Jaravel (2022), our shares sum up to 1 for each port-year observation.

4.2 Modal Complementarity and Diversion

Infrastructure improvements on one transport mode will have both direct and indirect effects within the general equilibrium multimodal framework. We illustrate these effects using the example of an improvement in road infrastructure. Directly, truck transport costs will go down which will increase road traffic use as established in our theory model (Equation (18)). Indirectly,

Table. 3. Congestion Elasticity of Port Traffic with respect to Ship Dwell Times

	(1) OLS	(2) OLS	(3) First-Stage	(4) IV	(5) First-Stage	(6) IV
Port Traffic	0.09**	0.10**		0.26**		0.24**
	(0.04)	(0.04)		(0.12)		(0.11)
Port Trade Exposure by Weight			0.23***		0.23***	
			(0.05)		(0.05)	
Day-Month-Year FE	✓	✓	✓	✓	✓	✓
Port-Year FE	✓	✓	✓	✓	✓	✓
Ship-Port FE		✓			✓	✓
Ship FE	✓		✓	✓		
Observations	90516	90516	90516	90516	90516	90516
First Stage KP-F				18.27		18.19

Standard errors in parentheses

* $p < 0.10$, ** $p < 0.05$, *** $p < 0.01$

***Notes*:** Robust standard errors in parentheses are clustered by port. All variables are in logs. Port traffic is the 28-day moving average of total daily net tonnage at the port. Weighted by ship net tonnage.

Table. 4. Value IV for robustness

	(1) OLS	(2) OLS	(3) First-Stage	(4) IV	(5) First-Stage	(6) IV
Port Traffic	0.09**	0.10**		0.25		0.19
	(0.04)	(0.04)		(0.28)		(0.31)
Port Trade Exposure by Value			0.11***		0.11***	
			(0.04)		(0.04)	
Day-Month-Year FE	✓	✓	✓	✓	✓	✓
Port-Year FE	✓	✓	✓	✓	✓	✓
Ship-Port FE		✓			✓	✓
Ship FE	✓		✓	✓		
Observations	90516	90516	90516	90516	90516	90516
First Stage KP-F				8.53		8.51

Standard errors in parentheses

* $p < 0.10$, ** $p < 0.05$, *** $p < 0.01$

***Notes*:** Robust standard errors in parentheses are two-way clustered by ship and port. All variables are in logs. Port traffic is the 28-day moving average of total daily net tonnage at the port. Weighted by ship net tonnage.

we find two important effects. First, an improvement in road access would generally decrease trade costs in and out of these cities and improve their general market access. This is in line with our general market access measures outlined in Equation (19), where destination-level road infrastructure improvement would impact the inward market access measure P_k and origin-level

improvement would impact the outward market access measure Π_l. Second, however, this road access improvement would also have a modal diversion or substitution effect—rail transport costs are now relatively more expensive and this will decrease overall rail traffic use. The indirect impact of a mode-specific infrastructure improvement on the traffic use of alternate modes is ultimately an empirical question. We estimate these indirect effects by building on the seminal work by Duranton and Turner (2011).

Duranton and Turner (2011) find that building more roads, as measured by lane kilometers of interstate highways, increases the vehicle-kilometers traveled (VKT) in US metropolitan cities. In order to overcome the potential endogeneity between the demand for VKT and changes to the stock of roads at the metropolitan statistical areas (MSAs) level, they utilize three instruments: kilometers of preliminary interstate highway in each MSA as part of the 1947 highway plan (Baum-Snow, 2007; Michaels, 2008), kilometers of 1898 railroads in each MSA, and exploration routes between 1528-1850.[21] In particular, they find that commercial truck traffic plays an important role in this VKT increase. By aggregating our waybill rail data to the MSA level and matching it to their data, we find empirical evidence of modal diversion dominating with respect to infrastructure investments: when road infrastructure improves, the ratio of rail to road traffic use decreases.[22]

We first consider the following OLS specification with fixed effects from Duranton and Turner (2011):

$$\ln Y_{cy} = \alpha \ln \text{Interstate Highway Lanes}_{cy} + \psi C_{cy} + \zeta_c + \iota_y + \varepsilon_{cy} \tag{37}$$

where $\ln Y_{cy}$ is the log traffic use outcomes for MSA c in year y, $\ln \text{Interstate Highway Lanes}_{cy}$ is the log number of interstate highway lanes going through MSA c which proxies for the road infrastructure for that MSA in year y. C_{jt} are city-specific time-varying controls including population, physical geography, census divisions, and socioeconomic characteristics that are taken from Duranton and Turner (2011). ζ_c is a MSA city-level fixed effect, and ι_y is a year fixed effect.

[21] Using the same three instruments, Duranton and Turner (2012) estimates the impact of interstate highways on urban growth between 1983 and 2003 and finds that a 10% increase in a city's stock of interstate highways increases its employment by about 1.5%. With the same instruments, Duranton, Morrow and Turner (2014) estimates the impact of highways on the trade composition of US cities and finds that more highways result in cities specializing in exporting goods with higher weight-to-value ratios.

[22] We have 221 MSAs due to the matching process between MSAs and our rail traffic data which is 7 less compared to Duranton and Turner (2011) (see Section C.1.5 for more information). We first show that we are able to replicate the Duranton and Turner (2011) results in Table 5. Our fixed effects and IV estimates have the same sign and are within one standard deviation of the results from Duranton and Turner (2011) (Columns (6) to (10), Table 9, Duranton and Turner (2011)).

To measure road traffic use, we employ the truck VKT from Duranton and Turner (2011). To construct a rail traffic use variable that is commensurate with truck VKT that is measured in vehicle-kilometers traveled, we calculate rail traffic in railcar-kilometers-traveled for each city. Our more detailed data allows us to calculate the rail VKT by destination—the amount of incoming rail traffic use—and by origin—outgoing rail traffic use. We also observe the amount of weight in these rail cars, and can construct an alternative measure of rail traffic use by weight in weight-kilometers-traveled. In order to measure modal diversion for US cities in response to road infrastructure improvements, we take the ratio of rail traffic use (measured in railcar-km or weight-km) to road traffic (measured in truck vehicle-km) for city c in year t ($\frac{\text{Rail Traffic Use}_{cy}}{\text{Road Traffic Use}_{cy}}$).

As previously mentioned and established in our theory model (Equation (18)), Duranton and Turner (2011) finds that commercial truck traffic has a positive relationship with road infrastructure improvements as measured by inter-state highways. We replicate these results using our matched dataset (Columns (1) and (2), Table 5). Our OLS estimates with fixed effects have the same sign and are within one standard deviation of the results from Duranton and Turner (2011) (Columns (6) and (7), Table 9, Duranton and Turner (2011)).

Using railcar-kilometers traveled as our rail traffic use measure in Equation (37), we find that rail traffic use has a negative relationship with road infrastructure improvement in US cities as proxied by inter-state highways (Columns (1) and (2), Table 6). These relationships are imprecisely estimated due to two opposing forces. First, an improvement in road access would generally decrease trade cost in and out of these cities and improve their general market access. This is inline with our general market access measures predicted in Equation (**??**), where destination-level road infrastructure improvement would impact the inward market access measure P_k and origin-level improvement would impact the outward market access measure Π_l. Second, however, this road access improvement would also have a modal substitution or diversion effect—rail transport costs are now relatively more expensive and this will decrease overall rail traffic use. We find similar results using rail traffic measured in weight-kilometers (Columns (1) and (2), Table A.10).

Next, we compare these changes in rail and road traffic use by estimating Equation (37) using the ratio of rail traffic use to road traffic use. In Columns (1) and (2) of Table 7, we find that the ratio of rail to truck traffic use has a negative and significant relationship with road infrastructure improvement in US cities. This result is robust to the inclusion of city-level fixed effects and year-level fixed effects, as well including time-varying city-level controls like socioeconomic characteristics and population. We note that this result, a regression coefficient

Table. 5. Elasticity of Truck VKT with respect to Interstate Highway Lane Kilometers

	(1) OLS	(2) OLS	(3) IV	(4) IV	(5) IV
Inter-State Highway Lane KM	1.606***	1.616***	1.746***	2.083***	2.099***
	(0.328)	(0.338)	(0.427)	(0.483)	(0.530)
Population		0.967*	-0.278	-0.615	-0.484
		(0.550)	(0.303)	(0.376)	(0.393)
Geography				✓	✓
Census Divisions				✓	✓
Socioeconomic Characteristics		✓			✓
MSA FE	✓	✓			
Year FE	✓	✓	✓	✓	✓
Observations	663	663	663	663	663
R-squared	0.77	0.78	-	-	-
KP F-stat			13.48	10.08	10.02

Notes: * $p < 0.1$, ** $p < 0.05$, *** $p < 0.01$. Robust standard errors clustered by MSAs in parentheses. All variables are in logs. Instruments are 1835 exploration routes, 1898 railroad route kilometers, and 1947 planned interstate highways. 663 observations corresponding to 221 MSAs for each regression. See Table A.3 for first-stage regressions.

Table. 6. Elasticity of Rail Car Traffic-Kilometers with respect to Interstate Highway Lane Kilometers

	(1) OLS	(2) OLS	(3) IV	(4) IV	(5) IV
Interstate Highway Lane KM	-0.103	-0.0993	0.434	0.254	0.401
	(0.173)	(0.175)	(0.314)	(0.337)	(0.315)
Population		0.346	0.695***	0.878***	0.757***
		(0.299)	(0.245)	(0.286)	(0.273)
Geography				✓	✓
Census Divisions				✓	✓
Socioeconomic Characteristics		✓			✓
MSA FE	✓	✓			
Year FE	✓	✓	✓	✓	✓
Observations	663	663	663	663	663
R-squared	0.94	0.94	-	-	-
KP F-stat			13.48	10.08	10.02

Notes: * $p < 0.1$, ** $p < 0.05$, *** $p < 0.01$. Robust standard errors clustered by MSAs in parentheses. All variables are in logs. Instruments are 1835 exploration routes, 1898 railroad route kilometers, and 1947 planned interstate highways. 663 observations corresponding to 221 MSAs for each regression. See Table A.7 for first stage regressions.

of around -1.4, is not entirely driven by the inverse of truck traffic use result: our estimates are lower in absolute terms and beyond one standard error from the replicated truck VKT estimates of positive 1.6 from Table 5 (Columns (1) and (2)). This suggests that while rail traffic use has

a positive relationship with road infrastructure improvement, as we have shown in Table 6, this rail increase is less than the road traffic use increase. This negative relationship is robust to measuring rail traffic use in terms of rail weight as well (Columns (1) and (2), Table A.21).

Since transport infrastructure and traffic use may be simultaneously determined, we required an instrumental variable approach in order to identify the causal effects of road infrastructure on rail traffic use and modal substitution. We employ the three instruments by Duranton and Turner (2011) to predict the stock of roads in US cities: kilometers of preliminary interstate highway in each MSA as part of the 1947 highway plan (Baum-Snow, 2007; Michaels, 2008), kilometers of 1898 railroads in each MSA, and exploration routes between 1528-1850. We estimate the following two-stage least squares IV regression:

$$\begin{aligned} \ln \text{Interstate Highway Lanes}_{cy} &= \eta_1 \ln \text{Instruments}_c + \kappa C_{cy} + \iota_y + \nu_{cy} \\ \ln Y_{cy} &= \eta_2 \ln \text{Interstate Highway Lanes}_{cy} + \phi C_{cy} + \iota_y + \mu_{cy} \end{aligned} \tag{38}$$

where $\ln Y_{cy}$ is the log traffic use outcomes for MSA c in year y, $\ln \text{Instruments}_c$ is the set of three instruments discussed earlier, $\ln \text{Interstate Highway Lanes}_{cy}$ is the log number of interstate highway lanes going through each city c which proxies for the road infrastructure for that city in year y. C_{jt} are city-specific time-varying controls including population, physical geography, census divisions, and socioeconomic characteristics that are taken from Duranton and Turner (2011), and ι_y is year fixed effects.

The validity of the IV strategy here requires that the instrument be uncorrelated with unobserved changes in road and rail traffic use conditional on the control variables and fixed effects in Equation (38). We first show that we can replicate the IV results in Duranton and Turner (2011): our IV estimates in Columns (3) and (4) (Table 5) have the same sign and are within one standard error of the results from Duranton and Turner (2011) (Columns (9) and (10), Table 9, Duranton and Turner (2011)). Similar to them, we find that the IV estimates are slightly higher than the OLS estimates. Our results are also robust to including socioeconomic characteristics (Column (5), Table 5). We then show that road infrastructure has a positive and noisy impact on rail traffic (Columns (3) to (5), Table 6). Using rail traffic measured in weight-kilometers, we again find similar positive but noisy effects (Columns (3) to (5), Table A.10).

Comparing these increases in rail and road traffic use, we find that road infrastructure improvements result in a larger increase in road traffic use relative to the rail increase—resulting in a decrease in the ratio of rail traffic use to road traffic use. A 1 percent increase in interstate highways causes a 0.9-1.2 percent decrease in rail to road traffic use (Columns (3) to (5), Table

Table. 7. Elasticity of Rail to Truck Traffic Use with respect to Road Infrastructure Improvements

	(1)	(2)	(3)	(4)	(5)
Rail to Road Traffic Use	OLS	OLS	IV	IV	IV
Interstate Highway Lane KM	-1.432***	-1.432***	-0.867**	-1.249***	-1.099***
	(0.195)	(0.196)	(0.376)	(0.388)	(0.364)
Population		-0.150	0.699**	1.092***	0.891***
		(0.337)	(0.289)	(0.328)	(0.306)
Geography				✓	✓
Census Divisions				✓	✓
Socioeconomic Characteristics		✓			✓
MSA FE	✓	✓			
Year FE	✓	✓	✓	✓	✓
Observations	658	658	658	658	658
R-squared	0.88	0.88	-	-	-
KP F-stat			14.48	10.76	10.04

Notes: * $p < 0.1$, ** $p < 0.05$, *** $p < 0.01$. Robust standard errors clustered by MSAs in parentheses. All variables are in logs. Rail traffic use, measured in railcar-kilometers, is constructed using confidential rail waybill data. Truck traffic use (in vehicle-kilometers) and other variables are from Duranton and Turner (2011). Instruments are 1835 exploration routes, 1898 railroad route kilometers, and 1947 planned interstate highways. 663 observations corresponding to 221 MSAs for each regression. See Table A.16 for first stage regressions.

7). It is important to note that this result is not driven by the inverse of truck traffic use result: our estimates are lower in absolute terms and beyond one standard error from the replicated truck VKT estimates where a 1 percent increase in interstate highways causes a 1.7-2.1 percent increase in truck VKT (Columns (3) to (5), Table 5). These estimates are similar in magnitude when measuring rail traffic by weight (Columns (3) to (5), Table A.21).

Robustness Since our rail traffic data is more disaggregated, we are able investigate incoming and outgoing rail traffic use separately. We find that these directional results retain the same signs and are within one standard error of most of our main results, suggesting that both incoming and outgoing rail traffic use respond similarly to road infrastructure improvements. While both rail traffic use measures are imprecisely estimated, they are similar in magnitude (Tables A.6 and A.8 respectively for incoming and outgoing rail traffic use measured in railcar-km). We find similar results using incoming and outgoing rail traffic measured in weight-kilometers (Tables A.12 and A.14 respectively). Comparing the ratio of directional rail traffic use to road traffic use, we find that a 1 percent increase in interstate highways increases the elasticity of incoming rail traffic use to road traffic use by 1-1.2 percent (Columns (3) to (5), Table A.17) while a 1 percent increase in interstate highways increases the elasticity of outgoing rail traffic use to road traffic use by about 1.2 percent (Columns (3) to (5), Table A.19). These results are slightly

higher using rail traffic use measured in weight-kilometers (Tables A.23 and A.25 respectively for incoming and outgoing rail traffic use measured in railcar-km).

5 Calibration and Counterfactuals

In this section, we apply our multimodal economic geography framework to evaluate the aggregate implications of the multimodal transport network for infrastructure investments and disruptions. First, we discuss how we construct the US multimodal transport network using detailed traffic and geography data, and the calibration of key parameters in the model.

5.1 Calibration

In order to calibrate our framework to the US multimodal network, we require data on income, population, as well as geo-spatial and traffic data on roads, rail, waterways, ports, and inland intermodal terminals. We utilize income, population, as well as road geo-spatial and traffic data from Allen and Arkolakis (2022). The additional rail, waterways, ports, and intermodal terminals data have been introduced in Section 2.1. Our resultant sparse graph representation of the multimodal transport network collapses the high-dimensional geo-spatial information from each mode-specific shapefiles and retains nodes at endpoints or intersections. Cities containing at least 10,000 people (CBSAs) are also represented by a single node within the network. The resulting graph comprises of 228 nodes and and 704 edges.

In a last step before conducting the counterfactual analysis we discuss our choice of the model parameters $\{\alpha, \beta, \theta, \lambda_1, \lambda_2, \eta\}$. For the local productivity spillover α, local amenity spillovers β, and shape parameter θ, we follow the literature (Allen and Arkolakis, 2022) and set $\theta = 8$, $\alpha = .1$ and $\beta = -.3$. For the road congestion elasticity, we use $\lambda_1 = 0.092$ following Allen and Arkolakis (2022) who estimates this parameter by regressing the observed speed on individual highway segments against a measure of instrumented traffic.

The last two parameters come from our own estimates. For the intermodal terminal congestion parameter λ_2, we first determine the impact of port traffic on the observed duration a ship spends at port using an instrument which measures the trade exposure at these ports (Section 4.1). We use $\lambda_2 = 0.096$ after converting this time elasticity into a cost measure, relying on the ad valorem tariff estimate on an additional day in transit from Hummels and Schaur (2013). For the modal elasticity of substitution η, we estimate the impact of road infrastructure improvements on rail relative to road traffic flows using the instruments from Duranton and Turner (2011). We

Table. 8. Elasticity of Rail Dwell Times with respect to Port Traffic

	(1)	(2)	(3)	(4)	(5)
Nearest Port Traffic (Net Tons)	0.05**		0.05**		0.03
	(0.02)		(0.02)		(0.02)
Nearest Port Traffic (Ships)		0.04**		0.04**	
		(0.01)		(0.01)	
Port Buffer Area	150km	150km	150km	150km	200km
Week-Year FE	✓	✓	✓	✓	✓
Rail Station-Port FE			✓	✓	
Port FE	✓	✓			
Rail Station FE	✓	✓			
Observations	3327	3327	3327	3327	4316
R^2	0.80	0.80	0.80	0.80	0.79
F	9.08	6.80	9.08	6.80	2.06

Notes: Robust standard errors in parentheses are clustered by port. All variables are in logs. Local railroads are determined by a 150km buffer area around the ports.

use $\eta = 1.099$.

5.2 Gains from Intermodal Terminal Investments

While previous papers have focused on estimating the welfare effects of improving individual segments of the US road network, and in particular of the US highway network, less is known about the welfare impact of improving the degree to which the US multimodal transport network is interconnected. In order to evaluate this, we will use the counterfactual equations of Proposition (1) to estimate the aggregate welfare impact ($\hat{W} = \hat{\chi}^{-\frac{1}{\theta}}$) of a small (1%) improvement to the switching cost, $s_{ii,m}$, at each intermodal node across the system, given the calibrated parameters and observed traffic on road, rail, waterways, and ports.

Our results are visualized in Figure 7 and the top 10 highest impact nodes are listed in Table 9. For the welfare benefits, we convert the welfare elasticity into a dollar amount using a compensating variation approach by calculating the necessary increase, in millions of chained 2012 US dollars, in annual US real GDP (valued at $19 trillion) to achieve the same welfare improvement that we estimate. Unsurprisingly, some of the intermodal terminals that generate the largest welfare impacts are populous coastal cities New York City and Los Angeles (which also includes Long Beach). New York City and Los Angeles both rank top two and three respectively (Table 9). However, many of the most impactful terminals are located in center of the United States like Chicago, Dallas, and Atlanta—highlighting the role of multimodal network transporting goods

Figure 7. Welfare Benefits of Intermodal Terminal Improvements

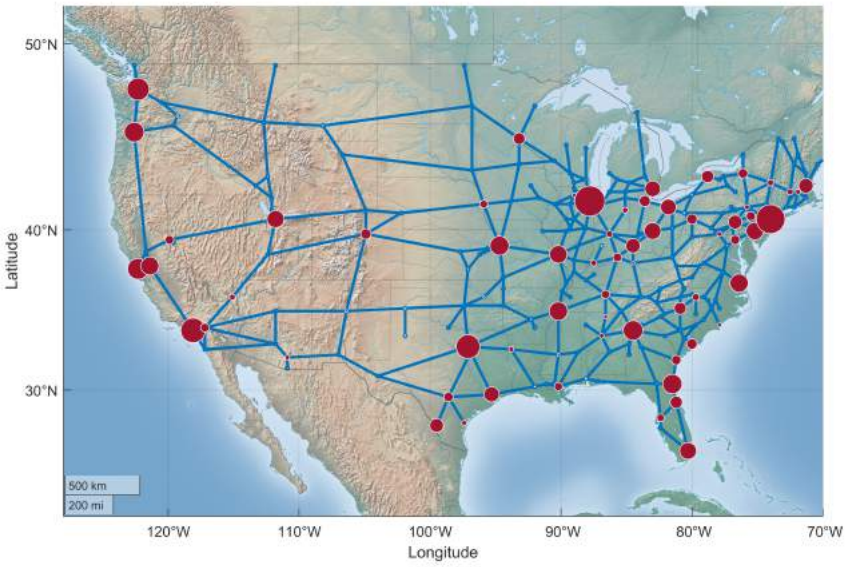

Notes: The figure visualizes the welfare impact of lowering the transshipment cost in each node by 1 percent. The larger the dots, the larger the welfare gains. The blue lines indicate the graph representation of the primary road network. State boundaries are included. See Table 9 for the top ten list of .

from coastal regions to the interior (Figure 7). Chicago, the top ranked terminal, has the highest rail throughput indicating its central role as a intermodal hub for the Midwest (Table 9, Column (4)). Several of these terminals, like Dallas, Kansas City, and Salt Lake City, do not have large throughput flows or a lot of terminals. However, their importance lies in their strategic geographical position along the multimodal network that facilitates the connection between coastal areas and the interior regions. These locations are highly central to the transportation system and represent potential bottlenecks within the US system. The implied welfare benefit of lowering the switching costs in some of the most central nodes could represent a welfare gain equivalent to increasing US GDP between 300-700 million USD (in 2012 USD).

Additionally, we combine our welfare benefits with cost assessments in order to compute the return on investment (ROI) for each of these terminal investments. To operationalize this, we utilize equation (42) in AA2022 adapted for terminal operations to determine the amount of container volume required to achieve a one percent reduction in switching cost at these terminals.[23] Next, we calculate the number of gantry cranes in container terminals required to achieve

[23]This implies a (log) proportional relationship between number of terminals and switching costs, i.e.

$$\hat{s}_{kk,m} = \hat{terminals}_{kk,m}^{-\lambda_m}.$$

where $\hat{s}_{kk,m}$ denotes the mode specific (log) change in the switching cost and $\hat{terminals}_{kk,m}$ denotes the necessary (log) change in terminal capacity.

Table. 9. Ranking: Welfare Benefits of Intermodal Terminal Improvements

	(1) CBSA Name	(2) Population	(3) Terminals	(4) Throughput	(5) ROI	(6) Benefit ($m)	(7) Cost ($m)
1	Chicago	9368268	88	3456228	0.249	691	553
2	New York City	14745610	29	497852	1.820	635	225
3	Los Angeles	9639715	38	2278880	-0.624	490	1301
4	Dallas	4513776	13	564160	4.581	465	83
5	Seattle	2189215	20	644052	1.917	418	143
6	San Francisco	3863536	14	104312	2.757	384	102
7	Portland	1641801	30	141432	8.891	352	36
8	Atlanta	1627623	28	610280	3.237	347	82
9	Jacksonville	936317	18	265960	6.995	341	43
10	Kansas City	1767872	55	362920	7.225	333	40

Notes: The table shows the ten terminals where a one percent reduction of the transshipment cost generates the highest benefit. Column (1) indicates the core based statistical areas (CBSA) name of the node, which includes both metropolitan and micropolitan areas. The terminal's population, number of terminals, and rail throughput in TEUs are reported in Columns (2), (3), and (4) respectively. Column (5) shows the imputed return on investment (ROI), Column (6) calculates how much 2012 US GDP would need to increase in order to match the overall welfare gain, while Column (6) presents the required cost of making this one percent cost decrease. For an extended version including the top 30 terminals see Table A.1.

this higher container volume using industry estimates. Since these terminals require land, each location will have a different construction cost based on local property prices. We obtain land values from Albouy, Ehrlich and Shin (2018). Assuming a 20-year depreciation schedule, a 5% annual maintenance cost, and a 3% borrowing cost, we estimate that 10% of the construction cost is accrued on an annual basis (Allen and Arkolakis, 2022).

We compare our results to improvements to a unimodal highway network like in Allen and Arkolakis (2022), where they identify gains in short coastal segments linking densely populated areas (like Boston-Philadelphia and Los Angeles-San Diego), and in trade thoroughfares via Indiana. Our gains instead are mostly in the central US, highlighting the role of multimodal transportation taking place over longer distances and linking coastal to interior regions. When implementing the same counterfactual of highway link improvements within our multimodal network setting, we find similar relative rankings for the links that are consistent with their results. However, the gains that we are estimating for the improvements of these links are lower because of the presence of other transport modes in our network.

Terminal improvements within a multimodal network can generate complementarity and substitution effects. On one hand, better access to the multimodal transport network means that locations can have better market access overall (for both consumer and producers). This would increase their overall demand for transportation across all modes. On the other hand, the improvement increases the relative costs of other transport modes, and transport use for other modes will decline relatively. This is the modal substitution effect. In practice, aggregate growth

outweighs the partial equilibrium effect and leads to a global increase in greenhouse gas emissions. Instead we isolate the partial equilibrium effect by keeping overall (GHG weighted) traffic constant. In order to calculate the environmental impact from this counterfactual, we obtain data on transport mode-specific greenhouse gas (GHG) emissions from EPA (2022*a*). For each counterfactual improvement of the intermodal terminals, we calculate the change in mode-specific traffic flows using Corollary 1 and multiply this change with the mode-specific GHG emissions in order to determine the change in GHG emissions. We employ EPA (2022*b*)'s estimates when calculating the social cost of GHG emissions.

Table 10 reports the environmental impacts of the intermodal terminal improvements. For all terminals, this decrease in the cost of accessing multimodal transport raises the relative cost of using truck transport which decreases road traffic flows, resulting in a decrease in GHG emissions from trucks (Table 10, Column (4)). Since the switching cost of intermodal terminals have decreased, rail traffic flows will increase in response which increases GHG emissions for rail. However, since rail is much less polluting than road, the overall GHG emission change is net decrease for all the terminals. The implied welfare benefit of lowering the switching costs in some of the most central nodes could result in an unintended environmental benefit, equivalent to between 22 to 45 million USD.

5.3 Impact of Policy Scenarios: Rail Strike, Jones Act Repeal, and Panama Canal Disruption

Next, we quantify the impact of several policy-relevant scenarios taking into account the multimodal transport network. First, we evaluate the impact of a strike by rail workers which would shut down the entire rail transport. Second, we study the impact of repealing the Jones Act, a currently active US trade restriction which requires all ships transporting freight between US ports to be built in the US, owned by US citizens, and mostly crewed by US citizen. Third, we study the impact of the Panama Canal disruptions due to drought conditions. In each of these scenarios, we further evaluate how congestion within the multimodal network affects the welfare impacts. We do this by comparing our baseline welfare number—with congestion at intermodal terminals and roads—to the welfare estimates without terminal congestion and without both terminal and road congestion. Last but not least, we study the environmental consequences of each of these scenarios.

Table. 10. Ranking: Environmental Impact of Intermodal Terminal Improvements

	(1) CBSA Name	(2) Benefit ($m)	(3) Cost ($m)	(4) Truck GHG (kt)	(5) Rail GHG (kt)	(6) GHG Benefit ($m)
1	Chicago	691	553	-148.62	19.15	45.33
2	New York City	635	225	-148.09	19.05	45.13
3	Los Angeles	490	1301	-107.17	13.36	32.64
4	Dallas	465	83	-89.36	11.82	27.23
5	Seattle	418	143	-101.76	12.92	31.00
6	San Francisco	384	102	-100.82	12.97	30.73
7	Portland	352	36	-72.86	9.54	22.21
8	Atlanta	347	82	-82.83	11.12	25.24
9	Jacksonville	341	43	-81.10	10.37	24.74
10	Kansas City	333	40	-76.64	9.89	23.37

Notes: The table shows the environmental impact from the ten terminals where a one percent reduction of the transshipment cost generates the highest benefit. Column (1) indicates the core based statistical areas (CBSA) name of the node, which includes both metropolitan and micropolitan areas. olumn (2) calculates how much 2012 US GDP would need to increase in order to match the overall welfare gain, while Column (3) presents the required cost of making this one percent cost decrease. Column (4) shows the change in truck GHG emissions which comes from the change in road traffic flows. Column (5) shows the change in rail GHG emissions which comes from the change in rail traffic flows. Column (6) presents the net social cost or benefit from the changes in mode-specific GHG emissions. Waterway emissions are omitted here for brevity.

Rail Strike The potential of a rail strike loomed in the fall of 2022, and only averted due to US President Biden intervening (Kanno-Youngs and Cochrane, 2022). In order to evaluate this, we estimate the aggregate welfare impact of increasing the cost on all rail links to prohibitively high levels (twenty-fold). The first row in Table 11 shows that the welfare cost of losing the rail network is equivalent to decreasing US GDP by about 230 billion USD (in 2012 USD). This is about half the value of the US highway system as estimated by Jaworski, Kitchens and Nigai (2023), and about 40% more than the adjusted value of railroads to the agriculture sector as estimated by Donaldson and Hornbeck (2016).

How much does congestion within the network affect these results? We next estimate the same increase in rail link costs, but reducing the congestion at intermodal terminals to zero ($\lambda_2 = 0$). We find a very small increase in the negative welfare impact of 2.5%, which is expected since the terminal congestion effects are not binding due to prohibitively high cost of rail—there is very little traffic flows on the rail network. The small increase is likely due to intermodal terminals that are also ports. When we remove congestion on roads, however, we see a 21% larger negative impact of the rail strike which is equivalent to decreasing US GDP by about 279 billion USD (in 2012 USD, Table11, Column (4)). We see here that congestion can play a compounding effect.

Repeal of Jones Act Next, we examine the consequences of repealing the Jones Act, the Merchant Marine Act of 1920. This is an active US trade regulation which requires all ships

Table. 11. Welfare Impact of Policy Scenarios: The Role of Congestion

	(1) Scenario	(2) Benefit ($bn)	(3) Benefit without Terminal Congestion ($bn)	(4) Benefit without All Congestion ($bn)
1	Railroad Strike	-230.46	-236.40	-278.94
2	Removal of the Jones Act	3.15	11.73	16.16
3	Panama Canal	-2.67	-7.64	-10.29

Notes: The table shows the welfare impact each of the three scenarios indicated by each row. Column (1) labels each scenario. Column (2) calculates how much 2012 US GDP would need to change in order to match the overall welfare change from each scenario. Column (3) is calculated the same way as Column (2) except with the removal of congestion on intermodal terminals ($\lambda_2 = 0$). Column (4) is calculated the same way as Column (2) except with the removal of congestion on intermodal terminals ($\lambda_2 = 0$) and roads ($\lambda_1 = 0$).

transporting freight and passengers between US ports to be built in the US, owned by US citizens, and mostly crewed by US citizen. Jones Act ships on average cost 2.7 times to operate than foreign-flag equivalents (MARAD, 2011). We evaluate the repeal of the Jones Act by decrease the link cost of waterways by the 2.7 estimate by MARAD (2011). The second row in Table 11 shows that the welfare gain of repealing the Jones Act and allowing foreign ships to transport cargo between US ports is equivalent to increasing US GDP by about 3.2 billion USD (in 2012 USD). Our estimate is towards the lower end of the range of estimates by the USITC: $2.8 billion (USITC, 1995) to $9.8 billion (USITC, 1991). There are a few reasons that contribute to our estimate being lower. First, we are only estimating this impact for the continental United States. The Jones Act repeal will have much larger benefits for Hawaii, Alaska, and Puerto Rico since these locations rely a lot more on maritime transport and have less modal substitution options. Secondly, our estimates are based on the the US multimodal network today. The Jones Act, established in 1920, is more than 100 years old. Over this long time period, the multimodal network has adjusted to substitute for the expensive waterway transport. As an example, Figure 3 shows that there is rail and road networks up and down the coast lines. Had waterways been less expensive, potential these networks might have been built further inland.

In this scenario, the congestion effects of intermodal terminals play a much larger role in informing the welfare estimates. Without intermodal terminal congestion, the welfare benefits from repealing the Jones Act increase by 272% (Column (3) in Table 11). This is due to the gains from being able to increase waterway transport use once it is cheaper. Without all congestion (road and terminals), the welfare gains from the repeal increase by a further 38 percent.

Panama Canal Disruption Our third scenario studies the impact of the drought conditions in the Panama Canal, which decreases the number of ships that can access it. We evaluate this disruption by increasing the cost of accessing the canal by five times. The third row in Table 11 shows that the welfare cost of disruptions at the Panama Canal is equivalent to decreasing US

GDP by about 2.7 billion USD (in 2012 USD). To the best of our knowledge, this is the first estimate of this disruption allowing for modal and route substitution, including at ports. Here, removing congestion again compounds these effects. Without terminal congestion, the effects increase by more than 186 percent. This large increase is driven by the modal substitution from water to rail and road, and the intermodal terminals playing a crucial role in facilitating this transfer. Without terminal and road congestion, the increase is a further 35 percent.

Environmental Impact of Scenarios Next, we evaluate the environmental impact of each of these scenarios in Table 12. Here, the modal substitution mechanism is highlighted as each of the scenarios result in different modal substitution patterns. The rail strike scenarios pushes the cargo that would have gone via rail onto road instead, increasing the truck GHG emissions by a significant amount. Even though rail GHG emission decrease due to the lack of rail transport, trucks are much more polluting and this results in a huge decrease in the social cost of GHG by 12 billion dollars.

The repeal of the Jones Act, on the other hand, decreases emissions overall. This is because cargo would substitute towards using waterways due to the lower cost, and so road and rail traffic would decrease as a result. Since barge emissions are much lower, this results in a GHG benefit increase of 0.2 billion dollars.

The Panama Canal disruptions also result in modal substitution. This time cargo substitutes towards road and rail. The increase in truck and rail traffic flows increase GHG emissions on both modes, resulting in an overal decrease in the GHG benefit.

6 Conclusion

The movement of goods from origin to destination involves an extensive transport network of multiple modes, including highways, railroads, oceans, and waterways. This network, like production and trade networks, are extensive and can have large and compounding impacts on economic activity and welfare. Additionally, extensive reliance on particular transport modes like highways can result in negative externalities like congestion and pollution. While recognizing that transport is fundamental to the economy and society and attempting to make it more sustainable, the European Commission calls for multimodal transport solutions relying on waterborne and rail modes for long-hauls (European Commission, 2011).

We study the multimodal transport network and their impact on the economic and environ-

Table. 12. Environmental Impact of Policy Scenarios

	(1) Scenario	(2) Truck GHG Change (kt)	(3) Rail GHG Change (kt)	(4) GHG Benefit ($bn)	(5) Benefit ($bn)
1	Railroad Strike	38947	-5171	-11.88	-230.46
2	Removal of the Jones Act	-589	-47	0.19	3.15
3	Panama Canal	1524	111	-0.45	-2.67

Notes: The table shows the environmental impact of each of the three scenarios indicated by each row. Column (1) labels each scenario. Column (2) shows the change in truck GHG emissions which comes from the change in road traffic flows. Column (3) shows the change in rail GHG emissions which comes from the change in rail traffic flows. Column (4) presents the net social cost or benefit from the changes in mode-specific GHG emissions. Column (5) calculates how much 2012 US GDP would need to change in order to match the overall welfare change from each scenario. Waterway emissions are omitted here for brevity.

mental returns to new technology and infrastructure investments. In particular, we focus on how these outcomes will depend on the geography of the multimodal transportation network, the placement of intermodal terminals that allow for switches between modes of transportation, as well as the relative cost of transportation across modes. By incorporating these features we provide a framework that allows us to realistically evaluate infrastructure policies taking the complete domestic transportation network into account.

References

Akamatsu, Takashi. 1997. "Decomposition of Path Choice Entropy in General Transport Networks." *Transportation Science*, 31(4): 349–362.

Albouy, David, Gabriel Ehrlich, and Minchul Shin. 2018. "Metropolitan land values." *Review of Economics and Statistics*, 100(3): 454–466.

Allen, Treb, and Costas Arkolakis. 2014. "Trade and the Topography of the Spatial Economy." *The Quarterly Journal of Economics*, 129(3): 1085–1140.

Allen, Treb, and Costas Arkolakis. 2022. "The Welfare Effects of Transportation Infrastructure Improvements." *The Review of Economic Studies*.

Anderson, James E., and Eric van Wincoop. 2003. "Gravity with Gravitas: A Solution to the Border Puzzle." *American Economic Review*, 93(1): 170–192.

Antràs, Pol, and Alonso Gortari. 2020. "On the geography of global value chains." *Econometrica*, 88(4): 1553–1598.

Baum-Snow, Nathaniel. 2007. "Did highways cause suburbanization?" *The quarterly journal of economics*, 122(2): 775–805.

Beuthe, Michel, Bart Jourquin, and Natalie Urbain. 2014. "Estimating Freight Transport Price Elasticity in Multi-mode Studies: A Review and Additional Results from a Multimodal Network Model." *Transport Reviews*, 34(5): 626–644.

Bonadio, Barthélémy. 2021. "Ports vs. Roads: Infrastructure, Market Access and Regional Outcomes." Working Paper.

Borusyak, Kirill, Peter Hull, and Xavier Jaravel. 2022. "Quasi-experimental shift-share research designs." *The Review of Economic Studies*, 89(1): 181–213.

Boyles, Stephen D., Nicholas E. Lownes, and Avinash Unnikrishnan. 2021. *Transportation Network Analysis.* Vol. 1. 0.89 ed.

Brancaccio, Giulia, Myrto Kalouptsidi, and Theodore Papageorgiou. 2020. "Geography, transportation, and endogenous trade costs." *Econometrica*, 88(2): 657–691.

Congressional Budget Office (CBO). 2022. "Emissions of Carbon Dioxide in the Transportation Sector." CBO Publication 58566.

Coşar, A Kerem, and Banu Demir. 2018. "Shipping inside the box: Containerization and trade." *Journal of International Economics*, 114: 331–345.

Cristea, Anca, David Hummels, Laura Puzzello, and Misak Avetisyan. 2013. "Trade and the greenhouse gas emissions from international freight transport." *Journal of environmental economics and management*, 65(1): 153–173.

Daly, Andrew, and Michel Bierlaire. 2006. "A general and operational representation of Generalised Extreme Value models." *Trans. Res. Part B: Methodol.*, 40(4): 285–305.

Degiovanni, Pedro, and Ron Yang Yang. 2023. "Economies of Scale and Scope in Railroading." Working Paper.

Dekle, Robert, Jonathan Eaton, and Samuel Kortum. 2008. "Global Rebalancing with Gravity: Measuring the Burden of Adjustment." National Bureau of Economic Research, Inc NBER Working Papers 13846.

Donaldson, Dave, and Richard Hornbeck. 2016. "Railroads and American economic growth: A "market access" approach." *The Quarterly Journal of Economics*, 131(2): 799–858.

Duranton, Gilles, and Matthew A Turner. 2011. "The fundamental law of road congestion: Evidence from US cities." *American Economic Review*, 101(6): 2616–52.

Duranton, Gilles, and Matthew A Turner. 2012. "Urban growth and transportation." *Review of Economic Studies*, 79(4): 1407–1440.

Duranton, Gilles, Peter M Morrow, and Matthew A Turner. 2014. "Roads and Trade: Evidence from the US." *Review of Economic Studies*, 81(2): 681–724.

Eaton, Jonathan, and Samuel Kortum. 2002. "Technology, Geography, and Trade." *Econometrica*, 70(5): 1741–1779.

EPA. 2022*a*. "Inventory of US Greenhouse Gas Emissions and Sinks: 1990-2020." *https://www.epa.gov/ghgemissions/draft-inventory-us-greenhouse-gas-emissions-and-sinks-1990-2020*, US Environmental Protection Agency, EPA 430-R-22-0003.

EPA. 2022*b*. "Report on the social cost of greenhouse gases: Estimates incorporating recent scientific advances." US Environmental Protection Agency Washington, DC.

European Commission. 2011. "Roadmap to a Single European Transport Area-Towards a competitive and resource efficient transport system." *White Paper*, 144.

Fajgelbaum, Pablo D, and Edouard Schaal. 2017. "Optimal Transport Networks in Spatial Equilibrium." National Bureau of Economic Research Working Paper 23200.

Fajgelbaum, Pablo D, Cecile Gaubert, Nicole Gorton, Eduardo Morales, and Edouard Schaal. 2023. "Political Preferences and the Spatial Distribution of Infrastructure: Evidence from California's High-Speed Rail." National Bureau of Economic Research.

Fan, Jingting, and Wenlan Luo. 2020. "A Tractable Model of Transshipment." Working Paper.

Fan, Jingting, Yi Lu, and Wenlan Luo. 2019. "Valuing domestic transport infrastructure: a view from the route choice of exporters." *The Review of Economics and Statistics*, 1–46.

Ganapati, Sharat, Woan Foong Wong, and Oren Ziv. 2021. "Entrepot: Hubs, scale, and trade costs." National Bureau of Economic Research Working Paper 29015.

Heiland, Inga, Andreas Moxnes, Karen-Helene Ulltveit-Moe, and Yuan Zi. 2019. "Trade From Space: Shipping Networks and The Global Implications of Local Shocks." C.E.P.R. Discussion Papers CEPR Discussion Papers 14193.

Horn, Roger A, and Charles R Johnson. 2012. *Matrix analysis.* Cambridge university press.

Hummels, David L, and Georg Schaur. 2013. "Time as a trade barrier." *American Economic Review*, 103(7): 2935–2959.

Jaworski, Taylor, Carl Kitchens, and Sergey Nigai. 2023. "Highways and globalization." *International Economic Review*, 64(4): 1615–1648.

Kanno-Youngs, Zolan, and Emily Cochrane. 2022. "Biden Signs Legislation to Avert Nationwide Rail Strike." *https://www.nytimes.com/2022/12/02/us/politics/rail-strike-biden.html*, New York Times.

Kitthamkesorn, Songyot, Anthony Chen, and Xiangdong Xu. 2015. "Elastic demand with weibit stochastic user equilibrium flows and application in a motorised and non-motorised network." *Transportmetrica A: Transport Science*, 11(2): 158–185.

Lind, Nelson, and Natalia Ramondo. 2023. "Trade with Correlation." *Am. Econ. Rev.*, 113(2): 317–353.

Li, Xinyan, Chi Xie, and Zhaoyao Bao. 2022. "A multimodal multicommodity network equilibrium model with service capacity and bottleneck congestion for China-Europe containerized freight flows." *Transportation Research Part E: Logistics and Transportation Review*, 164: 102786.

Lugovskyy, Volodymyr, Alexandre Skiba, and David Terner. 2022. "Unintended Consequences of Environmental Regulation of Maritime Shipping: Carbon Leakage to Air Shipping." Working Paper.

MARAD. 2011. "Comparison of US and Foreign-flag Operating Costs." US Department of Transportation, Maritime Administration.

McFadden, Daniel. 1977. "Modelling the Choice of Residential Location." Cowles Foundation for Research in Economics, Yale University 477, Cowles Foundation for Research in Economics, Yale University.

McFadden, Daniel, Clifford Winston, and Axel Boersch-Supan. 1986. "Joint estimation of freight transportation decisions under nonrandom sampling." *Analytical Studies in Transport Economics*, , ed. Andrew F.Editor Daughety, 137–158. Cambridge University Press.

Michaels, Guy. 2008. "The effect of trade on the demand for skill: Evidence from the interstate highway system." *The Review of Economics and Statistics*, 90(4): 683–701.

Mundaca, Gabriela, Jon Strand, and Ian R Young. 2021. "Carbon pricing of international transport fuels: Impacts on carbon emissions and trade activity." *Journal of Environmental Economics and Management*, 110: 102517.

Oyama, Yuki, Yusuke Hara, and Takashi Akamatsu. 2022. "Markovian traffic equilibrium assignment based on network generalized extreme value model." *Trans. Res. Part B: Methodol.*, 135–159.

Papola, Andrea, and Vittorio Marzano. 2013. "A Network Generalized Extreme Value Model for Route Choice Allowing Implicit Route Enumeration." *Comput.-aided civ. infrastruct. eng.*, 28(8): 560–580.

Ranieri, Luigi, Salvatore Digiesi, Bartolomeo Silvestri, and Michele Roccotelli. 2018. "A review of last mile logistics innovations in an externalities cost reduction vision." *Sustainability*, 10(3): 782.

Redding, Stephen, and Anthony J. Venables. 2004. "Economic geography and international inequality." *Journal of International Economics*, 62(1): 53–82.

Redding, Stephen J. 2016. "Goods trade, factor mobility and welfare." *Journal of International Economics*, 101: 148–167.

Redding, Stephen J. 2020. "Trade and Geography." NBER Working Paper 27821.

Rich, J., O. Kveiborg, and C.O. Hansen. 2011. "On structural inelasticity of modal substitution in freight transport." *Journal of Transport Geography*, 19(1): 134–146.

Rodrigue, Jean-Paul. 2020. *The geography of transport systems.* Routledge.

Shapiro, Joseph S. 2016. "Trade Costs, CO2, and the Environment." *American Economic Journal: Economic Policy*, 8(4): 220–54.

Surface Transportation Board. 2009. "A Study of Competition in the US Freight Railroad Industry and Analysis of Proposals that might Enhance Competition." Report prepared by Laurits R. Christensen Associates.

USITC. 1991. "The Economic Effects of Significant US Import Restraints." *Investigation No.332-325, Publication 3201.*

USITC. 1995. "The Economic Effects of Significant US Import Restraints."

Winston, Clifford. 1981. "A Disaggregate Model of the Demand for Intercity Freight Transportation." *Econometrica*, 49(4): 981–1006.

Wong, Woan Foong. 2022. "The round trip effect: Endogenous transport costs and international trade." *American Economic Journal: Applied Economics*, 14(4): 127–66.

Zgonc, Borut, Metka Tekavčič, and Marko Jakšič. 2019. "The impact of distance on mode choice in freight transport." *European Transport Research Review*, 11(1): 1–18.

Part

Appendix

Table of Contents

A Additional Tables and Figures

Figure A.1. US Transport Mode Weight Shares by Distance, 2018

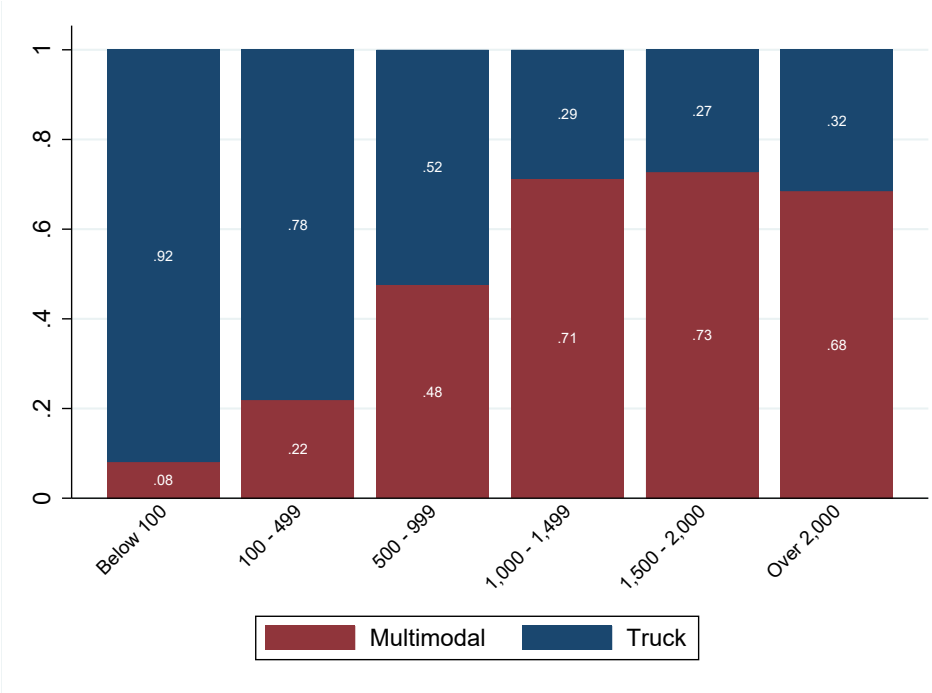

Notes: This figure plots the observed weight share of cargo transported by different modes across various distances. Multimodal indicates cargo movement that involves more than one mode. Source: Freight Analysis Framework, US Department of Transportation, and authors' calculations.

Table. A.1. Top 30 Ranking: Welfare Benefit of Investing in Terminal Operations

	(1) CBSA Name	(2) Population	(3) Terminals	(4) Throughput	(5) ROI	(6) Benefit ($m)	(7) Cost ($m)
1	Chicago	9368268	88	3456228	0.249	691	553
2	New York City	14745610	29	497852	1.820	635	225
3	Los Angeles	9639715	38	2278880	-0.624	490	1301
4	Dallas	4513776	13	564160	4.581	465	83
5	Seattle	2189215	20	644052	1.917	418	143
6	San Francisco	3863536	14	104312	2.757	384	102
7	Portland	1641801	30	141432	8.891	352	36
8	Atlanta	1627623	28	610280	3.237	347	82
9	Jacksonville	936317	18	265960	6.995	341	43
10	Kansas City	1767872	55	362920	7.225	333	40
11	Memphis	997862	28	472040	6.385	320	43
12	Virginia Beach	1457869	11	173840	7.454	313	37
13	Stockton	901910	11	288320	4.876	310	53
14	St. Louis	1901086	38	197440	13.038	299	21
15	Philadelphia	4532390	33	99800	17.443	293	16
16	Salt Lake City	1198360	5	87432	11.420	289	23
17	Miami	3184615	13	96120	2.208	281	88
18	Columbus	1902095	18	176600	12.261	278	21
19	Detroit	2732964	31	185920	13.479	257	18
20	Cleveland	2175988	23	143480	15.637	255	15
21	Houston	3133212	27	210100	8.064	245	27
22	Boston	3714540	13	58720	23.948	230	9
23	Cincinnati	1744673	23	85720	22.048	230	10
24	Laredo	265111	3	43640	38.249	215	5
25	Harrisburg	655561	1	264640	5.002	215	36
26	Deltona	411646	1	35280	19.714	186	9
27	Buffalo	1150833	17	42200	44.058	186	4
28	Charlotte	1502267	20	117480	27.506	182	6
29	Minneapolis	2886766	26	134560	5.070	177	29
30	Toledo	710352	16	39040	65.768	166	2

Notes: The table shows the thirty terminals where a one percent reduction of the switching cost generates the highest benefit. Column (1) indicates the core based statistical areas (CBSA) name of the node, which includes both metropolitan and micropolitan areas. The terminal's population, number of terminals, and rail throughput in TEUs are reported in Columns (2), (3), and (4) respectively. Column (5) shows the imputed return on investment (ROI), Column (6) calculates how much 2012 US GDP would need to increase in order to match the overall welfare gain, while Column (6) presents the required cost of making this one percent cost decrease.

B Theoretical Derivations

This appendix presents derivations for the results in Section 3. Additional derivations are presented in Online Appendix D.1.

B.1 Section 3.3.1: Recursive choice probabilities and transport costs

A consumer resides in location j and makes a route-sourcing choice comparing prices across all sourcing locations i and transportation costs across multiple routes r. Our aim is to characterize the choice probability that

We make the assumption that transport cost are multiplicative and that they are furthermore the product of edge-specific transport costs along the route r, i.e. $\tau_{ij,r}^{-\theta} = \left(\prod_{l=1}^{K} t_{r_{t-1},r_l}^{-\theta}\right)$. Finally, we assume that the consumer makes a recursive route-sourcing choice, beginning at the origin location j comparing the sourcing prices across neighboring nodes $k \in \mathcal{F}(j)$ and net the transportation cost of traversing via the neighboring nodes, t_{jk}. Below we will furthermore define the edge-specific transportation cost t_{jk} as arising as the expected minimum cost of traversing to the neighboring node along a multimodal transport network. For now - without loss of generality - we simply assume that the consumer faces a routing problem along a single-layered graph. In summary, the consumer at location j faces the following set of (recursively defined) prices:

$$p_{ij,k}(\nu) = \frac{t_{jk}\tau_{ki}w_i}{\varepsilon_{ij,k}(\nu)}$$

where $\varepsilon_{ij,k}(\nu)$ is a random variable drawn from a Frechet distribution with cumulative distribution given by,

$$F_{ijk}(\epsilon) = e^{-T_{ijk}\epsilon^{-\theta}}$$

The consumer in location j is presented with a set of route-source specific prices across sourcing locations i and choosing a route by traversing towards neighboring node k, i.e.

$$\begin{aligned} G_{ijk}(p) = \Pr\left(P_{ijk} \leq p\right) &= 1 - F_{ijk}\left(\frac{t_{jk}\tau_{ki}w_i}{p}\right) \\ &= 1 - e^{-T_{ijk}\left(t_{jk}\tau_{ki}w_i\right)^{-\theta}p^{\theta}} \end{aligned}$$

We can use this distribution to characterize the lowest route-source specific price that consumer in location j faces. To do so, fix an arbitrary threshold price p. The lowest price will be less than p, unless each route-source specific price is greater than p. We therefore seek to characterize, $G_{ijk}(p) = \Pr\left(P_{ijk} \leq p\right)$, which is given by,

$$\begin{aligned} G_j(p) &= 1 - \prod_{i,k}\left(1 - G_{ijk}(p)\right) \\ &= 1 - \prod_{i,k} e^{-T_{ijk}\left(t_{jk}\tau_{ki}w_i\right)^{-\theta}p^{\theta}} \\ &= 1 - e^{-\Phi_j p^{\theta}} \end{aligned}$$

where,

$$\Phi_j = \sum_{ik} T_{ijk}\left(t_{jk}\tau_{ki}w_i\right)^{-\theta}$$

If $p_{ij,k}(\nu) = p$ then the probability that ijk is the cost minimizing route-source choice is given by,

$$\begin{aligned} \prod_{i' \neq i, k' \neq k} \Pr\left[P_{ijrm} \geq p\right] &= \prod_{i' \neq i, k' \neq k}\left[1 - G_{i'jk'}\right] \\ &= \prod_{i' \neq i, k' \neq k} e^{-T_{ijk}\left(t_{jk}\tau_{ki}w_i\right)^{-\theta}p^{\theta}} \\ &= e^{-\left(\sum_{i,k} T_{ijr}\left(t_{jk}\tau_{ki}w_i\right)^{-\theta}\right)p^{\theta}} \end{aligned}$$

Integrating over all possible equilibrium prices p we can characterize the probability that country i and node

Variable Name	Variable
Multi-layered graph	$\mathcal{G} \equiv (\mathcal{N}, \mathcal{L})$
Successor nodes	$\mathcal{B}(i)$
Predecessor nodes	$\mathcal{F}(i)$
Route of length K	$r \equiv \{i = r_0, r_1, \ldots, r_K = j\}$
Elasticity of substitution (goods)	σ
Dispersion parameter (route)	θ
Dispersion parameter (mode)	η
Expected minimal transport cost between i and j	τ_{ij}
(Expected minimal) Edge-specific transport cost between i and k	t_{ik}
Mode-specific transport cost between i and k for mode m	$\tilde{t}_{ik,m}$
Link intensity	π_{ij}^{kl}
Link-sourcing probability	$\pi_{ij,k}$
Link choice probability conditional on sourcing from i to j	π_{ij}^{k}
Mode choice probability conditional on link ik	$\pi_{ij,k}^{m}$
Mode-link-sourcing probability	$\pi_{ij,k,m}$

Table. A.2. Overview of notation

k are the cost minimizing route-source choices:

$$\begin{aligned}\pi_{ij,k} &= \int_0^\infty \prod_{i' \neq i, k' \neq k} \left[1 - G_{i'jk'}\right] dG_{ijk}(p) \\ &= \int_0^\infty \prod_{i' \neq i, k' \neq k} e^{-T_{i'jk'}\left(t_{jk'}\tau_{ji'}w_{i'}\right)^{-\theta}p^\theta} dG_{ijk}(p)\end{aligned}$$

Replacing with $dG_{ijk}(p) = \left[T_{ijk}\left(t_{jk}\tau_{ji}w_i\right)^{-\theta}\theta p^{\theta-1}\right] e^{-T_{ijk}\left(t_{jk}\tau_{ji}w_i\right)^{-\theta}p^\theta} dp$, we obtain,

$$\begin{aligned}\pi_{ij,k} &= \int_0^\infty \prod_{i' \neq i, k' \neq k} e^{-T_{i'jk'}\left(t_{jk'}\tau_{ji'}w_{i'}\right)^{-\theta}p^\theta} dG_{ijk}(p) \\ &= \int_0^\infty \prod_{i' \neq i, k' \neq k} e^{-T_{i'jk'}\left(t_{jk'}\tau_{ji'}w_{i'}\right)^{-\theta}p^\theta} \left[T_{ijk}\left(t_{jk}\tau_{ji}w_i\right)^{-\theta}\theta p^{\theta-1}\right] e^{-T_{ijk}\left(t_{jk}\tau_{ji}w_i\right)^{-\theta}p^\theta} dp \\ &= T_{ijk}\left(t_{jk}\tau_{ji}w_i\right)^{-\theta} \int_0^\infty \prod_{i,k} e^{-T_{ijk}\left(t_{jk}\tau_{ji}w_i\right)^{-\theta}p^\theta} \left[\theta p^{\theta-1}\right] dp \\ &= T_{ijk}\left(t_{jk}\tau_{ji}w_i\right)^{-\theta} \int_0^\infty e^{-\left(\sum_{i,k} T_{ijk}\left(t_{jk}\tau_{ji}w_i\right)^{-\theta}\right)p^\theta} \left[\theta p^{\theta-1}\right] dp \\ &= T_{ijk}\left(t_{jk}\tau_{ji}w_i\right)^{-\theta} \int_0^\infty e^{-\Phi_j p^\theta} \left[\theta p^{\theta-1}\right] dp \\ &= T_{ijk}\left(t_{jk}\tau_{ji}w_i\right)^{-\theta} \left[\frac{1}{\Phi_j} e^{-\Phi_j p^\theta}\right]_0^\infty \\ &= \frac{T_{ijk}\left(t_{jk}\tau_{ji}w_i\right)^{-\theta}}{\Phi_j}\end{aligned}$$

Replacing with $\Phi_j = \sum_{ik} T_{ijk} \left(t_{jk}\tau_{ji}w_i\right)^{-\theta}$, we obtain,

$$\pi_{ij,k} = \frac{T_{ijk} \left(t_{jk}\tau_{ji}w_i\right)^{-\theta}}{\sum_{ik} T_{ijk} \left(t_{jk}\tau_{ji}w_i\right)^{-\theta}}$$

replacing $T_{ijk} \equiv \left(\frac{1}{A_i}\right)^{\theta}$, we obtain,

$$\pi_{ij,k} = \frac{\left(w_i/A_i\right)^{-\theta} \left(t_{jk}\tau_{ki}\right)^{-\theta}}{\sum_{i\in\mathcal{N}} \left(w_i/A_i\right)^{-\theta} \sum_{k'\in\mathcal{F}(i)} \left(t_{jk'}\tau_{k'i}\right)^{-\theta}}$$

as stated above. Furthermore, the expected minimal price is given by,

$$\begin{aligned} p_{ij,k} &= \mathbb{E}\left[\min_{k\in\mathcal{F}(i)} \left\{t_{jk}\tau_{ki}w_i\right\}\right] \\ &\propto \sum_{i\in\mathcal{N}} \left(w_i/A_i\right)^{-\theta} \sum_{k'\in\mathcal{F}(i)} \left(t_{jk'}\tau_{k'i}\right)^{-\theta} \\ &= \sum_{i\in\mathcal{N}} \left(w_i/A_i\right)^{-\theta} \tau_{ij}^{-\theta} \end{aligned}$$

where in the last line we have used the result that if we consider separately the routing problem this implies an expected transport cost that is in itself recursively defined, i.e.

$$\tau_{id} = \mathbb{E}\left[\min_{j\in\mathcal{F}(i)} \left\{t_{ij}\tau_{jd}\varepsilon_{ij}\right\}\right] = \left(\sum_{j\in\mathcal{F}(i)} \left(t_{ij}\tau_{jd}\right)^{-\theta}\right)^{-\frac{1}{\theta}}$$

which expressed the transport cost as an index of the continuation values along the different edges of the graph.

B.2 Section 3.3.: Gravity with Recursive Routing

We follow the derivations for the general equilibrium gravity equation in Anderson and van Wincoop (2003) to derive the gravity formula,

$$X_{ij} = \tau_{ij}^{-\theta_j} \times \frac{\gamma_i}{\Pi_i^{-\theta_j}} \times \frac{\delta_j}{P_j^{-\theta_j}}$$

Same derivations, alternatively,

$$\pi_{ij} = \frac{\delta_i^{-\theta_i}\tau_{ij}^{-\theta_i}}{\sum_{i\in N} \delta_i^{-\theta_i}\tau_{ij}^{-\theta_i}} = \frac{\delta_i^{-\theta_i}\tau_{ij}^{-\theta_i}}{P_j^{\theta_j}}$$

$$x_{ij} = \left(\frac{\delta_i\tau_{ji}}{P_j}\right)^{-\theta_j} y_j$$

where as usual,

$$P_j = \left[\sum_{i\in N} \delta_i^{-\theta_j}\tau_{ij}^{-\theta_j}\right]^{-\frac{1}{\theta_j}}$$

In general equilibrium we have,

$$\begin{aligned} y_i &= \sum_j x_{ij} \\ &= \sum_j \left(\frac{\delta_i \tau_{ji}}{P_j}\right)^{-\theta_j} y_j \\ &= (\delta_i)^{-\bar{\theta}} \sum_j \delta_i^{-\Delta\theta_j} \left(\frac{t_{ij}}{P_j}\right)^{-\theta_j} y_j \end{aligned}$$

Solve out for $\delta_i^{-\bar{\theta}}$,

$$\left(\frac{y_i}{\sum_j \delta_i^{-\Delta\theta_j} \left(\frac{t_{ij}}{P_j}\right)^{-\theta_j} y_j}\right)^{-\frac{1}{\bar{\theta}}} = \delta_i$$

Get the gravity equation,

$$\begin{aligned} x_{ij} &= \left(\frac{\delta_i \tau_{ij}}{P_j}\right)^{-\theta_j} y_j = (\delta_i)^{-\bar{\theta}} \delta_i^{-\Delta\theta_j} \left(\frac{\tau_{ij}}{P_j}\right)^{-\theta_j} y_j \\ &= \left(\frac{y_i}{\sum_j \delta_i^{-\Delta\theta_j} \left(\frac{\tau_{ij}}{P_j}\right)^{-\theta_j} y_j}\right) \delta_i^{-\Delta\theta_j} \left(\frac{\tau_{ij}}{P_j}\right)^{-\theta_j} y_j \\ &= \frac{y_i y_j}{y^W} \left(\frac{\tau_{ij}}{\left[\sum_j \delta_i^{-\Delta\theta_j} \left(\frac{\tau_{ij}}{P_j}\right)^{-\theta_j} \frac{y_j}{y^W}\right]^{-\frac{1}{\theta_j}} P_j}\right)^{-\theta_j} \\ &= \frac{y_i y_j}{y^W} \left(\frac{\tau_{ij}}{\Pi_i P_j}\right)^{-\theta_j} \end{aligned}$$

for

$$\Pi_i \equiv \left[\sum_j \delta_i^{-\Delta\theta_j} \left(\frac{t_{ij}}{P_j}\right)^{-\theta_j} \frac{y_j}{y^W}\right]^{-\frac{1}{\theta_j}}$$

We can substitute in the equilibrium scaled prices to get,

$$\begin{aligned} P_j &= \left[\sum_i (\delta_i \tau_{ij})^{-\theta_j}\right]^{-\frac{1}{\theta_j}} \\ &= \left[\sum_i (\delta_i)^{-\theta_j} (\tau_{ij})^{-\theta_j}\right]^{-\frac{1}{\theta_j}} \\ &= \left[\sum_i \left(\frac{y_i}{\sum_j \delta_i^{-\Delta\theta_j} \left(\frac{\tau_{ij}}{P_j}\right)^{-\theta_j} y_j}\right) (\tau_{ij})^{-\theta_j}\right]^{-\frac{1}{\theta_j}} \\ &= \left[\sum_i \frac{\frac{y_i}{y^W}}{\sum_j \delta_i^{-\Delta\theta_j} \left(\frac{\tau_{ij}}{P_j}\right)^{-\theta_j} \frac{y_j}{y^W}} (\tau_{ij})^{-\theta_j}\right]^{-\frac{1}{\theta_j}} \\ &= \left[\sum_i \frac{y_i}{y^W} \left(\frac{\tau_{ij}}{\Pi_i}\right)^{-\theta_j}\right]^{-\frac{1}{\theta_j}} \end{aligned}$$

In conclusion we have,

$$\Pi_i \equiv \left(\sum_j \left(\frac{\tau_{ij}}{P_j} \right)^{-\theta_j} \theta_j \right)^{-\frac{1}{\theta_j}}$$

$$P_j = \left[\sum_i \theta_i \left(\frac{\tau_{ij}}{\Pi_i} \right)^{-\theta_j} \right]^{-\frac{1}{\theta_j}}$$

For gravity we obtain,

$$X_{ij} = \tau_{ij}^{-\theta_j} \times \frac{\gamma_i}{\Pi_i^{-\theta_j}} \times \frac{\delta_j}{P_j^{-\theta_j}}$$

B.3 Section 3.4: Multimodal Routing and Transportation Cost

As presented in the previous section, we consider a consumer that resides in location j and makes a route-sourcing choice by choosing sequentially edges along the graph. This provides a convenient characterization of routing that avoids the curse of dimensionality by expressing the problem as a recursive problem instead of considering the universe of possible routes along a possibly high-dimensional graph. To furthermore accommodate multimodal routing choices, we incorporate a nested modal choice. In that setting, conditional on the neighboring node chosen, the consumer makes a modal choice by choosing the cost minimizing mode out of all modes along the edge, i. to traverse the edge (subject to an extreme value distributed cost shock). To fix ideas, consider a consumer in location j having chosen to route towards the neighboring node k. The consumer then compares all the different modes that are available along this edge, i.e. $m \in \mathcal{M}_{jk}$, where $\mathcal{M}_{jk}$ is the set of modes available between nodes $j$and k, and where the edge mode specific transport costs given by,

$$\tilde{t}_{jk,m} = \begin{cases} \tilde{t}_{jk} & \text{if} \quad m = 1 \\ s_{jj,m} \tau_{jk,m} s_{kk,m} & \text{if} \quad m \neq 1 \end{cases}$$

where for the primary mode no switching cost is required, but for any non-primary mode ($m \neq 1$) a switching cost ist imposed, while $\tau_{jk,m}$ refers to the iceberg transport cost of traversing the edge between node j and k along mode m. Notice that this specification is extremeley general and allows for geographies where non-primary modes might connect an entirely different set of nodes than primary nodes. The consumer then faces a cost minimizing choice subject to an extreme-value distributed cost shock, i.e.

$$\min_{m \in \mathcal{M}(j,k)} \{ t_{jk} \varepsilon_m \}$$

where the properties of the Frechet distribution implies that the expected cost minimizing transport along any mode between nodes j and k is given by,

$$t_{ik}^{-\theta} \propto \left(\sum_{m \in \mathcal{M}(i,k)} \tilde{t}_{ik,m}^{-\eta} \right)^{\frac{\theta}{\eta}|}$$

Overall, the consumer's route-sourcing choice can be written as a nested minimization problem where we can characterize the overall expected minimal cost, i.e.

$$\begin{aligned} p_{ij} &= \mathbb{E} \left[\min_{j \in \mathcal{F}(i)} \left\{ \mathbb{E} \left[\min_{m \in \mathcal{M}(i,k)} \{ \tilde{t}_{ik,m} \varepsilon_m \} \right] \tau_{jd} w_i \varepsilon_{ij} \right\} \right] \\ &\propto \sum_{i \in \mathcal{N}} (w_i / A_i)^{-\theta} \sum_{k' \in \mathcal{F}(i)} \left(\left(\sum_{m \in \mathcal{M}(i,k)} \tilde{t}_{ik,m}^{-\eta} \right)^{-\frac{1}{\eta}} \tau_{k'i} \right)^{-\theta} \\ &= \sum_{i \in \mathcal{N}} (w_i / A_i)^{-\theta} \tau_{ij}^{-\theta} \end{aligned}$$

where in the last line we again have used the definition of the transportation cost in terms of the edge-specific

costs and associated continuation values along neighboring nodes.

$$\tau_{id} = \mathbb{E}\left[\min_{j\in\mathcal{F}(i)}\left\{t_{ij}\tau_{jd}\varepsilon_{ij}\right\}\right] = \left(\sum_{j\in\mathcal{F}(i)}\left(\left(\sum_{m\in\mathcal{M}(i,k)}\tilde{t}_{ik,m}^{-\eta}\right)^{-\frac{1}{\eta}|}\tau_{jd}\right)^{-\theta}\right)^{-\frac{1}{\theta}}$$

which expressed the transport cost as an index of the continuation values along the different edges of the graph.

where the mode-route-sourcing choice probability is given by,

$$\begin{aligned}\pi_{ij,k,m} &= \frac{\left(w_i/A_i\right)^{-\theta}\left(t_{ik}\tau_{ki}\right)^{-\theta}}{\sum_{i\in\mathcal{N}}\left(w_i/A_i\right)^{-\theta}\sum_{k'\in\mathcal{F}(i)}\left(t_{ik'}\tau_{k'i}\right)^{-\theta}}\frac{\tilde{t}_{ik,m}^{-\eta}}{t_{ik}} \\ &= \pi_{ij,k}\times\pi_{ij,k}^{m}\end{aligned}$$

where we can decompose in the last line the link choice probability and the mode choice probability along the link.

B.4 Isomorphism with Allen and Arkolakis (2022)

It might be insightful to link the recursive expression in our paper to the approach in AA2022 that instead relies on explicit enumeration of the universe of paths and utilizes matrix algebra to express the expected minimum transport cost in terms of the leontief inverse of the adjacency matrix that captures the underlying infrastructure network. As we will show, the model is isomorphic in the case where there is a simple unimodal transport network. Furthermore, we will also show that for the simplified case where the mode choice elasticity is equal to the route choice elasticity, we can show that their approach can be extended to provide a clean expression of the multimodal transport cost in terms of (leontief inverses) of the infrastructure matrices. First, let us demonstrate the isomorphism for unimodal transport network. Consider the recursive transport cost stated above,

$$\tau_{id} = \mathbb{E}\left[\min_{j\in\mathcal{F}(i)}\left\{t_{ij}\tau_{jd}\varepsilon_{ij}\right\}\right] = \left(\sum_{j\in\mathcal{F}(i)}\left(t_{ij}\tau_{jd}\right)^{-\theta}\right)^{-\frac{1}{\theta}}$$

If we assume a finite graph, then we can iteratively substitute and obtain a closed-form expression for the endogenous transport cost, i.e.

$$\begin{aligned}\left(\tau_{id}\right)^{-\theta} &= t_{d-1d}^{-\theta}\sum_{j\in F(i)}t_{ij}^{-\theta}\sum_{j'\in F(j)}\cdots\sum_{k'\in F(d-1)}t_{k'd-1}^{-\theta} \\ &= \sum_{r\in\Re_{ij}}\left(\prod_{l=1}^{K}t_{r_{l-1},r_l}^{-\theta}\right) \\ &= \sum_{K=0}^{\infty}A_{ij}^{K} \\ &= \left(\mathbf{I}-\mathbf{A}\right)^{-1}\equiv\mathbf{B}\end{aligned}$$

where in the second line we recognize that the recursive substitution on a finite graph results in a characterization of all possible routes of any length along the network. The resulting expression is identical to expression for endogenous transport cost in AA2022. In the third and fourth line we then employ the same argument as in their paper to show that the implied transport cost can be expressed as the leontief inverse of the underlying infrastructure matrix, where $\mathbf{A}\equiv\left[t_{ij}^{-\theta}\right]$ is an $N\times N$ matrix with (i,j) element $t_{ij}^{-\theta}$ and A_{ij}^{K} is the (ij) element of the matrix A to the matrix power K. This shows that in essence, the two different approaches are isomorphic and capture the same underlying endogenous transport cost, albeit in different ways.

We now turn towards showing that for the special case where the mode choice elasticity is equal to the route

choice elasticity, we can furthermore extend the approach in AA2022 to derive a clean decomposition of the multimodal transport cost in terms of a set of underlying mode-specific infrastructure matrices. Let us therefore consider the case where $\eta = \theta$. Notice that in this special case, the edge-specific transport cost is given by,

$$t_{ik}^{-\theta} \propto \sum_{m \in \mathcal{M}(i,k)} \tilde{t}_{ik,m}^{-\theta}$$

where $\tilde{t}_{ik,m}^{-\theta}$are the mode specific traversal costs between node i and k. As above, we can express recursively substitute the expected transport across modes between nodes, and obtain,

$$(\tau_{id})^{-\theta} = t_{d-1d}^{-\theta} \sum_{j \in F(i)} t_{ij}^{-\theta} \sum_{j' \in F(j)} \cdots \sum_{k' \in F(d-1)} t_{k'd-1}^{-\theta}$$

by substituting the edge-specific transport cost in terms of the mode-specific cost, we obtain,

$$\begin{aligned}(\tau_{id})^{-\theta} &= \left(\sum_{m \in \mathcal{M}(d-1,d)} \tilde{t}_{d-1d,m}^{-\theta} \right) \sum_{j \in F(i)} \left(\sum_{m \in \mathcal{M}(i,j)} \tilde{t}_{ij,m}^{-\theta} \right) \sum_{j' \in F(j)} \cdots \sum_{k' \in F(d-1)} \left(\sum_{m \in \mathcal{M}(k',d-1)} \tilde{t}_{k'd-1,m}^{-\theta} \right) \\ &= \sum_{r \in \Re_{ij}} \left(\prod_{l=1}^{K} \sum_{m \in \mathcal{M}(r_{l-1},r_l)} \tilde{t}_{r_{l-1},r_l,m}^{-\theta} \right)\end{aligned}$$

where the second line is a concise way of summarizing all possible uni and multi-modal paths along the multi-layered network.Without loss of generality, let us consider the case of two modes - one primary mode where flows originate and terminate, and a secondary mode that is accessible subject to some switching cost. Define the $(N_1 + N_2) \times (N_1 + N_2)$ matrix $\mathbf{A} = \left[a_{ij} \equiv t_{ij}^{-\theta}\right]$. Notice that this adjacency matrix forms a block partitioned matrix, i.e.

$$\mathbf{A} = \begin{bmatrix} \mathbf{A_1} & \mathbf{S} \\ \mathbf{S}' & \mathbf{A_2} \end{bmatrix}$$

where $\mathbf{A_1} = [a_{ij}] = \left[t_{ij}^{-\theta}\right]$ is the adjacency matrix for the primary transportation network, $\mathbf{A_2} = [a_{i'j'}] = \left[t_{i'j'}^{-\theta}\right]$ is the adjacency matrix for the secondary transportation network, and $\mathbf{S} = \left[s_{ii'}^{-\theta}\right]$ is the diagonal matrix that represents linkages between the primary and secondary transportation network. We can write τ_{ij} from by explicitly summing across all possible routes of all possible lengths. To do so, we sum across all locations that are traveled through all the possible paths as follows:

$$\begin{aligned}\tau_{ij}^{-\theta} &= \sum_{r \in \Re_{ij}} \left(\prod_{l=1}^{K} \sum_{m \in \mathcal{M}(r_{l-1},r_l)} \tilde{t}_{r_{l-1},r_l,m}^{-\theta} \right) \\ &= \sum_{K=0}^{\infty} \left(\sum_{k_1=1}^{(N_1+N_2)} \sum_{k_2=1}^{(N_1+N_2)} \cdots \sum_{k_{K-1}=1}^{(N_1+N_2)} a_{i,k_1} \times a_{k_1,k_2} \times \ldots \times a_{k_{K-2},k_{K-1}} \times a_{k_{K-1}j} \right)\end{aligned}$$

explicitly recognizing that this sum across all locations through all possible paths can be partitioned into unimodal paths on each transportation network and an arbitrary number of switches between transportation modes, we have,

$$\tau_{ij}^{-\theta} = \sum_{t_1=1}^{N} \sum_{t_2=1}^{N} \cdots \sum_{t_S=1}^{N} \left(\left(\sum_{K=0}^{\infty} \mathbf{A}_{1,it_1}^{K} \right) \times s_{t_1 t_1'}^{-\theta} \times \ldots \times s_{t_s' t_s}^{-\theta} \left(\sum_{K=0}^{\infty} \mathbf{A}_{1,T_S j}^{K} \right) \right)$$

which in matrix notation can be written as,

$$\tau_{ij}^{-\theta} = \sum_{K=0}^{\infty} \left(\left(\sum_{K=0}^{\infty} \mathbf{A}_1^K \right) \left(\mathbf{S} \left(\sum_{K=0}^{\infty} \mathbf{A}_2^K \right) \mathbf{S}' \right) \right)^K \left(\sum_{K=0}^{\infty} \mathbf{A}_1^K \right)$$

To simplify this expression let us first define the Leontief inverse for each infrastructure matrix separately, i.e.

$$\sum_{K=0}^{\infty} \mathbf{A}_1^K = (\mathbf{I} - \mathbf{A}_1)^{-1} \equiv \mathbf{B}$$

$$\sum_{K=0}^{\infty} \mathbf{A}_2^K = (\mathbf{I} - \mathbf{A}_2)^{-1} \equiv \mathbf{C}$$

We also define - for convenience - the sandwich matrix that adjusts the transport cost along the secondary transportation network for switching costs and therefore traces out the option value of having access to the secondary transportation network,

$$\mathbf{S} \left(\sum_{K=0}^{\infty} \mathbf{A}_2^K \right) \mathbf{S}' \equiv \mathbf{D}$$

From matrix calculus we can restate the following result that relates the inverse of the Schur complement of the partitioned infrastructure matrix to the geometric sum of matrix operations, specifically,

$$\sum_{K=0}^{\infty} \left(\mathbf{B}^{-1} \mathbf{D} \right)^K \mathbf{B}^{-1} = (\mathbf{B} - \mathbf{D})^{-1} \equiv \mathbf{E}$$

applying this result we can write,

$$\begin{aligned} \tau_{ij}^{-\theta} &= \sum_{K=0}^{\infty} \left((\mathbf{I} - \mathbf{A}_1)^{-1} \left(\mathbf{S} (\mathbf{I} - \mathbf{A}_2)^{-1} \mathbf{S}' \right) \right)^K (\mathbf{I} - \mathbf{A}_1)^{-1} \\ &= \left[(\mathbf{I} - \mathbf{A_1}) - \mathbf{S} \left(\mathbf{I} - \mathbf{A_2} \right)^{-1} \mathbf{S}' \right]_{ij}^{-1} \end{aligned}$$

therefore we can write,

$$\tau_{ij} = e_{ij}^{-\frac{1}{\theta}}$$

Furthermore, the Woodbury matrix identity (see e.g. Horn and Johnson (2012)) states,

$$(\mathbf{A} + \mathbf{UCV})^{-1} = \mathbf{A}^{-1} - \mathbf{A}^{-1} \mathbf{U} \left(\mathbf{C}^{-1} + \mathbf{V} \mathbf{A}^{-1} \mathbf{U} \right)^{-1} \mathbf{V} \mathbf{A}^{-1}$$

which implies

$$\begin{aligned} \tau_{ij}^{-\theta} &= \left[(\mathbf{I} - \mathbf{A_1}) - \mathbf{S} \left(\mathbf{I} - \mathbf{A_2} \right)^{-1} \mathbf{S}' \right]_{ij}^{-1} \\ &= \left[\mathbf{B} + \mathbf{B} \mathbf{S} \left(\mathbf{A} / \mathbf{A_1} \right)^{-1} \mathbf{S}' \mathbf{B} \right]_{ij} \\ &= \left[(\mathbf{I} - \mathbf{A_1})^{-1} + (\mathbf{I} - \mathbf{A_1})^{-1} \mathbf{S} \left(\mathbf{A} / \mathbf{A_1} \right)^{-1} \mathbf{S}' \left(\mathbf{I} - \mathbf{A_1} \right)^{-1} \right]_{ij} \end{aligned}$$

where $\mathbf{A}/\mathbf{A_1} := (\mathbf{I} - \mathbf{A_1})^{-1} - \mathbf{S} \left(\mathbf{A} / \mathbf{A_1} \right)^{-1} \mathbf{S}'$ defines the Schur complement of the adjacency matrix A. The expressions corresponds to the expression given in the main text and intuitively decomposes the transport cost into a component that originates from the unimodal paths and another component that originates from the multimodal paths. This result can also directly be obtained by applying to the partitioned matrix A the formula for the inverse of block-partitioned matrices (see e.g. Horn and Johnson (2012)).

B.5 Section 3.3.2: Modal Traffic Flows

We characterize equilibrium traffic at different nodes of the transportation network. First, we utilize the recursive routing choice to characterize aggregate traffic between any two nodes across any mode. Second, we characterize mode-specific traffic between nodes. Finally, we characterize traffic at terminal stations.

B.5.1 Traffic on the aggregate transport network

We start by characterizing the aggregate traffic between any two nodes across any mode. To do so we start by restating the (recursively defined) sourcing and link choice probability which is given by:

$$\pi_{ij,k} = \frac{\left(w_i/A_i\right)^{-\theta}\left(t_{jk}\tau_{ki}\right)^{-\theta}}{\sum_{i\in\mathcal{N}}\left(w_i/A_i\right)^{-\theta}\sum_{k'\in\mathcal{F}(i)}\left(t_{jk'}\tau_{k'i}\right)^{-\theta}}$$

which can be decomposed in the sourcing share and the link choice probability conditional on the sourcing choice, i.e.

$$\begin{aligned}
\pi_{ij,kl} &= \frac{\left(t_{ik}\tau_{ki}\right)^{-\theta}}{\sum_{k'\in\mathcal{F}(i)}\left(t_{ik'}\tau_{k'i}\right)^{-\theta}}\frac{\tau_{ij}^{-\theta}p_i^{-\theta}}{\sum_{i\in\mathcal{N}}\tau_{ij}^{-\theta}p_i^{-\theta}} \\
&= \frac{\left(t_{ik}\tau_{ki}\right)^{-\theta}}{\tau_{ij}^{-\theta}}\frac{\tau_{ij}^{-\theta}p_i^{-\theta}}{\sum_{i\in\mathcal{N}}\tau_{ij}^{-\theta}p_i^{-\theta}} \\
&= \pi_{ij}^{k}\times\pi_{ij}
\end{aligned}$$

The previous derivations only characterize the probability of choosing neighboring link k when routing between i and j. Notice that we can construct the probability of using any edge kl when transporting goods from i to j in straightforward way, i.e.

$$\begin{aligned}
\pi_{kj}^{kl} &= \frac{t_{kl}^{-\theta}\tau_{lj}^{-\theta}}{\tau_{kj}^{-\theta}} \\
&= \frac{\tau_{ik}^{-\theta}t_{kl}^{-\theta}\tau_{lj}^{-\theta}}{\tau_{ik}^{-\theta}\tau_{kj}^{-\theta}} \\
&= \frac{\tau_{ik}^{-\theta}t_{kl}^{-\theta}\tau_{lj}^{-\theta}}{\tau_{ij}^{-\theta}} \\
&= \pi_{ij}^{kl}
\end{aligned}$$

Notice that this arises naturally due to the markovian property of the recursive routing choice. To characterize traffic between nodes k and l along any mode, we characterize the share of goods that are being sourced from any location i to any location j and use the link kl along the way, i.e.

$$\begin{aligned}
\Xi_{kl} &= \sum_{i\in\mathcal{N}}\sum_{j\in\mathcal{N}}\pi_{ij,kl}E_j \iff \\
\Xi_{kl} &= \sum_{i\in\mathcal{N}}\sum_{j\in\mathcal{N}}\pi_{ij}^{kl}X_{ij} \iff \\
\Xi_{kl} &= \sum_{i\in\mathcal{N}}\sum_{j\in\mathcal{N}}\frac{\tau_{ik}^{-\theta}t_{kl}^{-\theta}\tau_{lj}^{-\theta}}{\tau_{ij}^{-\theta}}\times\tau_{ij}^{-\theta}\frac{Y_i}{\Pi_i^{-\theta}}\frac{E_j}{P_j^{-\theta}} \iff \\
\Xi_{kl} &= t_{kl}^{-\theta}\sum_{i\in\mathcal{N}}\tau_{ik}^{-\theta}\frac{Y_i}{\Pi_i^{-\theta}}\sum_{j\in\mathcal{N}}\tau_{lj}^{-\theta}\frac{E_j}{P_j^{-\theta}}, \\
\Xi_{kl} &= t_{kl}^{-\theta}\times P_k^{-\theta}\times\Pi_l^{-\theta}
\end{aligned}$$

where in the last line we used the definition of the consumer and producer market access terms. Furthermore,

replacing market access terms,

$$P_i = \frac{1}{\bar{W}} \bar{u}_i L_i^{\beta-1} Y_i$$
$$\Pi_i = \bar{A}_i L_i^{1+\alpha} Y_i^{-\frac{\theta+1}{\theta}}$$

we obtain,

$$\begin{aligned}
\Xi_{kl} &= t_{kl}^{-\theta} \times \left(\frac{1}{\bar{W}} \bar{u}_k L_k^{\beta-1} Y_k \right)^{-\theta} \times \left(\bar{A}_l L_l^{1+\alpha} Y_l^{-\frac{\theta+1}{\theta}} \right)^{-\theta} \\
&= t_{kl}^{-\theta} \left(\frac{\bar{L}^{-(\alpha+\beta)\theta}}{W^{-\theta}} \right) \bar{L} \bar{A}_l^{-\theta} \bar{u}_k^{-\theta} l_k^{-\theta(\beta-1)} l_l^{-\theta(1+\alpha)} y_k^{-\theta} y_l^{(1+\theta)} \\
&= t_{kl}^{-\theta} \chi \bar{L} \bar{A}_l^{-\theta} \bar{u}_k^{-\theta} l_k^{-\theta(\beta-1)} l_l^{-\theta(1+\alpha)} y_k^{-\theta} y_l^{(1+\theta)}
\end{aligned}$$

where in the last line we use the definition $\chi = \frac{\bar{L}^{(\alpha+\beta)\theta}}{W^{\theta}}$. We have,

$$\Xi_{kl} = t_{kl}^{-\theta} \chi^{-1} \bar{L} \bar{A}_l^{-\theta} \bar{u}_k^{-\theta} l_k^{-\theta} l_l^{-\theta} y_k^{-\theta} y_l^{(1+\theta)}$$

which characterizes aggregate flows between neighboring nodes k and l in terms of the endogenous variables along the network.

B.5.2 Mode-specific traffic

In the next step we now turn towards characterizing the probability of sourcing from location j to location i choosing neighboring node k as the cost-minimizing routing choice and furthermore opting for mode m between node i and k. The nested choice implies that this choice probability is given by,

$$\pi_{ijk,m} = \frac{\tilde{t}_{ik,m}^{-\eta}}{t_{ik}^{-\eta}} \frac{\left(t_{ik}\tau_{kj}\right)^{-\theta} p_i^{-\theta}}{\sum_{i \in \mathcal{N}} \tau_{ij}^{-\theta} p_i^{-\theta}}$$

which can be decomposed in the sourcing share, link choice probability conditional on sourcing choice, and the modal share conditional on both sourcing and link choice, i.e.

$$\begin{aligned}
\pi_{ij,kl,m} &= \frac{\tilde{t}_{ik,m}^{-\eta}}{t_{ik}^{-\eta}} \frac{\left(t_{ik}\tau_{ki}\right)^{-\theta}}{\sum_{k' \in \mathcal{F}(i)} \left(t_{ik'}\tau_{k'i}\right)^{-\theta}} \frac{\tau_{ij}^{-\theta} p_i^{-\theta}}{\sum_{i \in \mathcal{N}} \tau_{ij}^{-\theta} p_i^{-\theta}} \\
&= \pi_{ik}^{m} \times \pi_{ij}^{k} \times \pi_{ij}
\end{aligned}$$

We can apply similar calculations as above to extend this for any link kl when transporting goods from i to j, i.e.

$$\pi_{ij,kl,m} = \frac{\tilde{t}_{kl,m}^{-\eta}}{t_{kl}^{-\eta}} \frac{\tau_{ik}^{-\theta} t_{kl}^{-\theta} \tau_{lj}^{-\theta}}{\tau_{ij}^{-\theta}} \frac{\tau_{ij}^{-\theta} p_i^{-\theta}}{\sum_{i \in \mathcal{N}} \tau_{ij}^{-\theta} p_i^{-\theta}}$$

Given this choice probability we can characterize the mode-specific traffic between neighboring nodes k and

l, i.e.

$$\begin{aligned}
\Xi_{kl,m} &= \sum_{i\in\mathcal{N}}\sum_{j\in\mathcal{N}} \pi_{ijk,m} E_j \iff \\
&= \sum_{i\in\mathcal{N}}\sum_{j\in\mathcal{N}} \pi^m_{ik} \times \pi^k_{ij} \times X_{ij} \\
&= \frac{\tilde{t}^{-\eta}_{kl,m}}{t^{-\eta}_{kl}} \sum_{i\in\mathcal{N}}\sum_{j\in\mathcal{N}} \frac{\tau^{-\theta}_{ik} t^{-\theta}_{kl} \tau^{-\theta}_{lj}}{\tau^{-\theta}_{ij}} \times \tau^{-\theta}_{ij} \frac{Y_i}{\Pi^{-\theta}_i} \frac{E_j}{P^{-\theta}_j} \iff \\
&= \frac{\tilde{t}^{-\eta}_{kl,m}}{t^{-\eta}_{kl}} \times t^{-\theta}_{kl} \sum_{i\in\mathcal{N}} \tau^{-\theta}_{ik} \frac{Y_i}{\Pi^{-\theta}_i} \sum_{j\in\mathcal{N}} \tau^{-\theta}_{lj} \frac{E_j}{P^{-\theta}_j}, \\
&= \frac{\tilde{t}^{-\eta}_{kl,m}}{t^{-\eta}_{kl}} \times t^{-\theta}_{kl} \times P^{-\theta}_k \times \Pi^{-\theta}_l \\
&= \tilde{t}^{-\eta}_{kl,m} \times t^{\eta-\theta}_{kl} \times P^{-\theta}_k \times \Pi^{-\theta}_l
\end{aligned}$$

which gives us an expression for mode-specific traffic in terms of market access measures and the aggregate and mode specific iceberg transport cost along the edge. Note, that the nested formulation implies that mode-specific traffic is the conditional mode specific share of aggregate traffic, i.e. $\Xi_{kl,m} = \pi^m_{ik} \times \Xi_{kl}$.

B.5.3 Traffic at Terminals

In the final step we characterize the traffic at mode-specific terminals that allow multimodal movements between nodes kl. To do so we start by characterizing the probability of sourcing from location j to location i choosing any neighboring node $k' \in \mathcal{F}(i)$, but crucially choosing an alternative non-primary mode of transport and therefore traversing through a terminal while routing. This choice probability can be characterized in the following way,

$$\begin{aligned}
\pi_{ij,kk,m} &= \sum_{k\in\mathcal{F}(i)} \frac{\tilde{t}^{-\eta}_{ik,m}}{t^{-\eta}_{ik}} \frac{t^{-\theta}_{ik} \tau^{-\theta}_{kj} p^{-\theta}_j}{\sum_{j\in 0}\sum_{k'} t_{ik}\tau_{k_j j} p^{-\theta}_j} \\
&= s^{-\eta}_{ii} \sum_{k\in\mathcal{F}(i)} \frac{\left(\tau_{ik} s_{kk,m}\right)^{-\eta}}{t^{-\eta}_{ik}} \frac{t^{-\theta}_{ik} \tau^{-\theta}_{kj} p^{-\theta}_j}{\sum_{j\in 0}\sum_{k'} t_{ik}\tau_{k_j j} p^{-\theta}_j}
\end{aligned}$$

which can be decomposed into which can again be decomposed into sourcing shares, link choice shares conditional on sourcing choice, and mode choice conditional on link choice, i.e.

$$\begin{aligned}
\pi_{ij,kk,m} &= \sum_{k\in\mathcal{F}(i)} \frac{s^{-\eta}_{ii}\left(\tau_{ik} s_{kk,m}\right)^{-\eta}}{t^{-\eta}_{ik}} \frac{\left(t_{ik}\tau_{ki}\right)^{-\theta}}{\sum_{k'\in\mathcal{F}(i)}\left(t_{ik'}\tau_{k'i}\right)^{-\theta}} \frac{\tau^{-\theta}_{ij} p^{-\theta}_i}{\sum_{i\in\mathcal{N}} \tau^{-\theta}_{ij} p^{-\theta}_i} \\
&= \pi_{ij} \sum_{k\in\mathcal{F}(i)} \pi^m_{ik} \times \pi^k_{ij}
\end{aligned}$$

We can apply similar calculations as above to extend this for any link kl when transporting goods from i to j, i.e.

$$\begin{aligned}
\pi_{ij,kk,m} &= \sum_{l\in\mathcal{F}(k)} \frac{s^{-\eta}_{kk}\left(\tau_{kl} s_{ll,m}\right)^{-\eta}}{t^{-\eta}_{kl}} \frac{\tau^{-\theta}_{ik} t^{-\theta}_{kl} \tau^{-\theta}_{lj}}{\tau^{-\theta}_{ij}} \frac{\tau^{-\theta}_{ij} p^{-\theta}_i}{\sum_{i\in\mathcal{N}} \tau^{-\theta}_{ij} p^{-\theta}_i} \\
&= \pi_{ij} \sum_{l\in\mathcal{F}(k)} \pi^m_{kl} \times \pi^{kl}_{ij}
\end{aligned}$$

Given this choice probability we can characterize the mode-specific traffic between neighboring nodes k and

l, i.e.

$$\begin{aligned}
\Xi_{kk,m} &= \sum_{i\in\mathcal{N}}\sum_{j\in\mathcal{N}} \pi_{ij,kk,m} E_j \iff \\
&= \sum_{i\in\mathcal{N}}\sum_{j\in\mathcal{N}} \left(\sum_{l\in\mathcal{F}(k)} \pi_{kl}^{m} \times \pi_{ij}^{kl} \right) \times X_{ij} \\
&= \sum_{l\in\mathcal{F}(k)} \frac{s_{kk}^{-\eta}\left(\tau_{kl} s_{ll,m}\right)^{-\eta}}{t_{kl}^{-\eta}} \sum_{i\in\mathcal{N}}\sum_{j\in\mathcal{N}} \frac{\tau_{ik}^{-\theta} t_{kl}^{-\theta} \tau_{lj}^{-\theta}}{\tau_{ij}^{-\theta}} \times \tau_{ij}^{-\theta} \frac{Y_i}{\Pi_i^{-\theta}} \frac{E_j}{P_j^{-\theta}} \iff \\
&= \sum_{l\in\mathcal{F}(k)} \frac{s_{kk}^{-\eta}\left(\tau_{kl} s_{ll,m}\right)^{-\eta}}{t_{kl}^{-\eta}} \times t_{kl}^{-\theta} \sum_{i\in\mathcal{N}} \tau_{ik}^{-\theta} \frac{Y_i}{\Pi_i^{-\theta}} \sum_{j\in\mathcal{N}} \tau_{lj}^{-\theta} \frac{E_j}{P_j^{-\theta}}, \\
&= \sum_{l\in\mathcal{F}(k)} \frac{s_{kk}^{-\eta}\left(\tau_{kl} s_{ll,m}\right)^{-\eta}}{t_{kl}^{-\eta}} \times t_{kl}^{-\theta} \times P_k^{-\theta} \times \Pi_l^{-\theta} \\
&= s_{kk}^{-\eta} \times P_k^{-\theta} \times \sum_{l\in\mathcal{F}(k)} \left(\tau_{kl} s_{ll,m}\right)^{-\eta} \times t_{kl}^{\eta-\theta} \times \Pi_l^{-\theta}
\end{aligned}$$

B.5.4 Traffic with congestion: Primary Mode of transportation

Incorporating congestion, for the primary mode of transport ($m = 0$), we have the following relationship,

$$\begin{aligned}
t_{kl,0} &= \bar{t}_{kl,0} \left[\Xi_{ij,0}\right]^{\lambda_0} \iff \\
t_{kl,0} &= \bar{t}_{kl,0} \left[t_{kl,0}^{-\eta} \times t_{kl}^{\eta-\theta} \times P_k^{-\theta} \times \Pi_l^{-\theta} \right]^{\lambda_0} \iff \\
t_{kl,0} &= \bar{t}_{kl,0} \times t_{kl,0}^{-\eta\lambda_0} \times t_{kl}^{\lambda_0(\eta-\theta)} \times P_k^{-\theta\lambda_0} \times \Pi_l^{-\theta\lambda_0} \iff \\
t_{kl,0}^{1+\eta\lambda_0} &= \bar{t}_{kl,0} \times t_{kl}^{\lambda_0(\eta-\theta)} \times P_k^{-\theta\lambda_0} \times \Pi_l^{-\theta\lambda_0} \iff \\
t_{kl,0} &= \bar{t}_{kl,0}^{\frac{1}{1+\eta\lambda_0}} \times t_{kl}^{\frac{\lambda_0(\eta-\theta)}{1+\eta\lambda_0}} \times P_k^{\frac{-\theta\lambda_0}{1+\eta\lambda_0}} \times \Pi_l^{\frac{-\theta\lambda_0}{1+\eta\lambda_0}}
\end{aligned}$$

Replacing to derive the expression for traffic,

$$\begin{aligned}
\Xi_{kl,0} &= \left(\bar{t}_{kl,0}^{\frac{1}{1+\theta\lambda_1}} \times t_{kl}^{\frac{\lambda_0(\eta-\theta)}{1+\eta\lambda_0}} \times P_k^{-\frac{\theta\lambda_1}{1+\theta\lambda_1}} \times \Pi_l^{-\frac{\theta\lambda_1}{1+\theta\lambda_1}} \right)^{-\theta} \times P_k^{-\theta} \times \Pi_l^{-\theta}, \\
&= \bar{t}_{kl}^{-\frac{\theta}{1+\theta\lambda_1}} \times t_{kl}^{\frac{-\theta\lambda_0(\eta-\theta)}{1+\eta\lambda_0}} \times P_k^{\frac{\theta\theta\lambda_1}{1+\theta\lambda_1}-\theta} \times \Pi_l^{\frac{\theta\lambda_1\theta}{1+\theta\lambda_1}-\theta} \\
&= \bar{t}_{kl}^{-\frac{\theta}{1+\theta\lambda_1}} \times t_{kl}^{\frac{-\theta\lambda_0(\eta-\theta)}{1+\eta\lambda_0}} \times P_k^{-\frac{\theta}{1+\theta\lambda_1}} \times \Pi_l^{-\frac{\theta}{1+\theta\lambda_1}}
\end{aligned}$$

For any secondary mode of transportation, we have instead congestion at terminal stations. Let us characterize the transport cost net of congestion at any terminal, i.e.

$$
\begin{aligned}
s_{kk,m} &= \bar{s}_{kk,m} \left[\Xi_{kk,m}\right]^{\lambda_m} \\
s_{kk,m} &= \bar{s}_{kk,m} \left[s_{kk,m}^{-\eta} \times P_k^{-\theta} \times \sum_{l \in \mathcal{F}(k)} \left(\tau_{kl} s_{ll,m}\right)^{-\eta} \times t_{kl}^{\eta-\theta} \times \Pi_l^{-\theta} \right]^{\lambda_m} \\
s_{kk,m} &= \bar{s}_{kk,m} \times s_{kk,m}^{-\eta\lambda_m} \times P_k^{-\theta\lambda_m} \times \left(\sum_{l \in \mathcal{F}(k)} \left(\tau_{kl} s_{ll,m}\right)^{-\eta} \times t_{kl}^{\eta-\theta} \times \Pi_l^{-\theta} \right)^{\lambda_m} \\
s_{kk,m}^{1+\eta\lambda_m} &= \bar{s}_{kk,m} \times P_k^{-\theta\lambda_m} \times \left(\sum_{l \in \mathcal{F}(k)} \left(\tau_{kl} s_{ll,m}\right)^{-\eta} \times t_{kl}^{\eta-\theta} \times \Pi_l^{-\theta} \right)^{\lambda_m} \\
s_{kk,m} &= \bar{s}_{kk,m}^{1+\eta\lambda_m} \times P_k^{\frac{-\theta\lambda_m}{1+\eta\lambda_m}} \times \left(\sum_{l \in \mathcal{F}(k)} \left(\tau_{kl} s_{ll,m}\right)^{-\eta} \times t_{kl}^{\eta-\theta} \times \Pi_l^{-\theta} \right)^{\frac{\lambda_m}{1+\eta\lambda_m}} \\
s_{kk,m} &= \bar{s}_{kk,m}^{\frac{1}{1+\eta\lambda_m}} \times P_k^{\frac{-\theta\lambda_m}{1+\eta\lambda_m}} \times \left(\sum_{l \in \mathcal{F}(k)} \left(\tau_{kl} s_{ll,m}\right)^{-\eta} \times t_{kl}^{\eta-\theta} \times \Pi_l^{-\theta} \right)^{\frac{\lambda_m}{1+\eta\lambda_m}}
\end{aligned}
$$

Combining both the switching cost of access the non-primary transport network and the terminal cost of exiting it again, we obtain,

$$
\begin{aligned}
\tilde{t}_{kl,m} &= \bar{s}_{kk,m} \tau_{kl,m} \bar{s}_{ll,m} \left[\Xi_{kk,m}\right]^{\lambda_m} \left[\Xi_{ll,m}\right]^{\lambda_m} \\
&= \bar{s}_{kk,m} \tau_{kl,m} \bar{s}_{ll,m} \left[\sum_{l \in \mathcal{F}(k)} \Xi_{kl,m} \right]^{\lambda_m} \left[\sum_{k \in \mathcal{B}(l)} \Xi_{kl,m} \right]^{\lambda_m} \\
&= \bar{s}_{kk,m} \tau_{kl,m} \bar{s}_{ll,m} \left[P_k^{-\theta} \times \sum_{l \in \mathcal{F}(k)} \tilde{t}_{kl,m}^{-\eta} \times t_{kl}^{\eta-\theta} \times \Pi_l^{-\theta} \right]^{\lambda_m} \left[\Pi_l^{-\theta} \times \sum_{k \in \mathcal{B}(l)} \tilde{t}_{kl,m}^{-\eta} \times t_{kl}^{\eta-\theta} \times P_k^{-\theta} \right]^{\lambda_m} \\
&= \bar{s}_{kk,m} \tau_{kl,m} \bar{s}_{ll,m} \left[P_k^{-\theta} \times \Pi_{k,m}^{-\theta} \right]^{\lambda_m} \left[\Pi_l^{-\theta} \times P_{l,m}^{-\theta} \right]^{\lambda_m} \\
&= \bar{s}_{kk,m} \times \tau_{kl,m} \times \bar{s}_{ll,m} \times P_k^{-\theta\lambda_m} \times \Pi_l^{-\theta\lambda_m} \times P_{k,m}^{-\theta\lambda_m} \times \Pi_{l,m}^{-\theta\lambda_m}
\end{aligned}
$$

where $P_{l,m} \equiv \sum_{k \in \mathcal{B}(l)} t_{kl,m}^{-\eta} \times t_{kl}^{\eta-\theta} \times P_k^{-\theta}$ and $\Pi_{k,m} \equiv \sum_{l \in \mathcal{F}(k)} t_{kl,m}^{-\eta} \times t_{kl}^{\eta-\theta} \times \Pi_l^{-\theta}$.

C Data and Additional Results

C.1 Data Appendix

C.1.1 AIS Vessel Traffic Data

USACE only captures draft if it's for ships carrying foreign cargo since they have to report with customs. Our AIS data captures all ships big and small maybe going empty so have more ships but no draft measure.

We highlight two examples to show how we capture these ships and the time they spend at a port. Panel (A) Figure A.2 shows the path of containership CMA CGM Christophe Colomb as it enters the Port of Los Angeles (LA) on May 2, 2022. It is a containership with a cargo capacity of 86,100 tons (13,800 twenty-foot equivalent unit containers (TEUs)) and is operated by container shipping company CMA CGM. Panel (B) Figure A.2 shows the path of containership Guthorm Maersk entering and leaving the Port of Newark. Guthorm Maersk is a containership with a cargo capacity of 57,000 tons (11,000 TEUs) and is operated by container shipping company Maersk. The ship path entering the port is highlighted in the figure and the redder color indicates slower speed. The darker region of both figures indicate the port polygon for both ports as defined by the US Army Corps of Engineers.

C.1.2 Ports

While we include the top 30 container ports in the US in our analysis, we merge some of these ports into the one polygon due to the USACE-provided polygons either overlapping or being very close to each other. Specifically, Tacoma + Seattle are merged into a single polygon due to their port alliance (NWSA). Additionally, Tacoma and Seattle share a port alliance. Tampa + Manatee were merged do to overlap issues between the rather large Tampa region and the manually applied Manatee port statistical area. Lastly, we include Chester in the Philadelphia PSA because the USACE-provided polygon area includes Chester. All in all, we have 27 unique ports.

C.1.3 Rail Traffic Data

C.1.4 Rail Dwell Times Data

We obtain weekly rail station dwell times from the Surface Transportation Board (STB). Railroads provide the STB with the average time a railcar resides at a station, measured in hours, for their 10 largest stations in terms of railcars processed. This dwell time measure excludes cars on through trains—trains that travels without stops en route. Since this dataset only captures a subset of all rail stations (albeit the largest ones), we match the ports in the previous section to their local rail stations. We do this by expanding the port polygon areas in 50km intervals. The rail stations that are captured in the buffer areas of their closest port is be considered a rail station in the vicinity of this port and is likely to service traffic to and from the port. Due to their proximity, The ports of Los Angeles and Long Beach and combined into one port for this exercise. We use a buffer area of 150km which captures 7 ports and 12 rail stations. We test the robustness of this buffer area by increasing the interval in our analysis to 200km where we capture 8 ports and 14 rail stations. Further increases to this interval result in more muted responses of rail station dwell times to port traffic, as these rail stations are much further away.

Additionally, the rail dwell times dataset is reported at the weekly level. In order to match this to our daily port traffic measure for analysis, we aggregate our port traffic measure up to the weekly level. We start our week on a Monday since we observe in our data that most ships tend to enter a port on Mondays.

Summary Statistics Figure A.3 plots the average of rail station dwell times from June 2015 to December 2021. The average dwell time over this period is around 25.5 hours per station with a standard deviation of 2.5 hours. However, there is also a large decrease in dwell times around the start of the pandemic followed up a steep increase afterwards.

C.1.5 Matching Rail Traffic Data to MSAs

Using 1999 MSA polygons from the Census Bureau, we match the rail stations from the Waybill data to the 228 MSAs in Duranton and Turner (2011). By rail destination, we observe 224 MSAs and by origin we observe 223 MSAs. Since some of these unobserved MSAs overlap, we have 7 MSAs. We conduct our analysis on the

Figure A.2. Illustration of AIS Mooring Paths

(a) Port of Los Angeles

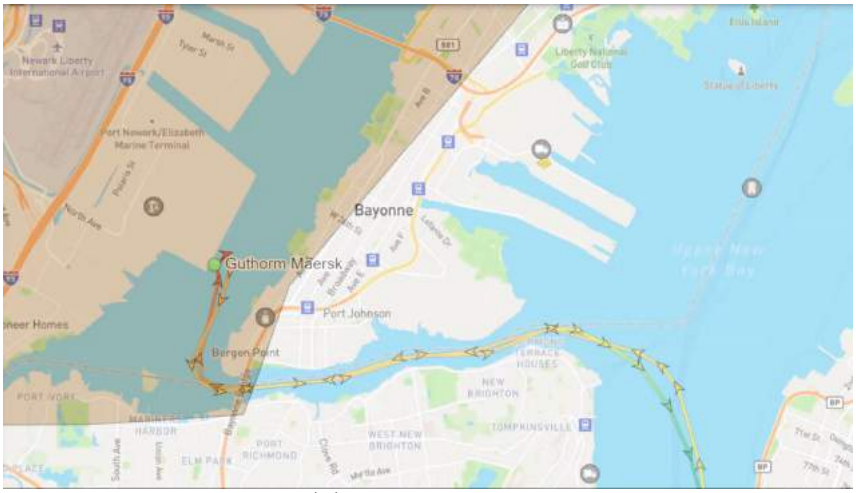

(b) Port of Newark

Notes: Panel (a) shows the containership CMA CGM Christophe Colomb at the Port of Los Angeles while Panel (b) shows the containership Guthorm Maersk at the Port of Newark. The path of each ship to and from the port shows its exact travel path. The darker regions at each port shows the port polygons as defined by the US Army Corps of Engineers.

remaining 221 MSAs, so that both the origin and destination results are comparable. The 7 MSAs that we do not have rail traffic for Daytona Beach FL, Fort Myers-Cape Coral FL, Fort Walton Beach FL, New Haven-Bridgeport-Stamford-Waterbury-Danbury CT, Providence-Warwick-Pawtucket RI, Punta Gorda FL, and Santa Fe NM.

To match the MSA-level truck vehicle-kilometers traveled (VKT) measure in Duranton and Turner (2011), we calculate the rail equivalent in two ways. First, we utilize the number of rail carloads, transported in and out of MSAs, multiplied by the weighted average of their distance traveled. We call this railcar-kilometers-traveled (rail VKT) and distinguish by destination for rail shipments transported into these MSAs, and by origin for shipments transported out of these MSAs. We also observe the weight of these rail shipments and can calculate rail weight VKT using the same method outlined previously.

Figure A.3. Rail Station Dwell Times

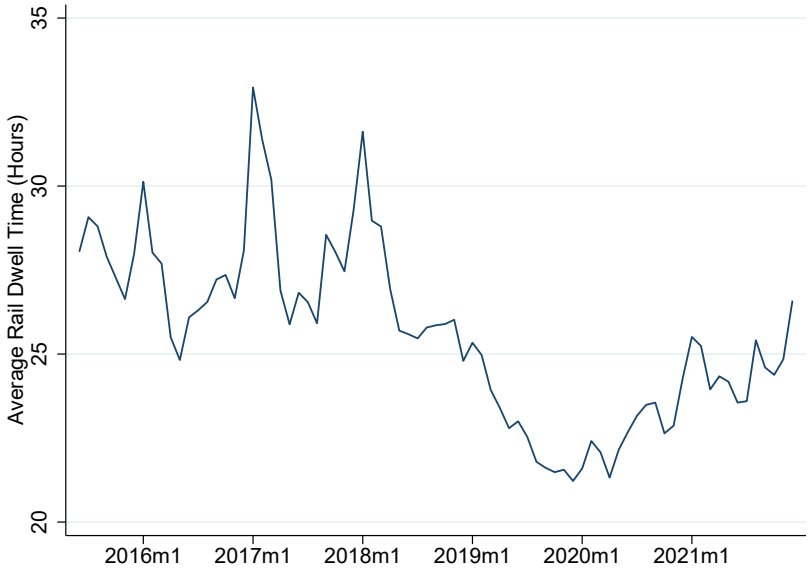

Notes: This figure plots the average time a railcar spends at a rail station from June 2015 to July 2022.

C.2 Modal Diversion: Additional Results

Since we have a slightly smaller set of MSAs due to the matching process between MSAs and our rail traffic data (see Section C.1.5 for more information), we first show that we are able to replicate the Duranton and Turner (2011) results in Table 5. We find that our fixed effects and IV estimates have the same sign and are within one standard deviation of the results from Duranton and Turner (2011) (Columns (6) to (10), Table 9, Duranton and Turner (2011)).[1]

[1] First stage results are in Table A.3.

Table. A.3. Elasticity of Truck VKT with respect to Interstate Highway Lane Kilometers: First Stage

	(1)	(2)	(3)
1898 Railroads	0.0879*	0.0939*	0.119**
	(0.0460)	(0.0499)	(0.0474)
1947 Planned Interstates	0.156***	0.127***	0.114***
	(0.0332)	(0.0322)	(0.0284)
1835 Exploration Routes	0.0249**	0.0268**	0.0222*
	(0.0117)	(0.0124)	(0.0122)
Population	0.516***	0.599***	0.545***
	(0.0393)	(0.0481)	(0.0597)
Geography		✓	✓
Census Divisions		✓	✓
Socioeconomic Characteristics			✓
Year FE	✓	✓	✓
Observations	663	663	663
KP F-stat	13.48	10.08	10.02

***Notes*:** Robust standard errors clustered by MSAs in parentheses. All variables are in logs. Instruments are 1835 exploration routes, 1898 railroad route kilometers, and 1947 planned interstate highways. 663 observations corresponding to 221 MSAs for each regression.

Table. A.4. Elasticity of Rail Traffic Use (in Railcar-Kilometers) with respect to Road Infrastructure Improvements: First Stage

	(1)	(2)	(3)
1898 Railroads	0.0879*	0.0939*	0.119**
	(0.0460)	(0.0499)	(0.0474)
1947 Planned Interstates	0.156***	0.127***	0.114***
	(0.0332)	(0.0322)	(0.0284)
1835 Exploration Routes	0.0249**	0.0268**	0.0222*
	(0.0117)	(0.0124)	(0.0122)
Population	0.516***	0.599***	0.545***
	(0.0393)	(0.0481)	(0.0597)
Geography		✓	✓
Census Divisions		✓	✓
Socioeconomic Characteristics			✓
Year FE	✓	✓	✓
Observations	663	663	663
KP F-stat	13.48	10.08	10.02

***Notes*:** Robust standard errors clustered by MSAs in parentheses. All variables are in logs. Instruments are ln 1835 exploration routes, ln 1898 railroads, and ln 1947 planned interstates; 684 observations corresponding to 228 MSAs for each regression.

Table. A.5. Elasticity of Rail to Truck Traffic Use by Destination with respect to Road Infrastructure Improvements

	(1) OLS	(2) OLS	(3) IV	(4) IV	(5) IV
Inter-State Highway Lane KM	-1.060***	-1.061***	-1.101***	-1.210***	-0.999**
	(0.185)	(0.185)	(0.405)	(0.426)	(0.405)
Population		0.0605	1.132***	1.303***	1.145***
		(0.337)	(0.298)	(0.351)	(0.336)
Geography				✓	✓
Census Divisions				✓	✓
Socioeconomic Characteristics		✓			✓
MSA FE	✓	✓			
Year FE	✓	✓	✓	✓	✓
Observations	658	658	658	658	658
R-squared	0.89	0.89	0.04	0.21	0.24
KP F-stat			14.48	10.76	10.04

Notes: * $p < 0.1$, ** $p < 0.05$, *** $p < 0.01$. Robust standard errors clustered by MSAs in parentheses. All variables are in logs. Rail traffic use, measured in railcar-kilometers, is constructed using confidential rail waybill data. Truck traffic use (in vehicle-kilometers) and other variables are from Duranton and Turner (2011). Instruments are 1835 exploration routes, 1898 railroad route kilometers, and 1947 planned interstate highways. 663 observations corresponding to 221 MSAs for each regression. See Table A.18 for first stage regressions.

Table. A.6. Elasticity of Rail Car Traffic-Kilometers by Destination with respect to Interstate Highway Lane Kilometers

Rail Traffic Use by Destination (railcar-km)	(1) OLS	(2) OLS	(3) IV	(4) IV	(5) IV
Interstate Highway Lane (km)	0.181	0.187	0.225	0.295	0.525
	(0.113)	(0.114)	(0.417)	(0.466)	(0.465)
Population		0.548**	1.110***	1.086***	0.986**
		(0.247)	(0.307)	(0.380)	(0.380)
Geography				✓	✓
Census Divisions				✓	✓
Socioeconomic Characteristics		✓			✓
MSA FE	✓	✓			
Year FE	✓	✓	✓	✓	✓
Observations	663	663	663	663	663
R-squared	0.95	0.95	-	-	-
KP F-stat			13.48	10.08	10.02

Notes: * $p < 0.1$, ** $p < 0.05$, *** $p < 0.01$. Robust standard errors clustered by MSAs in parentheses. All variables are in logs. Instruments are 1835 exploration routes, 1898 railroad route kilometers, and 1947 planned interstate highways. 663 observations corresponding to 221 MSAs for each regression. See Table A.7 for first stage regressions.

Table. A.7. Elasticity of Rail Traffic Use (in Railcar-Kilometers) by Destination with respect to Road Infrastructure Improvements: First Stage

	(1)	(2)	(3)
1898 Railroads	0.0879*	0.0939*	0.119**
	(0.0460)	(0.0499)	(0.0474)
1947 Planned Interstates	0.156***	0.127***	0.114***
	(0.0332)	(0.0322)	(0.0284)
1835 Exploration Routes	0.0249**	0.0268**	0.0222*
	(0.0117)	(0.0124)	(0.0122)
Population	0.516***	0.599***	0.545***
	(0.0393)	(0.0481)	(0.0597)
Geography		✓	✓
Census Divisions		✓	✓
Socioeconomic Characteristics			✓
Year FE	✓	✓	✓
Observations	663	663	663
KP F-stat	13.48	10.08	10.02

***Notes*:** Robust standard errors clustered by MSAs in parentheses. All variables are in logs. Instruments are ln 1835 exploration routes, ln 1898 railroads, and ln 1947 planned interstates; 684 observations corresponding to 228 MSAs for each regression.

Table. A.8. Elasticity of Rail Traffic Use (in railcar-km) by Origin with respect to Road Infrastructure Improvements

	(1)	(2)	(3)	(4)	(5)
Rail Traffic Use by Origin (railcar-km)	OLS	OLS	IV	IV	IV
Interstate Highway Lane (km)	0.197	0.200	0.630*	0.230	0.231
	(0.122)	(0.123)	(0.380)	(0.347)	(0.332)
Population		0.266	0.474	0.923***	0.905***
		(0.374)	(0.296)	(0.302)	(0.295)
Geography				✓	✓
Census Divisions				✓	✓
Socioeconomic Characteristics		✓			✓
MSA FE	✓	✓			
Year FE	✓	✓	✓	✓	✓
Observations	663	663	663	663	663
R-squared	0.94	0.94	-	-	-
KP F-stat			13.48	10.08	10.02

Notes: * $p < 0.1$, ** $p < 0.05$, *** $p < 0.01$. Robust standard errors clustered by MSAs in parentheses. All variables are in logs. Rail traffic use is constructed using the confidential rail waybill data. All other variables are from Duranton and Turner (2011). Instruments are 1835 exploration routes, 1898 railroad route kilometers, and 1947 planned interstate highways. 663 observations corresponding to 221 MSAs for each regression. See Table A.15 for first stage regressions.

Table. A.9. Elasticity of Rail Traffic Use (in Railcar-Kilometers) by Origin with respect to Road Infrastructure Improvements: First Stage

	(1)	(2)	(3)
1898 Railroads	0.0879*	0.0939*	0.119**
	(0.0460)	(0.0499)	(0.0474)
1947 Planned Interstates	0.156***	0.127***	0.114***
	(0.0332)	(0.0322)	(0.0284)
1835 Exploration Routes	0.0249**	0.0268**	0.0222*
	(0.0117)	(0.0124)	(0.0122)
Population	0.516***	0.599***	0.545***
	(0.0393)	(0.0481)	(0.0597)
Geography		✓	✓
Census Divisions		✓	✓
Socioeconomic Characteristics			✓
Year FE	✓	✓	✓
Observations	663	663	663
KP F-stat	13.48	10.08	10.02

***Notes*:** Robust standard errors clustered by MSAs in parentheses. All variables are in logs. Instruments are ln 1835 exploration routes, ln 1898 railroads, and ln 1947 planned interstates; 684 observations corresponding to 228 MSAs for each regression.

Table. A.10. Elasticity of Rail Traffic Use (in Weight-Kilometers) with respect to Road Infrastructure Improvements

	(1) OLS	(2) OLS	(3) IV	(4) IV	(5) IV
Interstate Highway Lane KM	-0.135	-0.131	0.367	0.131	0.292
	(0.161)	(0.163)	(0.320)	(0.335)	(0.314)
Population		0.393	0.524**	0.798***	0.647**
		(0.251)	(0.248)	(0.282)	(0.269)
Geography				✓	✓
Census Divisions				✓	✓
Socioeconomic Characteristics		✓			✓
MSA FE	✓	✓			
Year FE	✓	✓	✓	✓	✓
Observations	663	663	663	663	663
R-squared	0.94	0.94	0.29	0.49	0.52
KP F-stat			13.48	10.08	10.02

Notes: * $p < 0.1$, ** $p < 0.05$, *** $p < 0.01$. Robust standard errors clustered by MSAs in parentheses. All variables are in logs. Instruments are 1835 exploration routes, 1898 railroad route kilometers, and 1947 planned interstate highways. 663 observations corresponding to 221 MSAs for each regression. See Table A.3 for first stage regressions.

Table. A.11. Elasticity of Rail Traffic Use (in Weight-Kilometers) with respect to Road Infrastructure Improvements: First Stage

	(1)	(2)	(3)
1898 Railroads	0.0879*	0.0939*	0.119**
	(0.0460)	(0.0499)	(0.0474)
1947 Planned Interstates	0.156***	0.127***	0.114***
	(0.0332)	(0.0322)	(0.0284)
1835 Exploration Routes	0.0249**	0.0268**	0.0222*
	(0.0117)	(0.0124)	(0.0122)
Population	0.516***	0.599***	0.545***
	(0.0393)	(0.0481)	(0.0597)
Geography		✓	✓
Census Divisions		✓	✓
Socioeconomic Characteristics			✓
Year FE	✓	✓	✓
Observations	663	663	663
KP F-stat	13.48	10.08	10.02

***Notes*:** Robust standard errors clustered by MSAs in parentheses. All variables are in logs. Instruments are ln 1835 exploration routes, ln 1898 railroads, and ln 1947 planned interstates; 684 observations corresponding to 228 MSAs for each regression.

Table. A.12. Elasticity of Rail Traffic Use (in Weight-Kilometers) by Destination with respect to Road Infrastructure Improvements

	(1)	(2)	(3)	(4)	(5)
	OLS	OLS	IV	IV	IV
Inter-State Highway Lane KM	0.151	0.156	0.184	0.225	0.494
	(0.0972)	(0.0989)	(0.426)	(0.470)	(0.469)
Population		0.562**	0.939***	0.975**	0.824**
		(0.236)	(0.312)	(0.382)	(0.383)
Geography				✓	✓
Census Divisions				✓	✓
Socioeconomic Characteristics		✓			✓
MSA FE	✓	✓			
Year FE	✓	✓	✓	✓	✓
Observations	663	663	663	663	663
R-squared	0.95	0.95	0.37	0.48	0.50
KP F-stat			13.48	10.08	10.02

Notes: * $p < 0.1$, ** $p < 0.05$, *** $p < 0.01$. Robust standard errors clustered by MSAs in parentheses. All variables are in logs. Instruments are 1835 exploration routes, 1898 railroad route kilometers, and 1947 planned interstate highways. 663 observations corresponding to 221 MSAs for each regression. See Table A.3 for first stage regressions.

Table. A.13. Elasticity of Rail Traffic Use (in Weight-Kilometers) by Destination with respect to Road Infrastructure Improvements: First Stage

	(1)	(2)	(3)
1898 Railroads	0.0879*	0.0939*	0.119**
	(0.0460)	(0.0499)	(0.0474)
1947 Planned Interstates	0.156***	0.127***	0.114***
	(0.0332)	(0.0322)	(0.0284)
1835 Exploration Routes	0.0249**	0.0268**	0.0222*
	(0.0117)	(0.0124)	(0.0122)
Population	0.516***	0.599***	0.545***
	(0.0393)	(0.0481)	(0.0597)
Geography		✓	✓
Census Divisions		✓	✓
Socioeconomic Characteristics			✓
Year FE	✓	✓	✓
Observations	663	663	663
KP F-stat	13.48	10.08	10.02

***Notes*:** Robust standard errors clustered by MSAs in parentheses. All variables are in logs. Instruments are ln 1835 exploration routes, ln 1898 railroads, and ln 1947 planned interstates; 684 observations corresponding to 228 MSAs for each regression.

Table. A.14. Elasticity of Rail Traffic Use (in Weight-Kilometers) by Origin with respect to Road Infrastructure Improvements

	(1) OLS	(2) OLS	(3) IV	(4) IV	(5) IV
Inter-State Highway Lane KM	0.167	0.169	0.621	0.150	0.155
	(0.117)	(0.117)	(0.401)	(0.355)	(0.347)
Population		0.209	0.206	0.757**	0.707**
		(0.300)	(0.310)	(0.307)	(0.303)
Geography				✓	✓
Census Divisions				✓	✓
Socioeconomic Characteristics		✓			✓
MSA FE	✓	✓			
Year FE	✓	✓	✓	✓	✓
Observations	663	663	663	663	663
R-squared	0.94	0.94	0.17	0.44	0.48
KP F-stat			13.48	10.08	10.02

Notes: * $p < 0.1$, ** $p < 0.05$, *** $p < 0.01$. Robust standard errors clustered by MSAs in parentheses. All variables are in logs. Instruments are 1835 exploration routes, 1898 railroad route kilometers, and 1947 planned interstate highways. 663 observations corresponding to 221 MSAs for each regression. See Table A.3 for first stage regressions.

Table. A.15. Elasticity of Rail Traffic Use (in Weight-Kilometers) by Origin with respect to Road Infrastructure Improvements: First Stage

	(1)	(2)	(3)
1898 Railroads	0.0879*	0.0939*	0.119**
	(0.0460)	(0.0499)	(0.0474)
1947 Planned Interstates	0.156***	0.127***	0.114***
	(0.0332)	(0.0322)	(0.0284)
1835 Exploration Routes	0.0249**	0.0268**	0.0222*
	(0.0117)	(0.0124)	(0.0122)
Population	0.516***	0.599***	0.545***
	(0.0393)	(0.0481)	(0.0597)
Geography		✓	✓
Census Divisions		✓	✓
Socioeconomic Characteristics			✓
Year FE	✓	✓	✓
Observations	663	663	663
KP F-stat	13.48	10.08	10.02

***Notes*:** Robust standard errors clustered by MSAs in parentheses. All variables are in logs. Instruments are ln 1835 exploration routes, ln 1898 railroads, and ln 1947 planned interstates; 684 observations corresponding to 228 MSAs for each regression.

Table. A.16. Elasticity of Rail to Truck Traffic Use with respect to Road Infrastructure Improvements: First Stage

	(1)	(2)	(3)
1898 Railroads	0.102**	0.107**	0.129***
	(0.0445)	(0.0481)	(0.0478)
1947 Planned Interstates	0.148***	0.117***	0.108***
	(0.0317)	(0.0298)	(0.0274)
1835 Exploration Routes	0.0244**	0.0257**	0.0220*
	(0.0117)	(0.0124)	(0.0122)
Population	0.511***	0.597***	0.535***
	(0.0386)	(0.0474)	(0.0600)
Geography		✓	✓
Census Divisions		✓	✓
Socioeconomic Characteristics			✓
Year FE	✓	✓	✓
Observations	658	658	658
KP F-stat	14.48	10.76	10.04

***Notes*:** Robust standard errors clustered by MSAs in parentheses. All variables are in logs. Rail traffic use, measured in railcar-kilometers, is constructed using confidential rail waybill data. Instruments are ln 1835 exploration routes, ln 1898 railroads, and ln 1947 planned interstates; 684 observations corresponding to 228 MSAs for each regression.

Table. A.17. Elasticity of Rail to Truck Traffic Use by Destination with respect to Road Infrastructure Improvements

	(1) OLS	(2) OLS	(3) IV	(4) IV	(5) IV
Inter-State Highway Lane KM	-1.060***	-1.061***	-1.101***	-1.210***	-0.999**
	(0.185)	(0.185)	(0.405)	(0.426)	(0.405)
Population		0.0605	1.132***	1.303***	1.145***
		(0.337)	(0.298)	(0.351)	(0.336)
Geography				✓	✓
Census Divisions				✓	✓
Socioeconomic Characteristics		✓			✓
MSA FE	✓	✓			
Year FE	✓	✓	✓	✓	✓
Observations	658	658	658	658	658
R-squared	0.89	0.89	0.04	0.21	0.24
KP F-stat			14.48	10.76	10.04

Notes: * $p < 0.1$, ** $p < 0.05$, *** $p < 0.01$. Robust standard errors clustered by MSAs in parentheses. All variables are in logs. Rail traffic use, measured in railcar-kilometers, is constructed using confidential rail waybill data. Truck traffic use (in vehicle-kilometers) and other variables are from Duranton and Turner (2011). Instruments are 1835 exploration routes, 1898 railroad route kilometers, and 1947 planned interstate highways. 663 observations corresponding to 221 MSAs for each regression. See Table A.18 for first stage regressions.

Table. A.18. Elasticity of Rail to Truck Traffic Use by Destination with respect to Road Infrastructure Improvements: First Stage

	(1)	(2)	(3)
1898 Railroads	0.102**	0.107**	0.129***
	(0.0445)	(0.0481)	(0.0478)
1947 Planned Interstates	0.148***	0.117***	0.108***
	(0.0317)	(0.0298)	(0.0274)
1835 Exploration Routes	0.0244**	0.0257**	0.0220*
	(0.0117)	(0.0124)	(0.0122)
Population	0.511***	0.597***	0.535***
	(0.0386)	(0.0474)	(0.0600)
Geography		✓	✓
Census Divisions		✓	✓
Socioeconomic Characteristics			✓
Year FE	✓	✓	✓
Observations	658	658	658
KP F-stat	14.48	10.76	10.04

***Notes*:** Robust standard errors clustered by MSAs in parentheses. All variables are in logs. Rail traffic use, measured in railcar-kilometers, is constructed using confidential rail waybill data. Instruments are ln 1835 exploration routes, ln 1898 railroads, and ln 1947 planned interstates; 684 observations corresponding to 228 MSAs for each regression.

Table. A.19. Elasticity of Rail to Truck Traffic Use by Origin with respect to Road Infrastructure Improvements

	(1) OLS	(2) OLS	(3) IV	(4) IV	(5) IV
Inter-State Highway Lane KM	-1.075***	-1.075***	-0.635	-1.235***	-1.220***
	(0.207)	(0.207)	(0.468)	(0.451)	(0.444)
Population		-0.255	0.452	1.107***	1.000***
		(0.378)	(0.352)	(0.379)	(0.367)
Geography				✓	✓
Census Divisions				✓	✓
Socioeconomic Characteristics		✓			✓
MSA FE	✓	✓			
Year FE	✓	✓	✓	✓	✓
Observations	658	658	658	658	658
R-squared	0.90	0.90	-0.04	0.26	0.31
KP F-stat			14.48	10.76	10.04

Notes: * $p < 0.1$, ** $p < 0.05$, *** $p < 0.01$. Robust standard errors clustered by MSAs in parentheses. All variables are in logs. Rail traffic use, measured in railcar-kilometers, is constructed using the confidential rail waybill data. Truck traffic use (in vehicle-kilometers) and other variables are from Duranton and Turner (2011). Instruments are 1835 exploration routes, 1898 railroad route kilometers, and 1947 planned interstate highways. 663 observations corresponding to 221 MSAs for each regression. See Table A.20 for first stage regressions.

Table. A.20. Elasticity of Rail to Truck Traffic Use by Origin with respect to Road Infrastructure Improvements: First Stage

	(1)	(2)	(3)
1898 Railroads	0.102**	0.107**	0.129***
	(0.0445)	(0.0481)	(0.0478)
1947 Planned Interstates	0.148***	0.117***	0.108***
	(0.0317)	(0.0298)	(0.0274)
1835 Exploration Routes	0.0244**	0.0257**	0.0220*
	(0.0117)	(0.0124)	(0.0122)
Population	0.511***	0.597***	0.535***
	(0.0386)	(0.0474)	(0.0600)
Geography		✓	✓
Census Divisions		✓	✓
Socioeconomic Characteristics			✓
Year FE	✓	✓	✓
Observations	658	658	658
KP F-stat	14.48	10.76	10.04

***Notes*:** Robust standard errors clustered by MSAs in parentheses. All variables are in logs. Rail traffic use, measured in railcar-kilometers, is constructed using confidential rail waybill data. Instruments are ln 1835 exploration routes, ln 1898 railroads, and ln 1947 planned interstates; 684 observations corresponding to 228 MSAs for each regression.

Table. A.21. Elasticity of Rail to Truck Traffic Use with respect to Road Infrastructure Improvements, by Rail Weight

	(1) OLS	(2) OLS	(3) IV	(4) IV	(5) IV
Interstate Highway Lane KM	-1.473***	-1.472***	-0.930**	-1.373***	-1.203***
	(0.171)	(0.172)	(0.392)	(0.403)	(0.382)
Population		-0.101	0.524*	1.012***	0.774**
		(0.308)	(0.297)	(0.338)	(0.316)
Geography				✓	✓
Census Divisions				✓	✓
Socioeconomic Characteristics		✓			✓
MSA FE	✓	✓			
Year FE	✓	✓	✓	✓	✓
Observations	658	658	658	658	658
R-squared	0.89	0.89	-0.03	0.23	0.28
KP F-stat			14.48	10.76	10.04

Notes: * $p < 0.1$, ** $p < 0.05$, *** $p < 0.01$. Robust standard errors clustered by MSAs in parentheses. All variables are in logs. Rail traffic use, measured in rail weight-kilometers, is constructed using confidential rail waybill data. All other variables are from Duranton and Turner (2011). Instruments are 1835 exploration routes, 1898 railroad route kilometers, and 1947 planned interstate highways. 663 observations corresponding to 221 MSAs for each regression. See Table A.3 for first stage regressions.

Table. A.22. Elasticity of Rail to Truck Traffic Use with respect to Road Infrastructure Improvements, by Rail Weight: First Stage

	(1)	(2)	(3)
1898 Railroads	0.102**	0.107**	0.129***
	(0.0445)	(0.0481)	(0.0478)
1947 Planned Interstates	0.148***	0.117***	0.108***
	(0.0317)	(0.0298)	(0.0274)
1835 Exploration Routes	0.0244**	0.0257**	0.0220*
	(0.0117)	(0.0124)	(0.0122)
Population	0.511***	0.597***	0.535***
	(0.0386)	(0.0474)	(0.0600)
Geography		✓	✓
Census Divisions		✓	✓
Socioeconomic Characteristics			✓
Year FE	✓	✓	✓
Observations	658	658	658
KP F-stat	14.48	10.76	10.04

***Notes*:** Robust standard errors clustered by MSAs in parentheses. All variables are in logs. Rail traffic use, measured in rail weight-kilometers, is constructed using confidential rail waybill data. Instruments are ln 1835 exploration routes, ln 1898 railroads, and ln 1947 planned interstates; 684 observations corresponding to 228 MSAs for each regression.

Table. A.23. Elasticity of Rail to Truck Traffic Use by Destination with respect to Road Infrastructure Improvements, by Rail Weight

	(1) OLS	(2) OLS	(3) IV	(4) IV	(5) IV
Inter-State Highway Lane KM	-1.104***	-1.104***	-1.133***	-1.273***	-1.019**
	(0.167)	(0.167)	(0.421)	(0.447)	(0.430)
Population		0.0823	0.953***	1.185***	0.973***
		(0.331)	(0.306)	(0.366)	(0.352)
Geography				✓	✓
Census Divisions				✓	✓
Socioeconomic Characteristics		✓			✓
MSA FE	✓	✓			
Year FE	✓	✓	✓	✓	✓
Observations	658	658	658	658	658
R-squared	0.89	0.89	0.00	0.18	0.21
KP F-stat			14.48	10.76	10.04

Notes: * $p < 0.1$, ** $p < 0.05$, *** $p < 0.01$. Robust standard errors clustered by MSAs in parentheses. All variables are in logs. Rail traffic use, measured in rail weight-kilometers, is constructed using confidential rail waybill data. All other variables are from Duranton and Turner (2011). Instruments are 1835 exploration routes, 1898 railroad route kilometers, and 1947 planned interstate highways. 663 observations corresponding to 221 MSAs for each regression. See Table A.3 for first stage regressions.

Table. A.24. Elasticity of Rail to Truck Traffic Use by Destination with respect to Road Infrastructure Improvements, by Rail Weight: First Stage

	(1)	(2)	(3)
1898 Railroads	0.102**	0.107**	0.129***
	(0.0445)	(0.0481)	(0.0478)
1947 Planned Interstates	0.148***	0.117***	0.108***
	(0.0317)	(0.0298)	(0.0274)
1835 Exploration Routes	0.0244**	0.0257**	0.0220*
	(0.0117)	(0.0124)	(0.0122)
Population	0.511***	0.597***	0.535***
	(0.0386)	(0.0474)	(0.0600)
Geography		✓	✓
Census Divisions		✓	✓
Socioeconomic Characteristics			✓
Year FE	✓	✓	✓
Observations	658	658	658
KP F-stat	14.48	10.76	10.04

***Notes*:** Robust standard errors clustered by MSAs in parentheses. All variables are in logs. Rail traffic use, measured in rail weight-kilometers, is constructed using confidential rail waybill data. Instruments are ln 1835 exploration routes, ln 1898 railroads, and ln 1947 planned interstates; 684 observations corresponding to 228 MSAs for each regression.

Table. A.25. Elasticity of Rail to Truck Traffic Use by Origin with respect to Road Infrastructure Improvements, by Rail Weight

	(1) OLS	(2) OLS	(3) IV	(4) IV	(5) IV
Inter-State Highway Lane KM	-1.106***	-1.105***	-0.630	-1.308***	-1.283***
	(0.200)	(0.200)	(0.496)	(0.465)	(0.462)
Population		-0.314	0.176	0.936**	0.789**
		(0.326)	(0.370)	(0.388)	(0.376)
Geography				✓	✓
Census Divisions				✓	✓
Socioeconomic Characteristics		✓			✓
MSA FE	✓	✓			
Year FE	✓	✓	✓	✓	✓
Observations	658	658	658	658	658
R-squared	0.91	0.91	-0.02	0.29	0.34
KP F-stat			14.48	10.76	10.04

Notes: * $p < 0.1$, ** $p < 0.05$, *** $p < 0.01$. Robust standard errors clustered by MSAs in parentheses. All variables are in logs. Rail traffic use, measured in rail weight-kilometers, is constructed using confidential rail waybill data. All other variables are from Duranton and Turner (2011). Instruments are 1835 exploration routes, 1898 railroad route kilometers, and 1947 planned interstate highways. 663 observations corresponding to 221 MSAs for each regression. See Table A.3 for first stage regressions.

Table. A.26. Elasticity of Rail to Truck Traffic Use by Origin with respect to Road Infrastructure Improvements, by Rail Weight: First Stage

	(1)	(2)	(3)
1898 Railroads	0.102**	0.107**	0.129***
	(0.0445)	(0.0481)	(0.0478)
1947 Planned Interstates	0.148***	0.117***	0.108***
	(0.0317)	(0.0298)	(0.0274)
1835 Exploration Routes	0.0244**	0.0257**	0.0220*
	(0.0117)	(0.0124)	(0.0122)
Population	0.511***	0.597***	0.535***
	(0.0386)	(0.0474)	(0.0600)
Geography		✓	✓
Census Divisions		✓	✓
Socioeconomic Characteristics			✓
Year FE	✓	✓	✓
Observations	658	658	658
KP F-stat	14.48	10.76	10.04

***Notes*:** Robust standard errors clustered by MSAs in parentheses. All variables are in logs. Rail traffic use, measured in rail weight-kilometers, is constructed using confidential rail waybill data. Instruments are ln 1835 exploration routes, ln 1898 railroads, and ln 1947 planned interstates; 684 observations corresponding to 228 MSAs for each regression.

C.3 Multimodal Implications of Port Congestion

In this subsection, we study how port congestion can impact the multimodal network. In particular, we focus on how port traffic affects the amount of time a rail car spends at the rail station that is local to that port. We estimate the following regression (Columns (3) and (4), Table A.27):

$$\ln \text{Rail Dwell Time}_{rpwy} = \beta_2 \ln \text{Port Traffic}_{pwy} + \gamma_{wy} + \phi_{rp} + \epsilon_{rpwy} \tag{39}$$

where Rail Dwell Time_{rpwy} is the average number of hours a rail car spends at a rail station r that is in the vicinity of port p during week w in year y, Port Traffic_{pwy} is the average amount of port traffic at port p for that same week w in year y,[2] Port traffic is measured in both net tons of ships as in our congestion elasticity approach, as well as the number of ships. γ_{wy} is week-year fixed effects, and ϕ_{rp} is rail station-port fixed effects. The key parameter of interest, β_2, captures the link between rail dwell times and its nearest port traffic. Standard errors are clustered at the port level.

The week-year fixed effects control for aggregate events that affects all rail stations. The rail-port fixed effects control for fixed characteristics at the rail-port level. These include time-invariant comparative advantage differences across ports that result in larger capacity trains servicing the rail stations close to these ports which mechanically take longer time to unload. It also includes fixed rail station characteristics and fixed port characteristics that take into account their geography. In order to match the local rail stations in our rail dwell times dataset to ports, we extend the port areas in order to capture nearby rail stations. The buffer area we used in our baseline result is 150km which captures 6 ports and 11 rail stations. This small set of stations and ports is due to data restrictions from the rail dwell times dataset. The rail companies are only required to report the dwell times for the top 10 largest of their rail stations, and these rail stations sometimes overlap in geographic location.

We find that a one percent increase in port traffic, measured in average net tonnage, is correlated with a statistically significant increase in rail dwell times by 0.05 percent (Column (3), Table A.27). This elasticity is robust to specifications with rail station fixed effects and port fixed effects separately (Column (1), Table A.27). This elasticity is also robust to an alternative measures of port traffic by using the average number of ships (Columns (4) and (2), Table A.27).

As a robustness check, we extend the buffer area around the ports to 200km which captures 9 ports and 16 rail stations. We find that our estimate has the same sign and is within one standard error of our baseline estimate (Column (5), Table A.27). However, the magnitude of this estimate is smaller and noisy, due to the impact of port traffic being more muted on rail stations that are further away. Subsequent increases to the buffer area correspondingly result in even smaller estimates. Due to the small sample size, we are unable causally identify the multimodal impact of port traffic on rail dwell times, but we are able to show that there are statistically significant correlations between the two.

[2]This measure, as mentioned from the previous subsection, is at the daily level. In order to match the rail dwell time dataset, we aggregate it up to the weekly level. We start our week on a Monday since we observe in our data that most ships tend to enter a port on Mondays.

Table. A.27. Link between Rail Dwell Times and Nearest Port Traffic

	(1)	(2)	(3)	(4)	(5)
Nearest Port Traffic (Net Tons)	0.05**		0.05**		0.03
	(0.02)		(0.02)		(0.02)
Nearest Port Traffic (Ships)		0.04**		0.04**	
		(0.01)		(0.01)	
Port Buffer Area	150km	150km	150km	150km	200km
Week-Year FE	✓	✓	✓	✓	✓
Rail Station-Port FE			✓	✓	
Port FE	✓	✓			
Rail Station FE	✓	✓			
Observations	3327	3327	3327	3327	4316
R^2	0.80	0.80	0.80	0.80	0.79
F	9.08	6.80	9.08	6.80	2.06

Notes: Robust standard errors in parentheses are clustered by port. All variables are in logs. Local railroads are determined by a 150km or 200km buffer area around the ports as indicated in table.

D Additional Derivations

This section provides additional derivations for the equilibrium equations in Section 3, the derivations for the regression design as well as a comparison with Fan and Luo (2020).

D.1 Section 3.3: Equilibrium for Economic Geography Model with Multimodal Routing

In terms of market clearing and trade balance we have the following equilibrium conditions,

$$\gamma_i = \sum_j X_{ij}$$
$$\delta_i = \sum_j X_{ji}$$

Starting with the first equilibrium condition we have:

$$\begin{aligned}
\gamma_i &= \sum_j X_{ij} \iff \\
\gamma_i &= \sum_j \tau_{ij}^{-\theta} \times \frac{\gamma_i}{\Pi_i^{-\theta}} \times \frac{\delta_j}{P_j^{-\theta}} \iff \\
\Pi_i^{-\theta} &= \sum_j \tau_{ij}^{-\theta} \times \frac{\delta_j}{P_j^{-\theta}} \iff \\
\Pi_i^{-\theta} &= \tau_{ii}^{-\theta} \frac{\delta_i}{P_i^{-\theta}} + \sum_{j \neq i} \tau_{ij}^{-\theta} \frac{\delta_j}{P_j^{-\theta}} \iff \\
\Pi_i^{-\theta} &= \tau_{ii}^{-\theta} \frac{\delta_i}{P_i^{-\theta}} + \sum_{j \neq i} \left(\sum_{k \in \mathcal{F}(i)} t_{ik}^{-\theta} \tau_{kj}^{-\theta} \right) \frac{\delta_j}{P_j^{-\theta}} \iff \\
\Pi_i^{-\theta} &= \tau_{ii}^{-\theta} \frac{\delta_i}{P_i^{-\theta}} + \sum_{k \in \mathcal{F}(i)} t_{ik}^{-\theta} \left(-\tau_{ki}^{-\theta} \frac{\delta_i}{P_i^{-\theta}} + \sum_j \tau_{kj}^{-\theta} \frac{\delta_j}{P_j^{-\theta}} \right) \iff \\
\Pi_i^{-\theta} &= t_{ii}^{-\theta} \frac{\delta_i}{P_i^{-\theta}} + \sum_{k \in \mathcal{F}(i)} t_{ik}^{-\theta} \Pi_k^{-\theta}
\end{aligned}$$

where in the last line we used the definition of the recursive transport cost, $\tau_{ii}^{-\theta} = \left(t_{ii}^{-\theta} + \sum_{k \in \mathcal{F}(i)} (t_{ik} \tau_{kj})^{-\theta} \right)$.

Continuing with the second equilibrium condition,

$$
\begin{aligned}
\delta_i &= \sum_j X_{ji} \iff \\
\delta_i &= \sum_j \tau_{ji}^{-\theta} \times \frac{\gamma_j}{\Pi_j^{-\theta}} \times \frac{\delta_i}{P_i^{-\theta}} \iff \\
P_i^{-\theta} &= \sum_j \tau_{ji}^{-\theta} \times \frac{\gamma_j}{\Pi_j^{-\theta}} \iff \\
P_i^{-\theta} &= \tau_{ii}^{-\theta} \frac{\gamma_i}{\Pi_i^{-\theta}} + \sum_{j \neq i} \tau_{ji}^{-\theta} \frac{\gamma_j}{\Pi_j^{-\theta}} \iff \\
P_i^{-\theta} &= \tau_{ii}^{-\theta} \frac{\gamma_i}{\Pi_i^{-\theta}} + \sum_{j \neq i} \left(\sum_{k \in \mathcal{B}(i)} t_{ki}^{-\theta} \tau_{kj}^{-\theta} \right) \frac{\gamma_j}{\Pi_j^{-\theta}} \iff \\
P_i^{-\theta} &= \tau_{ii}^{-\theta} \frac{\gamma_i}{\Pi_i^{-\theta}} + \sum_{k \in \mathcal{F}(j)} t_{ki}^{-\theta} \left(-\tau_{ki}^{-\theta} \frac{\gamma_i}{\Pi_i^{-\theta}} + \sum_j \tau_{kj}^{-\theta} \frac{\gamma_j}{\Pi_j^{-\theta}} \right) \iff \\
P_i^{-\theta} &= t_{ii}^{-\theta} \frac{\gamma_i}{\Pi_i^{-\theta}} + \sum_{k \in \mathcal{F}(j)} t_{ki}^{-\theta} P_k^{-\theta}
\end{aligned}
$$

where in the last line we used the definition of the recursive transport cost, $\tau_{ii}^{-\theta} = \left(t_{ii}^{-\theta} + \sum_{k \in \mathcal{F}(i)} \left(t_{ik} \tau_{kj} \right)^{-\theta} \right)$.

D.2 Extension: International Trade

In this subsection, we extend the model to allow for both domestic locations $i, j \in \mathcal{D}$ and foreign locations $l \in \mathcal{F}$. Domestic locations consumer from both domestic and foreign locations, while foreign locations are modeled to only trade with domestic locations. Furthermore, we make a small open economy assumption such that changes in the domestic economy do not affect the labor allocations in the foreign economy. For the domestic economy we have the following conditions,

$$\gamma_i = \sum_{j \in \mathcal{D}} X_{ij} + \sum_{l \in \mathcal{F}} X_{il}$$
$$\delta_i = \sum_{j \in \mathcal{D}} X_{ji} + \sum_{l \in \mathcal{F}} X_{li}$$

Welfare equalization domestically implies,

$$P_i = \frac{w_i u_i}{W} \iff$$
$$P_i = Y_i \bar{u}_i L_i^{\beta-1} W^{-1} \implies$$
$$\hat{P}_i = \hat{y}_i \hat{l}_i^{\beta-1} \hat{W}^{-1}$$

and

$$\Pi_i = A_i L_i Y_i^{-\frac{\theta+1}{\theta}} \iff$$
$$\Pi_i = A_i L_i^{\alpha+1} Y_i^{-\frac{\partial+1}{\theta}} \implies$$
$$\hat{\Pi}_i = \hat{l}_i^{\alpha+1} \hat{y}_i^{-\frac{\theta+1}{\theta}}$$

For the foreign economy we have that market clearing implies,

$$\gamma_l = \sum_j X_{lj} \quad \forall l \in \mathcal{F}$$
$$\delta_l = \sum_j X_{jl} \quad \forall l \in \mathcal{F}$$

For the price indices for foreign locations we obtain,

$$P_l = \frac{w_l u_l}{W_l} \iff$$
$$P_l = Y_l \bar{u}_l L_l^{\beta-1} W_l^{-1} \implies$$
$$\hat{P}_l = \hat{y}_l \hat{W}_l^{-1}$$

and

$$\Pi_l = A_l L_l Y_l^{-\frac{\theta+1}{\theta}} \iff$$
$$\Pi_l = A_l L_l^{\alpha+1} Y_l^{-\frac{\theta+1}{\theta}} \implies$$
$$\hat{\Pi}_l = \hat{y}_l^{-\frac{\theta+1}{\theta}}$$

Considering now that the economy is situated on a graph with both foreign and domestic nodes, i.e. $\mathcal{G} \equiv (\mathcal{N}, \mathcal{L})$, where $\mathcal{N}$ is the union of domestic, $\mathcal{N}_D$, and foreign nodes, $\mathcal{N}_F$, and equivalently we define domestic and foreign successor nodes, $k \in \mathcal{F}_D(i)$, and $l \in \mathcal{F}_F(i)$.

Re-writing the equilibrium system for both foreign and domestic locations, defining domestic and foreign

neighboring notes

$$\hat{P}_i^{-\theta}\hat{\Pi}_i^{-\theta} = \left(\frac{E_i}{E_i + \sum_{k\in\mathcal{F}(i)}\Xi_{ik}}\right)\hat{\delta}_i + \sum_{k\in\mathcal{F}_D(i)}\left(\frac{\Xi_{ik}}{E_i + \sum_{k\in\mathcal{F}(i)}\Xi_{ik}}\right)\hat{t}_{ik}^{-\theta}\left(\hat{\Pi},\hat{P},\hat{t}_{ik,0},\hat{t}_{ik,m}\right)\hat{\Pi}_k^{-\theta}\hat{P}_i^{-\theta} + \sum_{l\in\mathcal{F}_F(i)}\left(\frac{\Xi_{il}}{E_i + \sum_{k\in\mathcal{F}(i)}\Xi_{ik}}\right)\hat{t}_{il}^{-\theta}\left(\hat{\Pi},\hat{P},\hat{t}_{ik,0},\hat{t}_{ik,m}\right)\hat{P}_i^{-\theta}\hat{\Pi}_l^{-\theta}$$

$$\hat{P}_i^{-\theta}\hat{\Pi}_i^{-\theta} = \left(\frac{Y_i}{Y_i + \sum_{k\in\mathcal{F}(i)}\Xi_{ki}}\right)\hat{\gamma}_i + \sum_{k\in\mathcal{F}_D(i)}\left(\frac{\Xi_{ki}}{Y_i + \sum_{k\in\mathcal{F}(i)}\Xi_{ki}}\right)\hat{t}_{ki}^{-\theta}\left(\hat{\Pi},\hat{P},\hat{t}_{ki,0},\hat{t}_{ki,m}\right)\hat{P}_k^{-\theta}\hat{\Pi}_i^{-\theta} + \sum_{l\in\mathcal{F}_F(i)}\left(\frac{\Xi_{li}}{Y_i + \sum_{k\in\mathcal{F}(i)}\Xi_{ki}}\right)\hat{t}_{li}^{-\theta}\left(\hat{\Pi},\hat{P},\hat{t}_{ki,0},\hat{t}_{ki,m}\right)\hat{P}_l^{-\theta}\hat{\Pi}_i^{-\theta}$$

And similarly for foreign locations, we have,

$$\hat{\Pi}_l^{-\theta}\hat{P}_l^{-\theta} = \left(\frac{E_l}{E_l + \sum_{k\in\mathcal{F}_D(l)}\Xi_{lk}}\right)\hat{y}_l + \sum_{k\in\mathcal{F}_D(l)}\left(\frac{\Xi_{lk}}{E_l + \sum_{k\in\mathcal{F}_D(l)}\Xi_{lk}}\right)\hat{t}_{lk}^{-\theta}\left(\hat{\Pi},\hat{P},\hat{t}_{lk,0},\hat{t}_{lk,m}\right)\hat{P}_l^{-\theta}\hat{\Pi}_k^{-\theta}$$

$$\hat{P}_l^{-\theta}\hat{\Pi}_l^{-\theta} = \left(\frac{Y_l}{Y_l + \sum_{k\in\mathcal{F}_D(l)}\Xi_{kl}}\right)\hat{y}_l + \sum_{k\in\mathcal{F}_D(l)}\left(\frac{\Xi_{kl}}{Y_l + \sum_{k\in\mathcal{F}_D(l)}\Xi_{kl}}\right)\hat{t}_{kl}^{-\theta}\left(\hat{\Pi},\hat{P},\hat{t}_{kl,0},\hat{t}_{kl,m}\right)\hat{P}_k^{-\theta}\hat{\Pi}_l^{-\theta}$$

Substituting,

$$\left(\hat{l}_i^{\alpha+1}\hat{y}_i^{-\frac{\theta+1}{\theta}}\right)^{-\theta}\left(\hat{y}_i\hat{l}_i^{\beta-1}\hat{W}^{-1}\right)^{-\theta} = \left(\frac{E_i}{E_i + \sum_{k\in\mathcal{F}(i)}\Xi_{ik}}\right)\hat{y}_i + \sum_{k\in\mathcal{F}_D(i)}\left(\frac{\Xi_{ik}}{E_i + \sum_{k\in\mathcal{F}(i)}\Xi_{ik}}\right)\hat{t}_{ik}^{-\theta}\left(\hat{\Pi},\hat{P},\hat{t}_{ik,0},\hat{t}_{ik,m}\right)\left(\hat{y}_i\hat{l}_i^{\beta-1}\hat{W}^{-1}\right)^{-\theta}\left(\hat{l}_k^{\alpha+1}\hat{y}_k^{-\frac{\theta+1}{\theta}}\right)^{-\theta} + \sum_{l\in\mathcal{F}_F(i)}\left(\frac{\Xi_{il}}{E_i + \sum_{k\in\mathcal{F}(i)}\Xi_{ik}}\right)\hat{t}_{il}^{-\theta}\left(\hat{\Pi},\hat{P},\hat{t}_{ik,0},\hat{t}_{ik,m}\right)\left(\hat{y}_i\hat{l}_i^{\beta-1}\hat{W}^{-1}\right)^{-\theta}\left(\hat{y}_l^{-\frac{\theta+1}{\theta}}\right)^{-\theta}$$

$$\left(\hat{l}_i^{\alpha+1}\hat{y}_i^{-\frac{\theta+1}{\theta}}\right)^{-\theta}\left(\hat{y}_i\hat{l}_i^{\beta-1}\hat{W}^{-1}\right)^{-\theta}=\left(\frac{Y_i}{Y_i+\sum_{k\in\mathcal{F}(i)}\Xi_{ki}}\right)\hat{y}_i$$
$$+\sum_{k\in\mathcal{F}_D(i)}\left(\frac{\Xi_{ki}}{Y_i+\sum_{k\in\mathcal{F}(i)}\Xi_{ki}}\right)\hat{t}_{ki}^{-\theta}\left(\hat{\Pi},\hat{P},\hat{t}_{ki,0},\hat{t}_{ki,m}\right)\left(\hat{y}_k\hat{l}_k^{\beta-1}\hat{W}^{-1}\right)^{-\theta}\left(\hat{l}_i^{\alpha+1}\hat{y}_i^{-\frac{\theta+1}{\theta}}\right)^{-\theta}$$
$$+\sum_{l\in\mathcal{F}_F(i)}\left(\frac{\Xi_{li}}{Y_i+\sum_{k\in\mathcal{F}(i)}\Xi_{ki}}\right)\hat{t}_{li}^{-\theta}\left(\hat{\Pi},\hat{P},\hat{t}_{ki,0},\hat{t}_{ki,m}\right)\left(\hat{y}_l\hat{W}_l^{-1}\right)^{-\theta}\left(\hat{l}_i^{\alpha+1}\hat{y}_i^{-\frac{\theta+1}{\theta}}\right)^{-\theta}$$

$$\left(\hat{y}_l^{-\frac{\theta+1}{\theta}}\right)^{-\theta}\left(\hat{y}_l\hat{W}_l^{-1}\right)^{-\theta}=\left(\frac{E_l}{E_l+\sum_{k\in\mathcal{F}_D(l)}\Xi_{lk}}\right)\hat{y}_l$$
$$+\sum_{k\in\mathcal{F}_D(l)}\left(\frac{\Xi_{lk}}{E_l+\sum_{k\in\mathcal{F}_D(l)}\Xi_{lk}}\right)\hat{t}_{lk}^{-\theta}\left(\hat{\Pi},\hat{P},\hat{t}_{lk,0},\hat{t}_{lk,m}\right)\left(\hat{y}_l\hat{W}_l^{-1}\right)^{-\theta}\left(\hat{l}_k^{\alpha+1}\hat{y}_k^{-\frac{\theta+1}{\theta}}\right)^{-\theta}$$

$$\left(\hat{y}_l^{-\frac{\theta+1}{\theta}}\right)^{-\theta}\left(\hat{y}_l\hat{W}_l^{-1}\right)^{-\theta}=\left(\frac{Y_l}{Y_l+\sum_{k\in\mathcal{F}_D(l)}\Xi_{kl}}\right)\hat{y}_l$$
$$+\sum_{k\in\mathcal{F}_D(l)}\left(\frac{\Xi_{kl}}{Y_l+\sum_{k\in\mathcal{F}_D(l)}\Xi_{kl}}\right)\hat{t}_{kl}^{-\theta}\left(\hat{\Pi},\hat{P},\hat{t}_{kl,0},\hat{t}_{kl,m}\right)\left(\hat{y}_k\hat{l}_k^{\beta-1}\hat{W}^{-1}\right)^{-\theta}\left(\hat{y}_l^{-\frac{\theta+1}{\theta}}\right)^{-\theta}$$

Multiplying both sides by $\hat{W}^{-\theta}$, and applying the definition $\hat{\chi}=\hat{W}^{-\theta}$,

$$\left(\hat{l}_i^{\alpha+1}\hat{y}_i^{-\frac{\theta+1}{\theta}}\right)^{-\theta}\left(\hat{y}_i\hat{l}_i^{\beta-1}\right)^{-\theta}\hat{\chi}^{-1}=\left(\frac{E_i}{E_i+\sum_{k\in\mathcal{F}(i)}\Xi_{ik}}\right)\hat{y}_i$$
$$+\hat{\chi}^{-1}\sum_{k\in\mathcal{F}_D(i)}\left(\frac{\Xi_{ik}}{E_i+\sum_{k\in\mathcal{F}(i)}\Xi_{ik}}\right)\hat{t}_{ik}^{-\theta}\left(\hat{\Pi},\hat{P},\hat{t}_{ik,0},\hat{t}_{ik,m}\right)\left(\hat{y}_i\hat{l}_i^{\beta-1}\right)^{-\theta}\left(\hat{l}_k^{\alpha+1}\hat{y}_k^{-\frac{\theta+1}{\theta}}\right)^{-\theta}$$
$$+\hat{\chi}^{-1}\sum_{l\in\mathcal{F}_F(i)}\left(\frac{\Xi_{il}}{E_i+\sum_{k\in\mathcal{F}(i)}\Xi_{ik}}\right)\hat{t}_{il}^{-\theta}\left(\hat{\Pi},\hat{P},\hat{t}_{ik,0},\hat{t}_{ik,m}\right)\left(\hat{y}_i\hat{l}_i^{\beta-1}\right)^{-\theta}\left(\hat{y}_l^{-\frac{\theta+1}{\theta}}\right)^{-\theta}$$

$$\left(\hat{l}_i^{\alpha+1}\hat{y}_i^{-\frac{\theta+1}{\theta}}\right)^{-\theta}\left(\hat{y}_i\hat{l}_i^{\beta-1}\right)^{-\theta}\hat{\chi}^{-1}=\left(\frac{Y_i}{Y_i+\sum_{k\in\mathcal{F}(i)}\Xi_{ki}}\right)\hat{y}_i$$
$$+\hat{\chi}^{-1}\sum_{k\in\mathcal{F}_D(i)}\left(\frac{\Xi_{ki}}{Y_i+\sum_{k\in\mathcal{F}(i)}\Xi_{ki}}\right)\hat{t}_{ki}^{-\theta}\left(\hat{\Pi},\hat{P},\hat{t}_{ki,0},\hat{t}_{ki,m}\right)\left(\hat{y}_k\hat{l}_k^{\beta-1}\right)^{-\theta}\left(\hat{l}_i^{\alpha+1}\hat{y}_i^{-\frac{\theta+1}{\theta}}\right)^{-\theta}$$
$$+\sum_{l\in\mathcal{F}_F(i)}\left(\frac{\Xi_{li}}{Y_i+\sum_{k\in\mathcal{F}(i)}\Xi_{ki}}\right)\hat{t}_{li}^{-\theta}\left(\hat{\Pi},\hat{P},\hat{t}_{ki,0},\hat{t}_{ki,m}\right)(\hat{y}_l)^{-\theta}\hat{\chi}_l^{-1}\left(\hat{l}_i^{\alpha+1}\hat{y}_i^{-\frac{\theta+1}{\theta}}\right)^{-\theta}$$

$$\left(\hat{y}_l^{-\frac{\theta+1}{\theta}}\right)^{-\theta}(\hat{y}_l)^{-\theta}\hat{\chi}_l^{-1}=\left(\frac{E_l}{E_l+\sum_{k\in\mathcal{F}_D(l)}\Xi_{lk}}\right)\hat{y}_l$$
$$+\sum_{k\in\mathcal{F}_D(l)}\left(\frac{\Xi_{lk}}{E_l+\sum_{k\in\mathcal{F}_D(l)}\Xi_{lk}}\right)\hat{t}_{lk}^{-\theta}\left(\hat{\Pi},\hat{P},\hat{t}_{lk,0},\hat{t}_{lk,m}\right)(\hat{y}_l)^{-\theta}\hat{\chi}_l^{-1}\left(\hat{l}_k^{\alpha+1}\hat{y}_k^{-\frac{\theta+1}{\theta}}\right)^{-\theta}$$

$$\left(\hat{y}_l^{-\frac{\theta+1}{\theta}}\right)^{-\theta}(\hat{y}_l)^{-\theta}\hat{\chi}_l^{-1} = \left(\frac{Y_l}{Y_l+\sum_{k\in\mathcal{F}_D(l)}\Xi_{kl}}\right)\hat{y}_l + \hat{\chi}^{-1}\sum_{k\in\mathcal{F}_D(l)}\left(\frac{\Xi_{kl}}{Y_l+\sum_{k\in\mathcal{F}_D(l)}\Xi_{kl}}\right)\hat{t}_{kl}^{-\theta}\left(\hat{\Pi},\hat{P},\hat{t}_{kl,0},\hat{t}_{kl,m}\right)\left(\hat{y}_k\hat{l}_k^{\beta-1}\right)^{-\theta}\left(\hat{y}_l^{-\frac{\theta+1}{\theta}}\right)^{-\theta}$$

Simplifying,

$$\begin{aligned}\left(\hat{l}_i^{\alpha+1}\hat{y}_i^{-\frac{\theta+1}{\theta}}\right)^{-\theta}\left(\hat{y}_i\hat{l}_i^{\beta-1}\right)^{-\theta} =&\hat{\chi}\left(\frac{E_i}{E_i+\sum_{k\in\mathcal{F}(i)}\Xi_{ik}}\right)\hat{y}_i\\ &+\sum_{k\in\mathcal{F}_D(i)}\left(\frac{\Xi_{ik}}{E_i+\sum_{k\in\mathcal{F}(i)}\Xi_{ik}}\right)\hat{t}_{ik}^{-\theta}\left(\hat{\Pi},\hat{P},\hat{t}_{ik,0},\hat{t}_{ik,m}\right)\left(\hat{y}_i\hat{l}_i^{\beta-1}\right)^{-\theta}\left(\hat{l}_k^{\alpha+1}\hat{y}_k^{-\frac{\theta+1}{\theta}}\right)^{-\theta}\\ &+\sum_{l\in\mathcal{F}_F(i)}\left(\frac{\Xi_{il}}{E_i+\sum_{k\in\mathcal{F}(i)}\Xi_{ik}}\right)\hat{t}_{il}^{-\theta}\left(\hat{\Pi},\hat{P},\hat{t}_{ik,0},\hat{t}_{ik,m}\right)\left(\hat{y}_i\hat{l}_i^{\beta-1}\right)^{-\theta}\left(\hat{y}_l^{-\frac{\theta+1}{\theta}}\right)^{-\theta}\end{aligned}$$

$$\begin{aligned}\left(\hat{l}_i^{\alpha+1}\hat{y}_i^{-\frac{\theta+1}{\theta}}\right)^{-\theta}\left(\hat{y}_i\hat{l}_i^{\beta-1}\right)^{-\theta} =&\hat{\chi}\left(\frac{Y_i}{Y_i+\sum_{k\in\mathcal{F}(i)}\Xi_{ki}}\right)\hat{y}_i\\ &+\sum_{k\in\mathcal{F}_D(i)}\left(\frac{\Xi_{ki}}{Y_i+\sum_{k\in\mathcal{F}(i)}\Xi_{ki}}\right)\hat{t}_{ki}^{-\theta}\left(\hat{\Pi},\hat{P},\hat{t}_{ki,0},\hat{t}_{ki,m}\right)\left(\hat{y}_k\hat{l}_k^{\beta-1}\right)^{-\theta}\left(\hat{l}_i^{\alpha+1}\hat{y}_i^{-\frac{\theta+1}{\theta}}\right)^{-\theta}\\ &+\sum_{l\in\mathcal{F}_F(i)}\left(\frac{\Xi_{li}}{Y_i+\sum_{k\in\mathcal{F}(i)}\Xi_{ki}}\right)\hat{t}_{li}^{-\theta}\left(\hat{\Pi},\hat{P},\hat{t}_{ki,0},\hat{t}_{ki,m}\right)\left(\frac{\hat{\chi}}{\hat{\chi}_l}\right)(\hat{y}_l)^{-\theta}\left(\hat{l}_i^{\alpha+1}\hat{y}_i^{-\frac{\theta+1}{\theta}}\right)^{-\theta}\end{aligned}$$

$$\left(\hat{y}_l^{-\frac{\theta+1}{\theta}}\right)^{-\theta}(\hat{y}_l)^{-\theta} = \hat{\chi}_l\left(\frac{E_l}{E_l+\sum_{k\in\mathcal{F}_D(l)}\Xi_{lk}}\right)\hat{y}_l + \sum_{k\in\mathcal{F}_D(l)}\left(\frac{\Xi_{lk}}{E_l+\sum_{k\in\mathcal{F}_D(l)}\Xi_{lk}}\right)\hat{t}_{lk}^{-\theta}\left(\hat{\Pi},\hat{P},\hat{t}_{lk,0},\hat{t}_{lk,m}\right)(\hat{y}_l)^{-\theta}\left(\hat{l}_k^{\alpha+1}\hat{y}_k^{-\frac{\theta+1}{\theta}}\right)^{-\theta}$$

$$\left(\hat{y}_l^{-\frac{\theta+1}{\theta}}\right)^{-\theta}(\hat{y}_l)^{-\theta}\hat{\chi}_l^{-1} = \left(\frac{Y_l}{Y_l+\sum_{k\in\mathcal{F}_D(l)}\Xi_{kl}}\right)\hat{y}_l + \hat{\chi}^{-1}\sum_{k\in\mathcal{F}_D(l)}\left(\frac{\Xi_{kl}}{Y_l+\sum_{k\in\mathcal{F}_D(l)}\Xi_{kl}}\right)\hat{t}_{kl}^{-\theta}\left(\hat{\Pi},\hat{P},\hat{t}_{kl,0},\hat{t}_{kl,m}\right)\left(\hat{y}_k\hat{l}_k^{\beta-1}\right)^{-\theta}\left(\hat{y}_l^{-\frac{\theta+1}{\theta}}\right)^{-\theta}$$

Simplifying on the LHS and isolating the i specific terms on the second summand on the RHS,

$$\begin{aligned}\left(\hat{l}_i^{\alpha+1}\hat{y}_i^{-\frac{\theta+1}{\theta}}\right)^{-\theta} =&\hat{\chi}\left(\frac{E_i}{E_i+\sum_{k\in\mathcal{F}(i)}\Xi_{ik}}\right)\hat{y}_i\left(\hat{y}_i\hat{l}_i^{\beta-1}\right)^{\theta}\\ &+\sum_{k\in\mathcal{F}_D(i)}\left(\frac{\Xi_{ik}}{E_i+\sum_{k\in\mathcal{F}(i)}\Xi_{ik}}\right)\hat{t}_{ik}^{-\theta}\left(\hat{\Pi},\hat{P},\hat{t}_{ik,0},\hat{t}_{ik,m}\right)\left(\hat{l}_k^{\alpha+1}\hat{y}_k^{-\frac{\theta+1}{\theta}}\right)^{-\theta}\\ &+\sum_{l\in\mathcal{F}_F(i)}\left(\frac{\Xi_{il}}{E_i+\sum_{k\in\mathcal{F}(i)}\Xi_{ik}}\right)\hat{t}_{il}^{-\theta}\left(\hat{\Pi},\hat{P},\hat{t}_{ik,0},\hat{t}_{ik,m}\right)\left(\hat{y}_l^{-\frac{\theta+1}{\theta}}\right)^{-\theta}\end{aligned}$$

$$\left(\hat{y}_i \hat{l}_i^{\beta-1}\right)^{-\theta} = \hat{\chi}\left(\frac{Y_i}{Y_i + \sum_{k\in\mathcal{F}(i)}\Xi_{ki}}\right)\hat{y}_i\left(\hat{l}_i^{\alpha+1}\hat{y}_i^{-\frac{\theta+1}{\theta}}\right)^{\theta} + \sum_{k\in\mathcal{F}_D(i)}\left(\frac{\Xi_{ki}}{Y_i + \sum_{k\in\mathcal{F}(i)}\Xi_{ki}}\right)\hat{t}_{ki}^{-\theta}\left(\hat{\Pi}, \hat{P}, \hat{t}_{ki,0}, \hat{t}_{ki,m}\right)\left(\hat{y}_k \hat{l}_k^{\beta-1}\right)^{-\theta} + \sum_{l\in\mathcal{F}_F(i)}\left(\frac{\Xi_{li}}{Y_i + \sum_{k\in\mathcal{F}(i)}\Xi_{ki}}\right)\hat{t}_{li}^{-\theta}\left(\hat{\Pi}, \hat{P}, \hat{t}_{ki,0}, \hat{t}_{ki,m}\right)\left(\frac{\hat{\chi}}{\hat{\chi}_l}\right)(\hat{y}_l)^{-\theta}$$

Similarly for foreign locations,

$$\left(\hat{y}_l^{-\frac{\theta+1}{\theta}}\right)^{-\theta} = \hat{\chi}_l\left(\frac{E_l}{E_l + \sum_{k\in\mathcal{F}_D(l)}\Xi_{lk}}\right)\hat{y}_l(\hat{y}_l)^{\theta} + \sum_{k\in\mathcal{F}_D(l)}\left(\frac{\Xi_{lk}}{E_l + \sum_{k\in\mathcal{F}_D(l)}\Xi_{lk}}\right)\hat{t}_{lk}^{-\theta}\left(\hat{\Pi}, \hat{P}, \hat{t}_{lk,0}, \hat{t}_{lk,m}\right)\left(\hat{l}_k^{\alpha+1}\hat{y}_k^{-\frac{\theta+1}{\theta}}\right)^{-\theta}$$

$$\left(\hat{y}_l \hat{W}_l^{-1}\right)^{-\theta}\hat{\chi}_l^{-1} = \left(\frac{Y_l}{Y_l + \sum_{k\in\mathcal{F}_D(l)}\Xi_{kl}}\right)\hat{y}_l\left(\hat{y}_l^{-\frac{\theta+1}{\theta}}\right)^{\theta} + \hat{\chi}^{-1}\sum_{k\in\mathcal{F}_D(l)}\left(\frac{\Xi_{kl}}{Y_l + \sum_{k\in\mathcal{F}_D(l)}\Xi_{kl}}\right)\hat{t}_{kl}^{-\theta}\left(\hat{\Pi}, \hat{P}, \hat{t}_{kl,0}, \hat{t}_{kl,m}\right)\left(\hat{y}_k \hat{l}_k^{\beta-1}\right)^{-\theta}$$

This system of equation pins down the equilibrium with foreign locations:

$$\hat{y}_i^{1+\theta}\hat{l}_i^{-\theta(\alpha+1)} = \hat{\chi}\left(\frac{E_i}{E_i + \sum_{k\in\mathcal{F}(i)}\Xi_{ik}}\right)\hat{y}_i^{1+\theta}\hat{l}_i^{\theta(\beta-1)} + \sum_{k\in\mathcal{F}_D(i)}\left(\frac{\Xi_{ik}}{E_i + \sum_{k\in\mathcal{F}(i)}\Xi_{ik}}\right)\hat{t}_{ik}^{-\theta}\left(\hat{\Pi}, \hat{P}, \hat{t}_{ik,0}, \hat{t}_{ik,m}\right)\hat{y}_k^{1+\theta}\hat{l}_k^{-\theta(1+\alpha)} + \sum_{l\in\mathcal{F}_F(i)}\left(\frac{\Xi_{il}}{E_i + \sum_{k\in\mathcal{F}(i)}\Xi_{ik}}\right)\hat{t}_{il}^{-\theta}\left(\hat{\Pi}, \hat{P}, \hat{t}_{ik,0}, \hat{t}_{ik,m}\right)\hat{y}_l^{1+\theta}$$

$$\hat{y}_i^{-\theta}\hat{l}_i^{\theta(1-\beta)} = \hat{\chi}\left(\frac{Y_i}{Y_i + \sum_{k\in\mathcal{F}(i)}\Xi_{ki}}\right)\hat{y}_i^{-\theta}\hat{l}_i^{\theta(\alpha+1)} + \sum_{k\in\mathcal{F}_D(i)}\left(\frac{\Xi_{ki}}{Y_i + \sum_{k\in\mathcal{F}(i)}\Xi_{ki}}\right)\hat{t}_{ki}^{-\theta}\left(\hat{\Pi}, \hat{P}, \hat{t}_{ki,0}, \hat{t}_{ki,m}\right)\hat{y}_k^{-\theta}\hat{l}_k^{\theta(1-\beta)} + \hat{\chi}\sum_{l\in\mathcal{F}_F(i)}\left(\frac{\Xi_{li}}{Y_i + \sum_{k\in\mathcal{F}(i)}\Xi_{ki}}\right)\hat{t}_{li}^{-\theta}\left(\hat{\Pi}, \hat{P}, \hat{t}_{ki,0}, \hat{t}_{ki,m}\right)\hat{\chi}_l^{-1}\hat{y}_l^{-\theta}$$

$$\hat{y}_l^{1+\theta} = \left(\frac{E_l}{E_l + \sum_{k\in\mathcal{F}_D(l)}\Xi_{lk}}\right)\hat{y}_l^{1+\theta}\hat{\chi}_l + \sum_{k\in\mathcal{F}_D(l)}\left(\frac{\Xi_{lk}}{E_l + \sum_{k\in\mathcal{F}_D(l)}\Xi_{lk}}\right)\hat{t}_{lk}^{-\theta}\left(\hat{\Pi}, \hat{P}, \hat{t}_{lk,0}, \hat{t}_{lk,m}\right)\hat{y}_k^{1+\theta}\hat{l}_k^{-\theta(1+\alpha)}$$

$$\hat{y}_l^{-\theta}\hat{\chi}_l^{-1} = \left(\frac{Y_l}{Y_l + \sum_{k\in\mathcal{F}_D(l)}\Xi_{kl}}\right)\hat{y}_l^{-\theta} + \hat{\chi}^{-1}\sum_{k\in\mathcal{F}_D(l)}\left(\frac{\Xi_{kl}}{Y_l + \sum_{k\in\mathcal{F}_D(l)}\Xi_{kl}}\right)\hat{t}_{kl}^{-\theta}\left(\hat{\Pi}, \hat{P}, \hat{t}_{kl,0}, \hat{t}_{kl,m}\right)\hat{y}_k^{-\theta}\hat{l}_k^{\theta(1-\beta)}$$

D.3 Regression design for modal diversion

We are interested in deriving a regression that studies the impact of secondary network traffic in a specific MSA with regard to plausibly exogenous changes in the primary network (road) transportation cost in the same location. Consider an MSA located at node k. We will make an additional assumption that there exists some localized primary network fully contained within the MSA that any unimodal route originating or terminating in k needs to transition through before accessing the national primary road network. Let this localized network be represented by the transportation cost $\bar{t}_k$. We are therefore interested in running the following regression,

$$d\ln \Xi_{kk'} = \alpha + \beta_k \times d\ln \bar{t}_k + \epsilon_{kk'}$$

where $\Xi_{kk'}$ refers to the amount of traffic at the intermodal station in k and represents traffic from the primary to the secondary network in that location and $d\ln \bar{t}_k$ refers to changes in transportation cost of the localized primary network.

Given the assumption above we can simplify the expression for the unimodal transportation cost (Equation XZ), i.e.

$$\begin{aligned}\left(\tau_{kj}^{1}\right)^{-\theta} &= \left(\sum_{r\in\mathcal{R}_{ij}^{1}}\left(\prod_{l=1}^{K} t_{r_{l-1},r_l}^{-\theta}\right)\right) \\ &= t_k^{-\theta}\left(\sum_{r\in\mathcal{R}_{ij}^{1}}\left(\prod_{l=2}^{K} t_{r_{l-1},r_l}^{-\theta}\right)\right)\end{aligned}$$

which factorizes out the transportation cost associated with the localized network, $t_k^{-\theta}$, since it is assumed to be used on all routes.

In order to derive the regression we start from equilibrium traffic at terminal stations (Equation XZ), i.e.

$$\Xi_{kk'}^{2} = \bar{s}_{kk'}^{-\frac{\theta}{1+\theta\lambda_2}} \times P_k^{-\frac{\theta}{1+\theta\lambda_2}} \times \left(\sum_l \tau_{k'l'}^{-\theta} s_{l'l}^{-\theta} \Pi_l^{-\theta}\right)^{\frac{1}{1+\theta\lambda_2}}$$

and we examine the responsiveness of traffic flows with regard to changes in the price index, $d\ln P_k$, which implies,

$$d\ln \Xi_{kk'} = d\ln P_k^{-\frac{\theta}{1+\theta\lambda_2}}$$

we then differentiate the price index and examine the responsiveness of the price index with regard to changes in the transportation cost,

$$P_k^{-\frac{\theta}{1+\theta\lambda_2}} = \left(\sum_{i=1}^{N} \tau_{ik}^{-\theta} Y_i \Pi_i^{\theta}\right)^{\frac{1}{1+\theta\lambda_2}}$$

$$dP_k^{-\frac{\theta}{1+\theta\lambda_2}} = \frac{1}{1+\theta\lambda_2} \times \left(\sum_{i=1}^{N} Y_i \Pi_i^{\theta} \tau_{ik}^{-\theta}\right)^{\frac{1}{1+\theta\lambda_2}-1} \times \sum_i Y_i \Pi_i^{\theta} d\tau_{ik}^{-\theta}$$

$$d\ln P_k^{-\frac{\theta}{1+\theta\lambda_2}} = \frac{1}{1+\theta\lambda_2} \sum_{i=1}^{N} \frac{\tau_{ik}^{-\theta} Y_i \Pi_i^{\theta}}{\sum_{i=1}^{N} \tau_{ik}^{-\theta} Y_i \Pi_i^{\theta}} d\ln \tau_{ik}^{-\theta}$$

Instead of considering arbitrary changes to the primary road transportation network instead focus on changes in the transportation cost at node k only. Totally differentiating the expression for unimodal transportation costs (Equation XZ), we obtain,

$$d\ln\left(\tau_{kj}^{1}\right)^{-\theta} = -\theta d\ln t_k \forall j$$

Combining we obtain,

$$\begin{aligned} d\ln P_k^{-\frac{\theta}{1+\theta\lambda_2}} &= -\frac{\theta}{1+\theta\lambda_2} d\ln t_k \sum_{i=1}^{N} \frac{\tau_{ik}^{-\theta} Y_i \Pi_i^{\theta}}{\sum_{i=1}^{N} \tau_{ik}^{-\theta} Y_i \Pi_i^{\theta}} d\ln \tau_{ik}^{-\theta} \\ &= -\frac{\theta}{1+\theta\lambda_2} d\ln t_k \end{aligned}$$

we have,

$$d\ln \Xi_{kk'} = d\ln P_k^{-\frac{\theta}{1+\theta\lambda_2}}$$

combining we have,

$$d\ln \Xi_{kk'} = -\frac{\theta}{1+\theta\lambda_2} d\ln t_{k,u}$$

Furthermore, we have,

$$t_{kl} = \bar{t}_{kl}^{\frac{1}{1+\theta\lambda_1}} \times P_k^{-\frac{\theta\lambda_1}{1+\theta\lambda_1}} \times \Pi_l^{-\frac{\theta\lambda_1}{1+\theta\lambda_1}}$$

which implies,

$$d\ln t_{kl} = \frac{1}{1+\theta\lambda_1} d\ln \bar{t}_{kl}$$

plugging in, we finally obtain,

$$d\ln \Xi_{kk'} = -\theta \frac{1}{1+\theta\lambda_2} \frac{1}{1+\theta\lambda_1} d\ln \bar{t}_{k,u}$$

which implies that the structural elasticity depends on the separate congestion forces on the primary and secondary network as well as the strength of substitution between routes and modes.

D.4 Comparison with Fan and Luo (2020)

Our project studies multimodal transport networks and their impact on the returns to new technology and infrastructure investment. In particular, we focus on how these outcomes depend on the geography of the multimodal network as well as the intermodal terminals which allows for switches between transport modes. To this end, we develop a quantitative spatial equilibrium model by extending the routing-based formulation of transport cost in Allen and Arkolakis (2022) to incorporate transportation across multiple transport modes and possible mode switching conditional on the geography of the multimodal transport network, including the location of intermodal terminals, and incurred switching costs. Employing the properties of partitioned matrices, we derive closed-form expressions for the expected transport cost over the multimodal transport network despite the increased dimensionality and complexity of the underlying network. This tractable model of routing allows for counterfactual experiments which allows us to evaluate the welfare consequences to new technology and modal or terminal infrastructure improvements.

In what follows, we demonstrate that our results are consistent with the transportation cost derived in Proposition 1 in Fan and Luo (2020). Fan and Luo (2020) is a note which presents a model of transshipment building on Allen and Arkolakis (2022) and Fan, Lu and Luo (2019).

We first restate our expected transport cost from origin i to destination j over the multimodal transportation network below for convenience:

$$\tau_{ij} = e_{ij}^{-\frac{1}{\theta}}$$

where $\mathbf{E} = [e_{ij}]$ refers to the inverse of the Schur complement of the Laplacian of the partitioned infrastructure matrix for the multimodal transport network and is defined as follows,

$$\mathbf{E} \equiv \left(\mathbf{B}^{-1} - \mathbf{D}\right)^{-1} \equiv S(\Omega)^{-1}$$

where $\mathbf{B} \equiv (\mathbf{I} - \mathbf{A}_1)^{-1}$ is the geometric sum of the primary transport network matrix $\mathbf{A}_1$ and $\mathbf{D} \equiv \mathbf{S}\left(\sum_{K=0}^{\infty} \mathbf{A}_2^K\right)\mathbf{S}'$ is the geometric sum of the secondary transport matrix $\mathbf{A}_2$ that is inclusive of intermodal switching linkages between the primary and secondary transport network $\mathbf{S}$.

To do so, instead of deriving the matrix representation from the explicit numeration and recursive formula as in the main text, we instead employ the inverse of the Leontief matrix of the underlying infrastructure matrix

$$\begin{aligned}
\tau_{ij} &\equiv \lim_{N\to\infty} \tau_{ij,N} \\
&= \lim_{N\to\infty} \Gamma\left(\frac{\theta-1}{\theta}\right)\left(\sum_{K=1}^{N}\left[\Omega_{(i,j)}^{K}\right]\right)^{-\frac{1}{\theta}} \\
&= \Gamma\left(\frac{\theta-1}{\theta}\right)\left(\left[(\mathbf{I}-\mathbf{\Omega})_{(i,j)}^{-1}\right]\right)^{-\frac{1}{\theta}}, i \neq j \\
&= \Gamma\left(\frac{\theta-1}{\theta}\right)\left(\left[\begin{array}{cc} \mathbf{B} + \mathbf{BS}\left(S(\Omega)^{-1}\right)\mathbf{S}'\mathbf{B} & \mathbf{BS}\left(S(\Omega)^{-1}\right) \\ \left(S(\Omega)^{-1}\right)\mathbf{SB} & \left(S(\Omega)^{-1}\right) \end{array}\right]_{(i,j)}\right)^{-\frac{1}{\theta}}
\end{aligned}$$

where N is maximum number of edges each ij pair can have, and $S(\Omega)$ defines the Schur complement of the Laplacian of the partitioned infrastructure matrix, as above.

If the freight shipment originates and terminates on the primary network, commonly known as the first and last mile in freight transportation, we can then express bilateral transportation costs more succinctly below as a decomposition of the transport costs that arise from (A) the universe of unimodal transportation over the primary network, and (B) the additional multimodal transportation over the primary network that traverses through the secondary network taking into account the possible linkages between the two networks:

$$\tau_{ij}^{-\theta} = \left[\underbrace{\mathbf{B}}_{\substack{\text{Unimodal costs over} \\ \text{primary network}}} + \underbrace{\mathbf{BS}\left(S(\Omega)^{-1}\right)\mathbf{S}'\mathbf{B}}_{\substack{\text{Multimodal costs over} \\ \text{primary \& secondary networks}}}\right]_{ij} = \left(\tau_{ij}^{1}\right)^{-\theta} + \left(\tau_{ij}^{1,2}\right)^{-\theta} \tag{40}$$

which corresponds to equation (**??**) in our draft and is an alternative expression that is equivalent to equation

(**??**). The first and second terms in the equation above corresponds to items (A) and (B) respectively.

If we abstract from this first and last mile assumption—that freight shipments originate and terminate on the primary network—then we can trace out the sum of paths that might either originate or terminate on either network. In matrix notation this corresponds to the following:

$$\begin{aligned}\tau_{ij} &= \Gamma\left(\frac{\theta-1}{\theta}\right)\cdot\left(\left[\left[\mathbf{A}_1\mathbf{A}_2\right]\begin{bmatrix}\mathbf{B}+\mathbf{BS}\left(S(\Omega)^{-1}\right)\mathbf{S'B} & \mathbf{BS}\left(S(\Omega)^{-1}\right)\\ \left(S(\Omega)^{-1}\right)\mathbf{SB} & \left(S(\Omega)^{-1}\right)\end{bmatrix}\begin{bmatrix}\mathbf{I}\\ \mathbf{I}\end{bmatrix}\right]_{ij}\right)^{-\frac{1}{\theta}} \\ &= \Gamma\left(\frac{\theta-1}{\theta}\right)\cdot\left(\left[\left[\mathbf{A}_1\mathbf{A}_2\right]\left(\mathbf{I}-\mathbf{\Omega}\right)^{-1}\begin{bmatrix}\mathbf{I}\\ \mathbf{I}\end{bmatrix}\right]_{ij}\right)^{-\frac{1}{\theta}}\end{aligned} \tag{41}$$

where the second line above corresponds to the expression for transportation costs in Proposition 1 Part (a) of Fan and Luo (2020), but where the first line utilizes the block matrix structure to make explicit the underlying decomposition that we are introducing in our framework.

E Proofs

This section presents the proof for Proposition 1 and 2.

E.1 Proof of Proposition 1: Counterfactual Equilibrium

We proceed in two steps. In a first step we derive the change in the equilibrium conditions in terms of market access terms before then substitution the model specific elements.

E.1.1 Preliminaries

We can write equilibrium trade flows as,

$$X_{ij} = \tau_{ij}^{-\theta} \times \frac{\gamma_i}{\Pi_i^{-\theta}} \times \frac{\delta_j}{P_j^{-\theta}}$$

where γ_i and δ_j are cumulative flows out of and origin and into a destination, respectively, and Π_i and P_j are origin and destination market access terms. Given the recursive routing formulation, trade costs can be represented as:

$$\tau_{ij} = \left(\sum_{k \in \mathcal{F}(i)} \left(t_{ik}\tau_{kj}\right)^{-\theta} \right)^{-\frac{1}{\theta}}$$

And furthermore from the nested choice along the multi-layered graph, we have,

$$t_{ik}^{-\theta} = \left(\sum_{m \in \mathcal{M}(i,k)} \tilde{t}_{ik,m}^{-\eta} \right)^{\frac{\theta}{\eta}|}$$

In terms of market clearing and trade balance we have the following equilibrium conditions,

$$\gamma_i = \sum_j X_{ij}$$
$$\delta_i = \sum_j X_{ji}$$

E.1.2 Deriving the equilibrium equation

Starting with the first equilibrium condition we have:

$$\begin{aligned}
\gamma_i &= \sum_j X_{ij} \iff \\
\gamma_i &= \sum_j \tau_{ij}^{-\theta} \times \frac{\gamma_i}{\Pi_i^{-\theta}} \times \frac{\delta_j}{P_j^{-\theta}} \iff \\
\Pi_i^{-\theta} &= \sum_j \tau_{ij}^{-\theta} \times \frac{\delta_j}{P_j^{-\theta}} \iff \\
\Pi_i^{-\theta} &= \tau_{ii}^{-\theta} \frac{\delta_i}{P_i^{-\theta}} + \sum_{j \neq i} \tau_{ij}^{-\theta} \frac{\delta_j}{P_j^{-\theta}} \iff \\
\Pi_i^{-\theta} &= \tau_{ii}^{-\theta} \frac{\delta_i}{P_i^{-\theta}} + \sum_{j \neq i} \left(\sum_{k \in \mathcal{F}(i)} t_{ik}^{-\theta} \tau_{kj}^{-\theta} \right) \frac{\delta_j}{P_j^{-\theta}} \iff \\
\Pi_i^{-\theta} &= \tau_{ii}^{-\theta} \frac{\delta_i}{P_i^{-\theta}} + \sum_{k \in \mathcal{F}(i)} t_{ik}^{-\theta} \left(-\tau_{ki}^{-\theta} \frac{\delta_i}{P_i^{-\theta}} + \sum_j \tau_{kj}^{-\theta} \frac{\delta_j}{P_j^{-\theta}} \right) \iff \\
\Pi_i^{-\theta} &= t_{ii}^{-\theta} \frac{\delta_i}{P_i^{-\theta}} + \sum_{k \in \mathcal{F}(i)} t_{ik}^{-\theta} \Pi_k^{-\theta}
\end{aligned}$$

where in the last line we used the definition of the recursive transport cost, $\tau_{ii}^{-\theta} = \left(t_{ii}^{-\theta} + \sum_{k \in \mathcal{F}(i)} \left(t_{ik} \tau_{kj} \right)^{-\theta} \right)$. Substituting the definition of the edge-specific transport cost in terms of the multi-layered mode specific transport cost,

$$\begin{aligned}
\Pi_i^{-\theta} &= t_{ii}^{-\theta} \frac{\delta_i}{P_i^{-\theta}} + \sum_{k \in \mathcal{F}(i)} \left(\sum_{m \in \mathcal{M}(i,k)} \tilde{t}_{ik,m}^{-\eta} \right)^{\frac{\theta}{\eta}|} \Pi_k^{-\theta} \\
&= t_{ii}^{-\theta} \frac{\delta_i}{P_i^{-\theta}} + \sum_{k \in \mathcal{F}(i)} \left(\sum_{m \in \mathcal{M}(i,k)} \tilde{t}_{ik,m}^{-\eta} \Pi_k^{-\eta} \right)^{\frac{\theta}{\eta}|}
\end{aligned}$$

Continuing with the second equilibrium condition,

$$
\begin{aligned}
\delta_i &= \sum_j X_{ji} \iff \\
\delta_i &= \sum_j \tau_{ji}^{-\theta} \times \frac{\gamma_j}{\Pi_j^{-\theta}} \times \frac{\delta_i}{P_i^{-\theta}} \iff \\
P_i^{-\theta} &= \sum_j \tau_{ji}^{-\theta} \times \frac{\gamma_j}{\Pi_j^{-\theta}} \iff \\
P_i^{-\theta} &= \tau_{ii}^{-\theta} \frac{\gamma_i}{\Pi_i^{-\theta}} + \sum_{j \neq i} \tau_{ji}^{-\theta} \frac{\gamma_j}{\Pi_j^{-\theta}} \iff \\
P_i^{-\theta} &= \tau_{ii}^{-\theta} \frac{\gamma_i}{\Pi_i^{-\theta}} + \sum_{j \neq i} \left(\sum_{k \in \mathcal{B}(i)} t_{ki}^{-\theta} \tau_{kj}^{-\theta} \right) \frac{\gamma_j}{\Pi_j^{-\theta}} \iff \\
P_i^{-\theta} &= \tau_{ii}^{-\theta} \frac{\gamma_i}{\Pi_i^{-\theta}} + \sum_{k \in \mathcal{F}(j)} t_{ki}^{-\theta} \left(-\tau_{ki}^{-\theta} \frac{\gamma_i}{\Pi_i^{-\theta}} + \sum_j \tau_{kj}^{-\theta} \frac{\gamma_j}{\Pi_j^{-\theta}} \right) \iff \\
P_i^{-\theta} &= t_{ii}^{-\theta} \frac{\gamma_i}{\Pi_i^{-\theta}} + \sum_{k \in \mathcal{F}(j)} t_{ki}^{-\theta} P_k^{-\theta}
\end{aligned}
$$

where in the last line we used the definition of the recursive transport cost, $\tau_{ii}^{-\theta} = \left(t_{ii}^{-\theta} + \sum_{k \in \mathcal{F}(i)} \left(t_{ik} \tau_{kj} \right)^{-\theta} \right)$. Substituting the definition of the edge-specific transport cost in terms of the multi-layered mode specific transport cost,

$$
\begin{aligned}
P_i^{-\theta} &= t_{ii}^{-\theta} \frac{\gamma_i}{\Pi_i^{-\theta}} + \sum_{k \in \mathcal{F}(j)} \left(\sum_{m \in \mathcal{M}(k,i)} \tilde{t}_{ki,m}^{-\eta} \right)^{\frac{\theta}{\eta}|} P_k^{-\theta} \\
&= t_{ii}^{-\theta} \frac{\gamma_i}{\Pi_i^{-\theta}} + \sum_{k \in \mathcal{F}(j)} \left(\sum_{m \in \mathcal{M}(k,i)} \tilde{t}_{ki,m}^{-\eta} P_k^{-\eta} \right)^{\frac{\theta}{\eta}|}
\end{aligned}
$$

E.1.3 Deriving the equilibrium system in changes

Start with (recursive) equilibrium condition from the previous subsection,

$$
\Pi_i^{-\theta} = t_{ii}^{-\theta} \frac{\delta_i}{P_i^{-\theta}} + \sum_{k \in \mathcal{F}(i)} t_{ik}^{-\theta} \Pi_k^{-\theta}
$$

$$
P_i^{-\theta} = t_{ii}^{-\theta} \frac{\gamma_i}{\Pi_i^{-\theta}} + \sum_{k \in \mathcal{F}(j)} t_{ki}^{-\theta} P_k^{-\theta}
$$

Expressed in changes,

$$
\begin{aligned}
\hat{\Pi}_i^{-\theta} = &\left(\frac{t_{ii}^{-\theta} \frac{\delta_i}{P_i^{-\theta}}}{t_{ii}^{-\theta} \frac{\delta_i}{P_i^{-\theta}} + \sum_{k \in \mathcal{F}(i)} t_{ik}^{-\theta} \Pi_k^{-\theta}} \right) \frac{\hat{\delta}_i}{\hat{P}_i^{-\theta}} \\
&+ \sum_{k \in \mathcal{F}(i)} \left(\frac{t_{ik}^{-\theta} \Pi_k^{-\theta}}{t_{ii}^{-\theta} \frac{\delta_i}{P_i^{-\theta}} + \sum_{k \in \mathcal{F}(i)} t_{ik}^{-\theta} \Pi_k^{-\theta}} \right) \hat{t}_{ik}^{-\theta} \hat{\Pi}_k^{-\theta}
\end{aligned}
$$

and,

$$\hat{P}_i^{-\theta} = \left(\frac{t_{ii}^{-\theta} \frac{\gamma_i}{\Pi_i^{-\theta}}}{t_{ii}^{-\theta} \frac{\gamma_i}{\Pi_i^{-\theta}} + \sum_{k \in \mathcal{F}(j)} t_{ki}^{-\theta} P_k^{-\theta}} \right) \frac{\hat{\gamma}_i}{\hat{\Pi}_i^{-\theta}} + \sum_{k \in \mathcal{F}(i)} \left(\frac{t_{ki}^{-\theta} P_k^{-\theta}}{t_{ii}^{-\theta} \frac{\gamma_i}{\Pi_i^{-\theta}} + \sum_{k \in \mathcal{F}(i)} t_{ki}^{-\theta} P_k^{-\theta}} \right) \hat{t}_{ki}^{-\theta} \hat{P}_k^{-\theta}$$

Multiplying both numerator and denominator by their appropriate market access terms, we obtain,

$$\hat{\Pi}_i^{-\theta} = \left(\frac{\delta_i}{\delta_i + \sum_{k \in \mathcal{F}(i)} t_{ik}^{-\theta} P_k^{-\theta} \Pi_j^{-\theta}} \right) \frac{\hat{\delta}_i}{\hat{P}_i^{-\theta}} + \sum_{k \in \mathcal{F}(i)} \left(\frac{t_{ik}^{-\theta} \Pi_j^{-\theta} P_i^{-\theta}}{\delta_i + \sum_{k \in \mathcal{F}(i)} t_{ik}^{-\theta} P_k^{-\theta} \Pi_j^{-\theta}} \right) \hat{t}_{ik}^{-\theta} \hat{\Pi}_k^{-\theta}$$

$$\hat{P}_i^{-\theta} = \left(\frac{\gamma_i}{\gamma_i + \sum_{k \in \mathcal{F}(i)} t_{ki}^{-\theta} P_k^{-\theta} \Pi_i^{-\theta}} \right) \frac{\hat{\gamma}_i}{\hat{\Pi}_i^{-\theta}} + \sum_{k \in \mathcal{F}(i)} \left(\frac{t_{ki}^{-\theta} P_k^{-\theta} \Pi_i^{-\theta}}{\gamma_i + \sum_{k \in \mathcal{F}(i)} t_{ki}^{-\theta} P_k^{-\theta} \Pi_i^{-\theta}} \right) \hat{t}_{ki}^{-\theta} \hat{P}_k^{-\theta}$$

Simplifying we obtain,

$$\hat{\Pi}_i^{-\theta} = \left(\frac{\delta_i}{\delta_i + \sum_{k \in \mathcal{F}(i)} \Xi_{ik}} \right) \frac{\hat{\delta}_i}{\hat{P}_i^{-\theta}} + \sum_{k \in \mathcal{F}(i)} \left(\frac{\Xi_{ik}}{\delta_i + \sum_{k \in \mathcal{F}(i)} \Xi_{ik}} \right) \hat{t}_{ik}^{-\theta} \hat{\Pi}_k^{-\theta}$$

$$\hat{P}_i^{-\theta} = \left(\frac{\gamma_i}{\gamma_i + \sum_{k \in \mathcal{F}(i)} \Xi_{ki}} \right) \frac{\hat{\gamma}_i}{\hat{\Pi}_i^{-\theta}} + \sum_{k \in \mathcal{F}(i)} \left(\frac{\Xi_{ki}}{\gamma_i + \sum_{k \in \mathcal{F}(i)} \Xi_{ki}} \right) \hat{t}_{ki}^{-\theta} \hat{P}_k^{-\theta}$$

Next, we proceed by deriving the nested transport equilibrium at the edge-level. Recall, that given the nested choice above the changes in aggregate transport cost is given by,

$$\hat{t}_{ik}^{-\theta} = \left(\sum_{m \in \mathcal{M}(i,k)} \frac{\left(t'_{ik,m} \right)^{-\eta}}{t_{ik}^{-\eta}} \right)^{\frac{\theta}{\eta}}$$

Multiplying with the appropriate market access terms, we obtain,

$$\hat{t}_{ik}^{-\theta} = \left(\sum_{m \in \mathcal{M}(i,k)} \frac{\Xi_{ik.m}}{\Xi_{ik}} \hat{t}_{ik,m}^{-\eta} \right)^{\frac{\theta}{\eta}}$$

For the changes in transport cost we have,

$$\hat{t}_{kl,0} = \hat{\hat{t}}_{kl,0}^{\frac{1}{1+\eta\lambda_0}} \times \hat{t}_{kl}^{\frac{\lambda_0(\eta-\theta)}{1+\eta\lambda_0}} \times \hat{P}_k^{\frac{-\theta\lambda_0}{1+\eta\lambda_0}} \times \hat{\Pi}_l^{\frac{-\theta\lambda_0}{1+\eta\lambda_0}}$$

And second, we have for any non-primary transport mode,

$$\hat{t}_{kl,m} = \hat{\hat{s}}_{kk,m} \hat{\tau}_{kl,m} \hat{\hat{s}}_{ll,m} \hat{P}_k^{-\theta\lambda_m} \hat{\Pi}_{k,m}^{-\theta\lambda_m} \hat{\Pi}_l^{-\theta\lambda_m} \hat{P}_{l,m}^{-\theta\lambda_m}$$

For the trade model here we have,

$$\delta_i = E_i$$
$$\gamma_i = Y_i$$

And for the price indices in changes we have,

$$\hat{P}_i = \hat{y}_i \hat{l}_i^{\beta-1} \hat{W}^{-1}$$

$$\hat{\Pi}_i = \hat{l}_i^{\alpha+1} \hat{y}_i^{-\frac{\theta+1}{\theta}}$$

and furthermore, we have the mode specific market access terms,

$$\hat{P}_{l,m}^{-\theta} \equiv \sum_{k \in \mathcal{B}(l)} \frac{\Xi_{kl,m}}{\sum_{k \in \mathcal{B}(l)} \Xi_{kl,m}} \hat{t}_{kl,m}^{-\eta} \times \hat{t}_{kl}^{\eta-\theta} \times \hat{P}_k^{-\theta}$$

$$\hat{\Pi}_{k,m}^{-\theta} \equiv \sum_{l \in \mathcal{F}(k)} \frac{\Xi_{kl,m}}{\sum_{l \in \mathcal{F}(k)} \Xi_{kl,m}} \times \hat{t}_{kl,m}^{-\eta} \times \hat{t}_{kl}^{\eta-\theta} \times \hat{\Pi}_l^{-\theta}$$

Given an initial guess for the market access terms, we can solve for the aggregate transport costs, $\hat{t}_{ik}^{-\theta}\left(\hat{\Pi}, \hat{P}, \hat{t}_{ik,0}, \hat{t}_{ik,m}\right)$, by iteratively updating the following equation until convergence,

$$\begin{aligned}
\hat{t}_{ik}^{-\theta} &= \left(\frac{\Xi_{ik.0}}{\Xi_{ik}} \hat{t}_{ik,0}^{-\eta} + \sum_{m \neq 0} \frac{\Xi_{ik.m}}{\Xi_{ik}} \hat{t}_{ik,m}^{\eta} \right)^{\frac{\theta}{\eta}} \\
&= \left(\frac{\Xi_{ik.0}}{\Xi_{ik}} \left[\hat{\hat{t}}_{ik,0}^{\frac{1}{1+\eta\eta\lambda_0}} \times \hat{t}_{ik}^{\frac{\lambda_0(\eta-\theta)}{1+\eta\lambda_0}} \times \hat{P}_i^{\frac{-\theta\lambda_0}{1+\eta\lambda_0}} \times \hat{\Pi}_k^{\frac{-\theta\lambda_0}{1+\eta\lambda_0}} \right]^{-\eta} + \sum_{m \neq 0} \frac{\Xi_{ik.m}}{\Xi_{ik}} \left[\hat{\hat{s}}_{ii,m} \hat{\tau}_{ik,m} \hat{\hat{s}}_{kk,m} \hat{P}_i^{-\theta\lambda_m} \hat{\Pi}_{i,m}^{-\theta\lambda_m} \hat{\Pi}_k^{-\theta\lambda_m} \hat{P}_{k,m}^{-\theta\lambda_m} \right]^{-\eta} \right)^{\frac{\theta}{\eta}}
\end{aligned}$$

Writing out and substituting for the transport cost terms,

$$\hat{P}_i^{-\theta} \hat{\Pi}_i^{-\theta} = \left(\frac{\delta_i}{\delta_i + \sum_{k \in \mathcal{F}(i)} \Xi_{ik}} \right) \hat{\delta}_i + \sum_{k \in \mathcal{F}(i)} \left(\frac{\Xi_{ik}}{\delta_i + \sum_{k \in \mathcal{F}(i)} \Xi_{ik}} \right) \hat{t}_{ik}^{-\theta} \left(\hat{\Pi}, \hat{P}, \hat{\hat{t}}_{ik,0}, \hat{\hat{t}}_{ik,m} \right) \hat{P}_i^{-\theta} \hat{\Pi}_k^{-\theta}$$

$$\hat{P}_i^{-\theta} \hat{\Pi}_i^{-\theta} = \left(\frac{\gamma_i}{\gamma_i + \sum_{k \in \mathcal{F}(i)} \Xi_{ki}} \right) \hat{\gamma}_i + \sum_{k \in \mathcal{F}(i)} \left(\frac{\Xi_{ki}}{\gamma_i + \sum_{k \in \mathcal{F}(i)} \Xi_{ki}} \right) \hat{t}_{ki}^{-\theta} \left(\hat{\Pi}, \hat{P}, \hat{\hat{t}}_{ki,0}, \hat{\hat{t}}_{ki,m} \right) \hat{P}_k^{-\theta} \hat{\Pi}_i^{-\theta}$$

Substituting the price indices in changes, we get,

$$\begin{aligned}
\left(\hat{l}_i^{\alpha+1} \hat{y}_i^{-\frac{\theta+1}{\theta}} \right)^{-\theta} \left(\hat{y}_i \hat{l}_i^{\beta-1} \hat{W}^{-1} \right)^{-\theta} &= \left(\frac{E_i}{E_i + \sum_{k \in \mathcal{F}(i)} \Xi_{ik}} \right) \hat{y}_i \\
&\quad + \sum_{k \in \mathcal{F}(i)} \left(\frac{\Xi_{ik}}{E_i + \sum_{k \in \mathcal{F}(i)} \Xi_{ik}} \right) \hat{t}_{ik}^{-\theta} \left(\hat{\Pi}, \hat{P}, \hat{t}_{ik,0}, \hat{t}_{ik,m} \right) \left(\hat{y}_i \hat{l}_i^{\beta-1} \hat{W}^{-1} \right)^{-\theta} \left(\hat{l}_k^{\alpha+1} \hat{y}_k^{-\frac{\theta+1}{\theta}} \right)^{-\theta} \\
\left(\hat{l}_i^{\alpha+1} \hat{y}_i^{-\frac{\theta+1}{\theta}} \right)^{-\theta} \left(\hat{y}_i \hat{l}_i^{\beta-1} \hat{W}^{-1} \right)^{-\theta} &= \left(\frac{Y_i}{Y_i + \sum_{k \in \mathcal{F}(i)} \Xi_{ki}} \right) \hat{y}_i \\
&\quad + \sum_{k \in \mathcal{F}(i)} \left(\frac{\Xi_{ki}}{Y_i + \sum_{k \in \mathcal{F}(i)} \Xi_{ki}} \right) \hat{t}_{ki}^{-\theta} \left(\hat{\Pi}, \hat{P}, \hat{t}_{ki,0}, \hat{t}_{ki,m} \right) \left(\hat{y}_k \hat{l}_k^{\beta-1} \hat{W}^{-1} \right)^{-\theta} \left(\hat{l}_i^{\alpha+1} \hat{y}_i^{-\frac{\theta+1}{\theta}} \right)^{-\theta}
\end{aligned}$$

Simplifying and defining, $\hat{\chi} = \hat{W}^{-\theta}$, we have,

$$\hat{y}_i^{1+\theta}\hat{l}_i^{-\theta(1+\alpha)} = \hat{\chi}\left(\frac{E_i}{E_i + \sum_{k\in\mathcal{F}(i)}\Xi_{ik}}\right)\hat{y}_i^{1+\theta}\hat{l}_i^{-\theta(1-\beta)} + \sum_{k\in\mathcal{F}(i)}\left(\frac{\Xi_{ik}}{E_i + \sum_{k\in\mathcal{F}(i)}\Xi_{ik}}\right)\hat{t}_{ik}^{-\theta}\hat{y}_k^{1+\theta}\hat{l}_k^{-\theta(1+\alpha)}$$

$$\hat{y}_i^{-\theta}\hat{l}_i^{\theta(1-\beta)} = \hat{\chi}\left(\frac{Y_i}{Y_i + \sum_{k\in\mathcal{F}(i)}\Xi_{ki}}\right)\hat{y}_i^{-\theta}\hat{l}_i^{\theta(1+\alpha)} + \sum_{k\in\mathcal{F}(i)}\left(\frac{\Xi_{ki}}{Y_i + \sum_{k\in\mathcal{F}(i)}\Xi_{ki}}\right)\hat{t}_{ki}^{-\theta}\hat{y}_k^{-\theta}\hat{l}_k^{\theta(1-\beta)}$$